TECHNISCHE UNIVERSITÄT DARMSTADT

EXPERIMENTAL RESULTS ON HADRON PRODUCTION

- In cold nuclear matter (π+A)
- In hot and dense matter (Au+Au):
  - Pions
  - Strangeness
  - Light resonances

Georgy Kornakov

High Acceptance Di-Electron Spectrometer

- Fix target
- A, p and π beams at SIS18, GSI, Darmstadt
- 1-4 GeV/c
- Low material budget
- Electron and charged particle identification

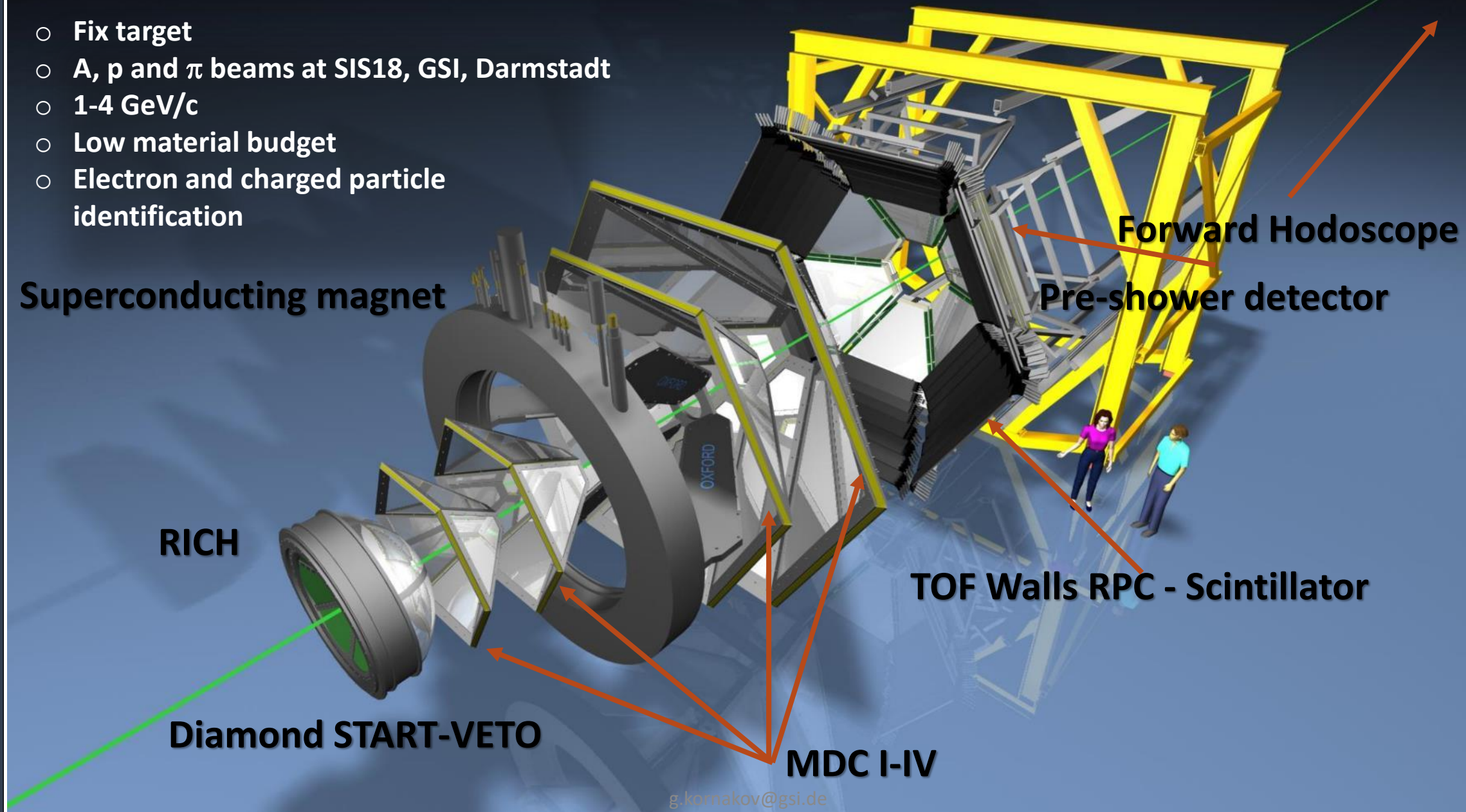

g.kornakov@gsi.de

Particle identification

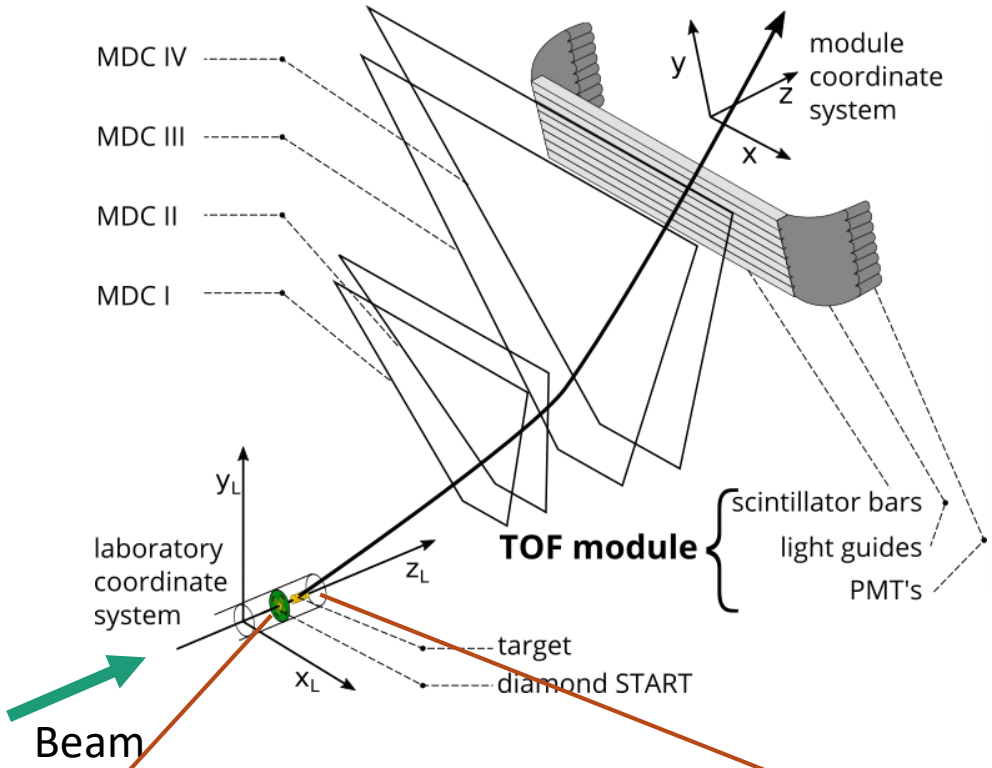

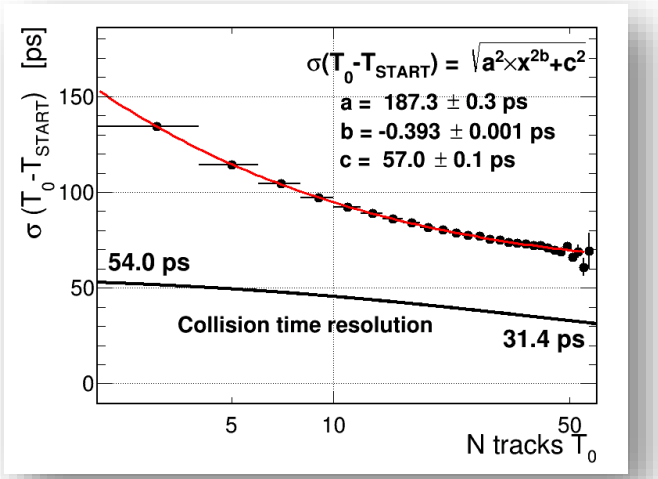

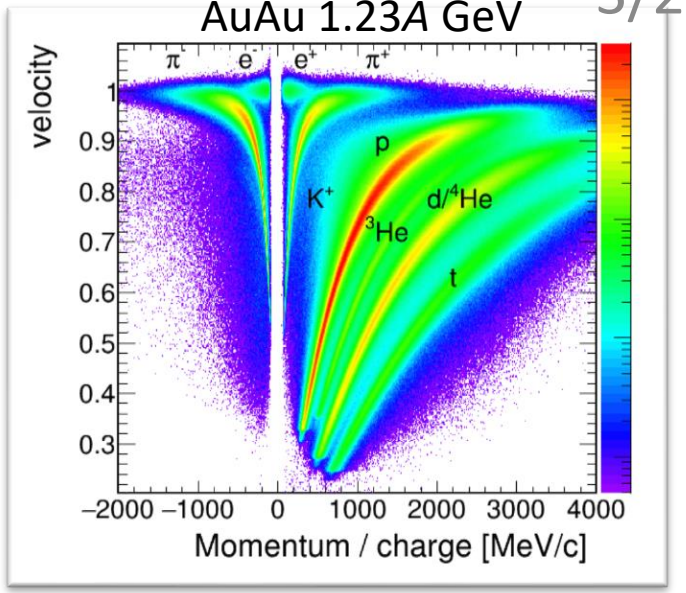

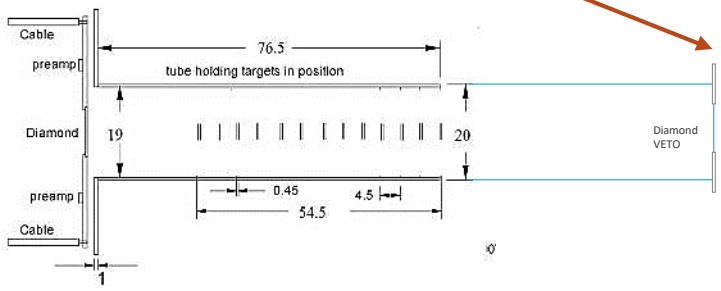

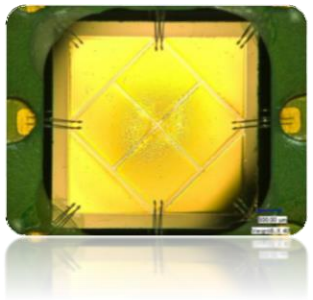

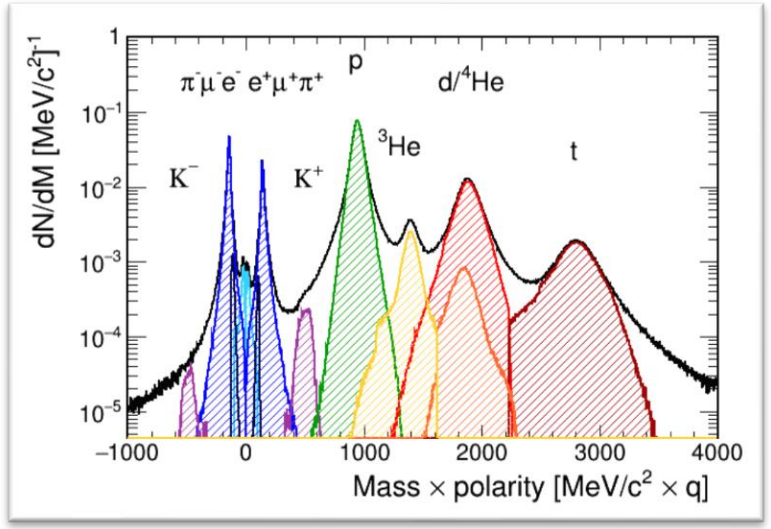

g.kornakov@gsi.de

Elementary and heavy-ion beams $\sqrt{s} = 2.3\text{-}2.7$ GeV at SIS18

- HADES explores baryon-rich matter
- Rare and penetrating probes

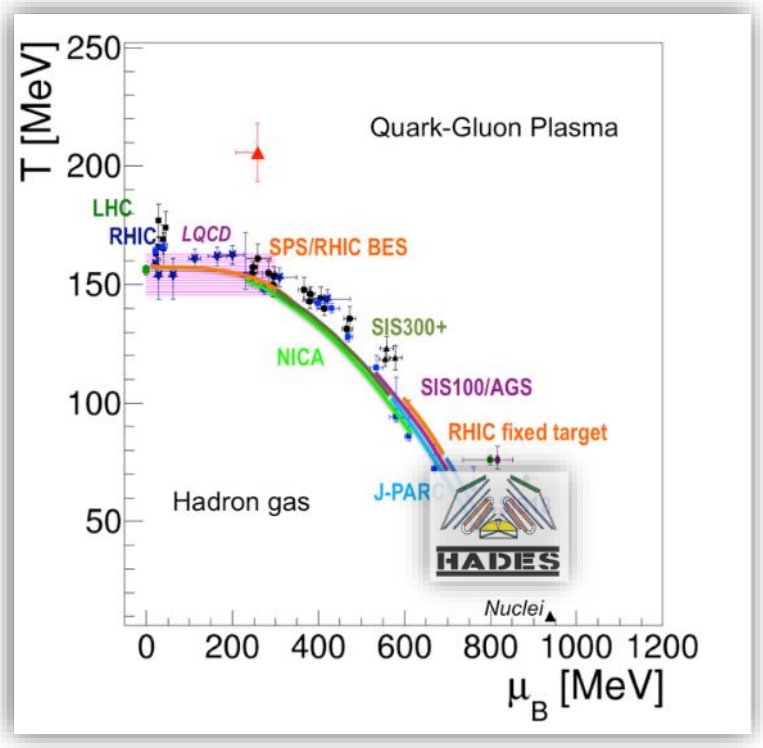

g.kornakov@gsi.de

Elementary and heavy-ion beams $\sqrt{s} = 2.3\text{-}2.7$ GeV at SIS18

- HADES explores baryon-rich matter
- Rare and penetrating probes
- Strangeness production below $\sqrt{s_{NN}}$ threshold

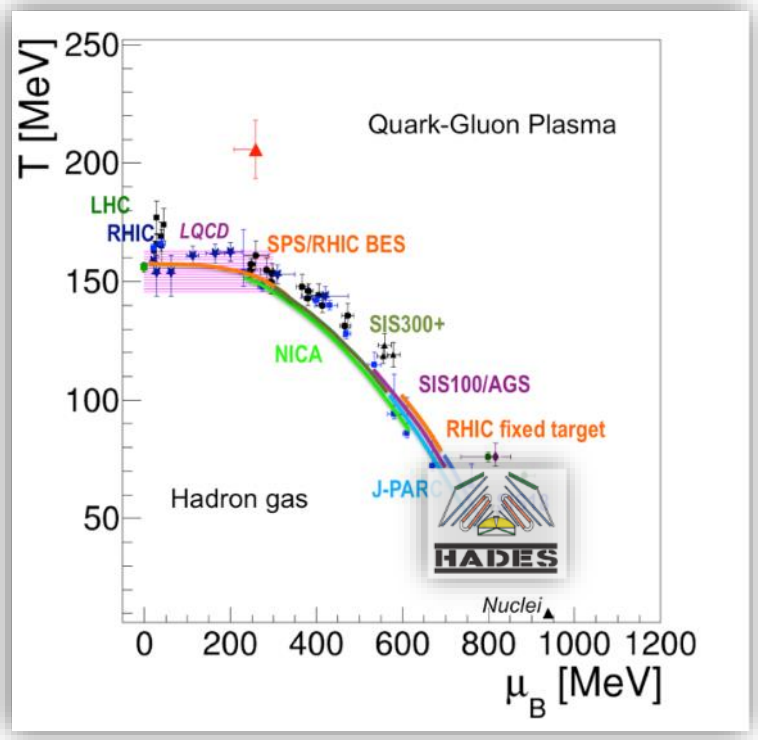

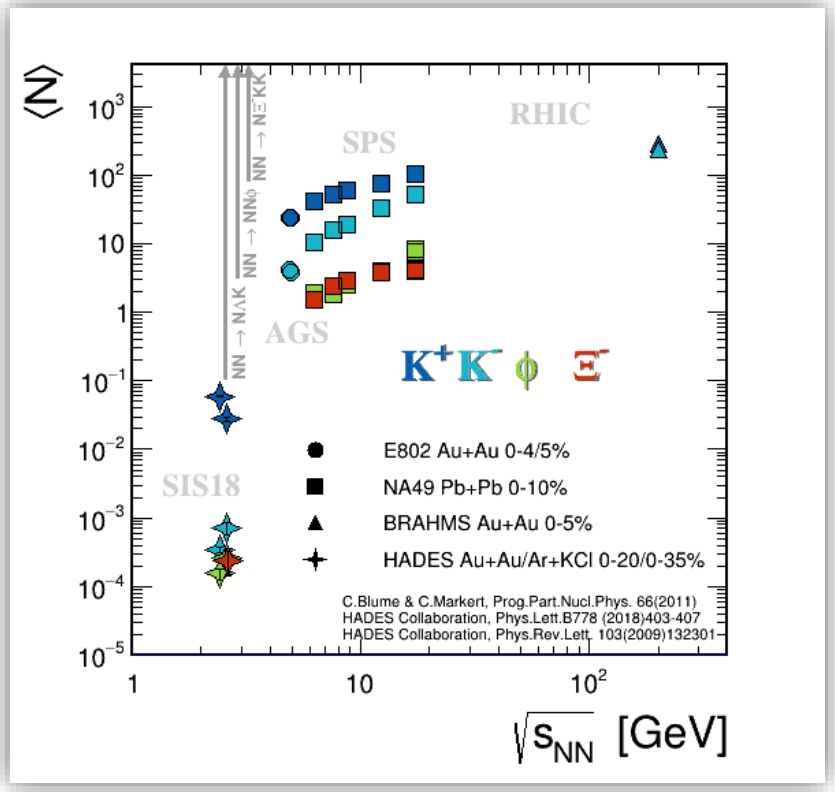

g.kornakov@gsi.de

Elementary and heavy-ion beams $\sqrt{s}$ = 2.3-2.7 GeV at SIS18

- HADES explores baryon-rich matter
- Rare and penetrating probes
- Strangeness production below $\sqrt{s_{NN}}$ threshold

Rare probes:
$\phi \rightarrow 2\times10^{-4}$/Event in K^+K^-
~1 decay in 5000 events!

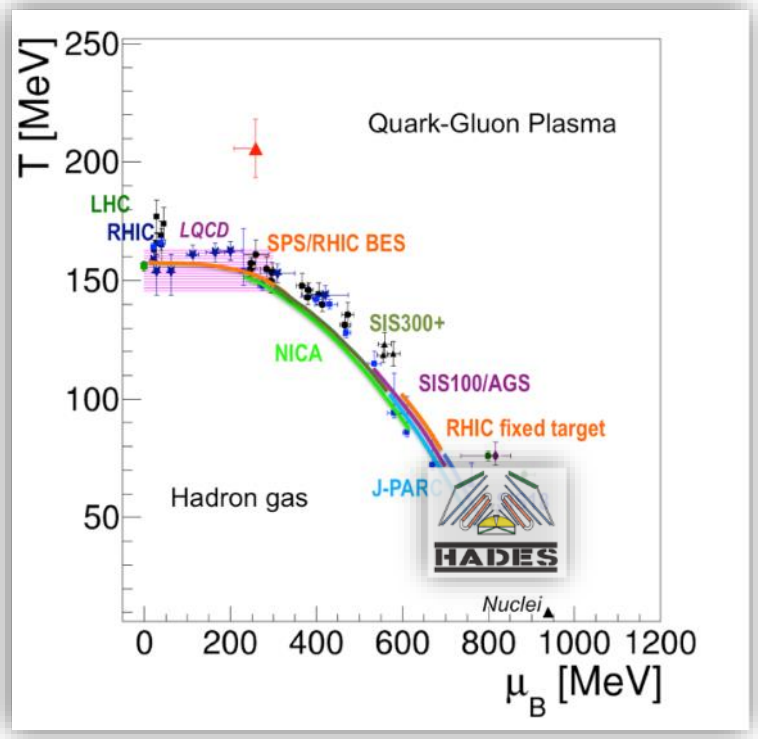

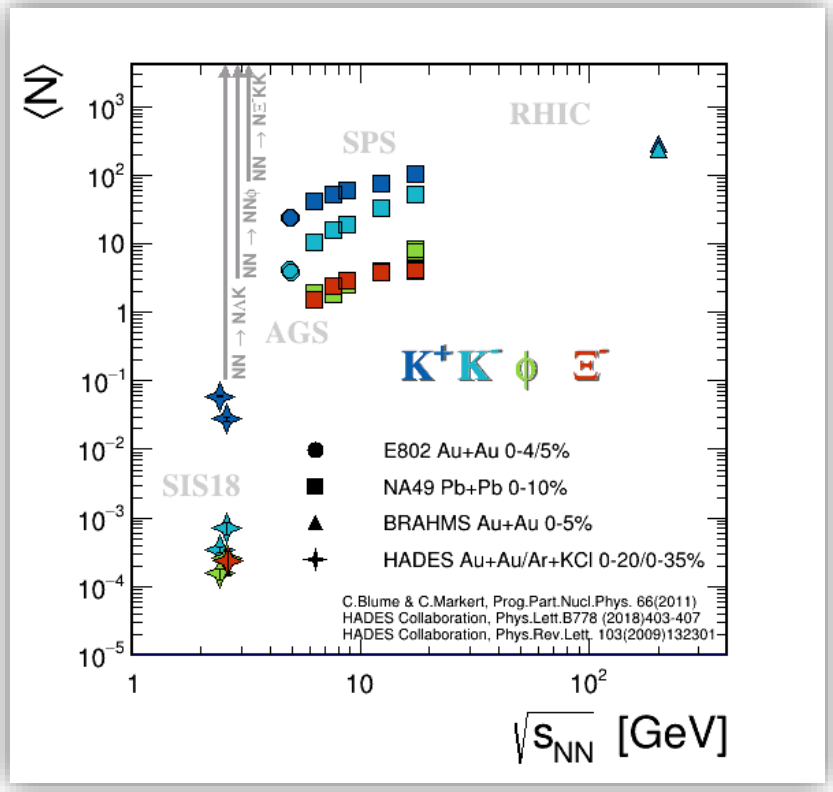

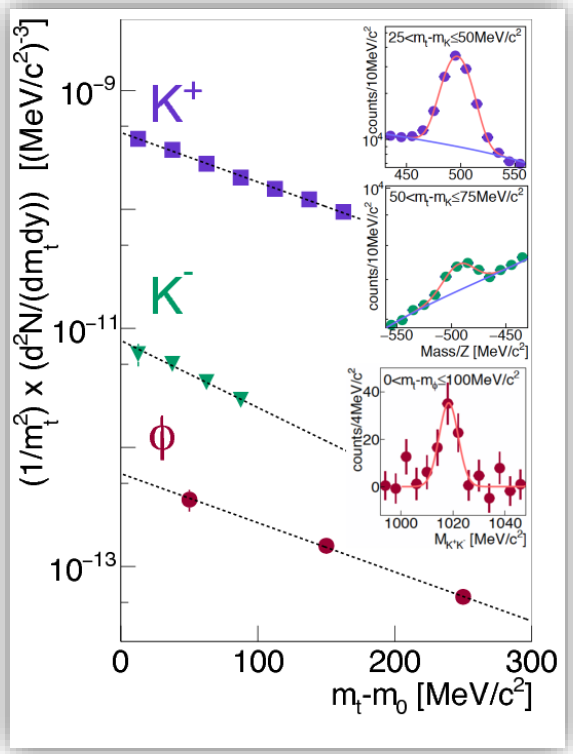

Phys.Lett. B778 (2018) 403-407

Models for strangeness production below NN threshold

- “Abundant” (multi)-strange particles demand an energy reservoir to be produced sub-threshold

Different approaches:

Models for strangeness production below NN threshold

❑ “Abundant” (multi)-strange particles demand an energy reservoir to be produced sub-threshold
Different approaches:

➢ Decays

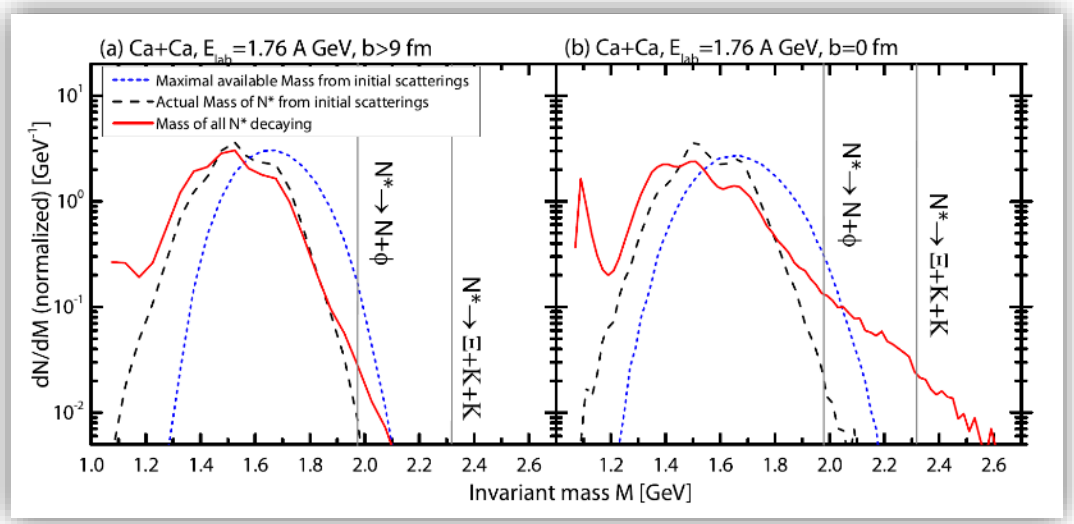

J. Steinheimer and M. Bleicher 2017
J. Phys. Conf. Ser. 779 012017

Models for strangeness production below NN threshold

❑ “Abundant” (multi)-strange particles demand an energy reservoir to be produced sub-threshold
Different approaches:

➢ Decays

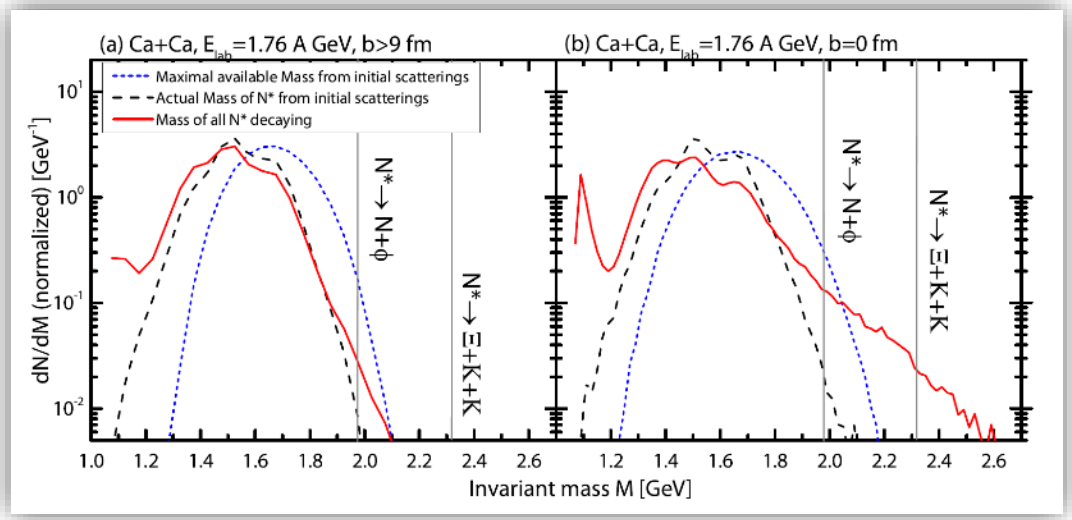

J. Steinheimer and M. Bleicher 2017
J. Phys. Conf. Ser. 779 012017

➢ Local forced thermalization

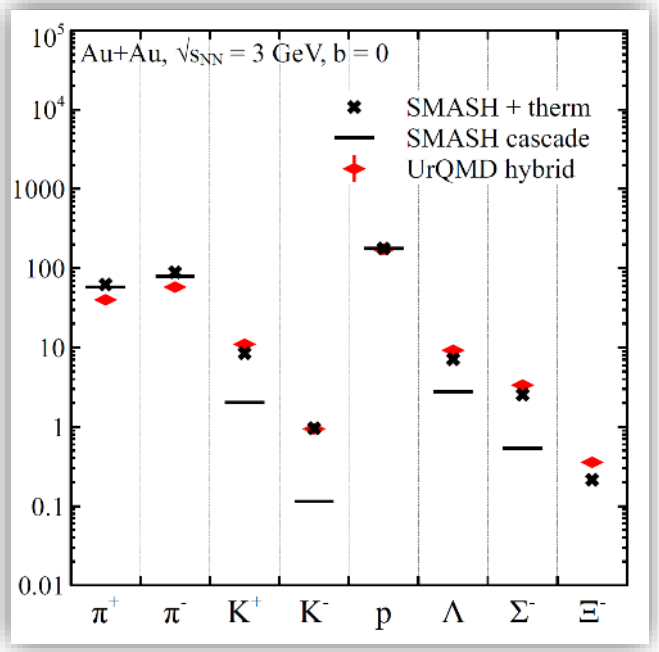

D. Oliinychenko and H. Petersen.
J.Phys. G44 (2017) no.3, 034001

Models for strangeness production below NN threshold

❑ “Abundant” (multi)-strange particles demand an energy reservoir to be produced sub-threshold

Different approaches:

➢ Decays

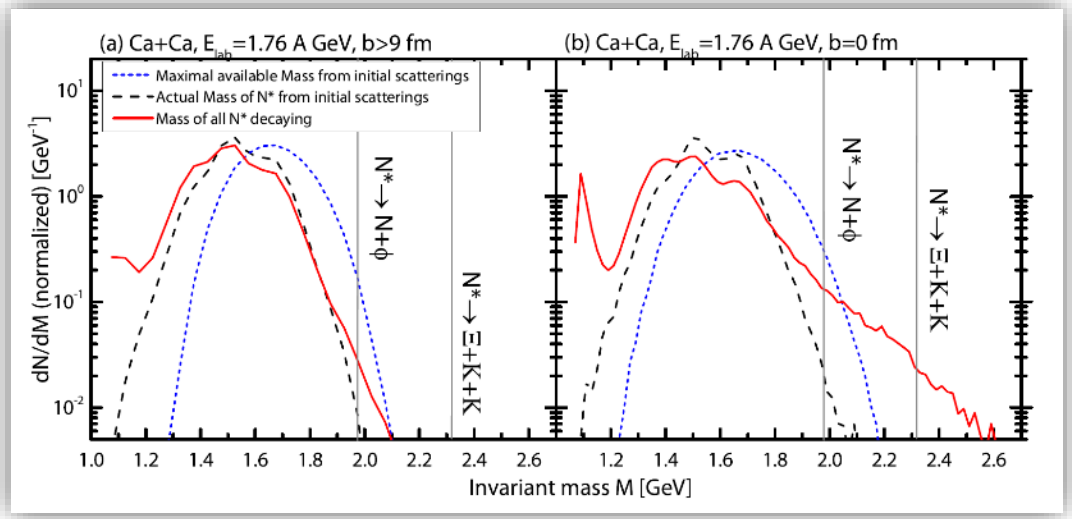

J. Steinheimer and M. Bleicher 2017
J. Phys. Conf. Ser. 779 012017

➢ Local forced thermalization

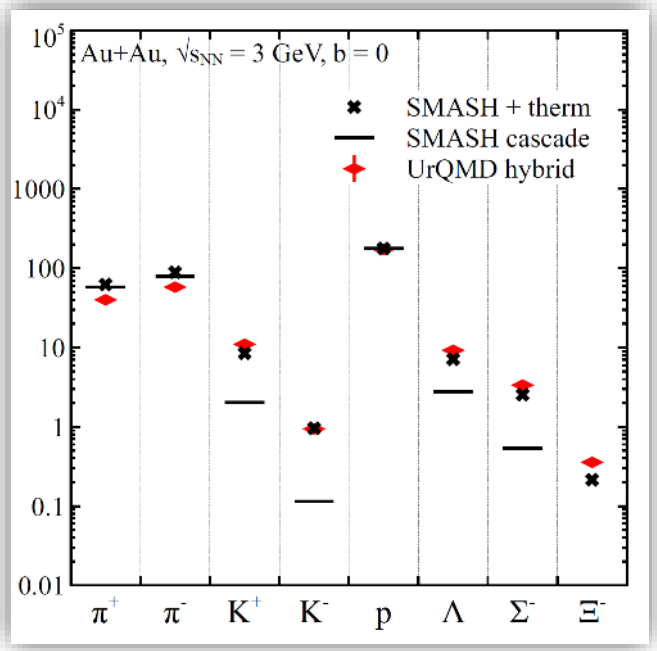

D. Oliinychenko and H. Petersen.
J.Phys. G44 (2017) no.3, 034001

➢ Hagedorn states

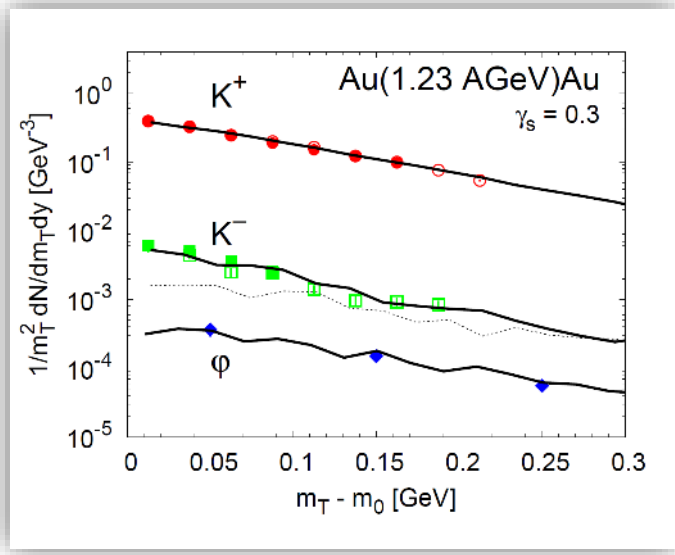

K. Gallmeister, M. Beitel, C. Greiner
arXiv:1712.04018 [hep-ph]

Models for strangeness production below NN threshold

❑ “Abundant” (multi)-strange particles demand an energy reservoir to be produced sub-threshold

Different approaches:

➢ Decays

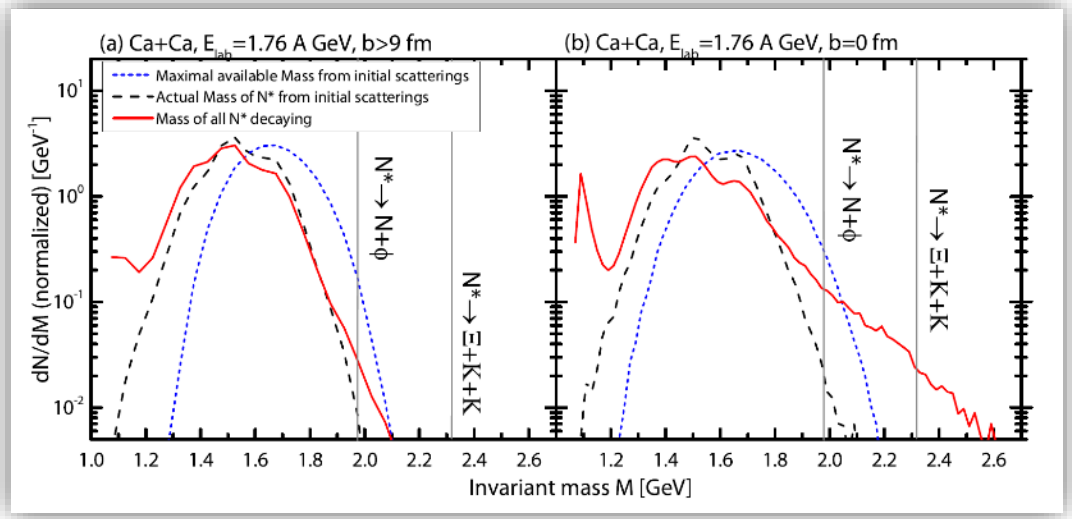

J. Steinheimer and M. Bleicher 2017
J. Phys. Conf. Ser. 779 012017

➢ Local forced thermalization

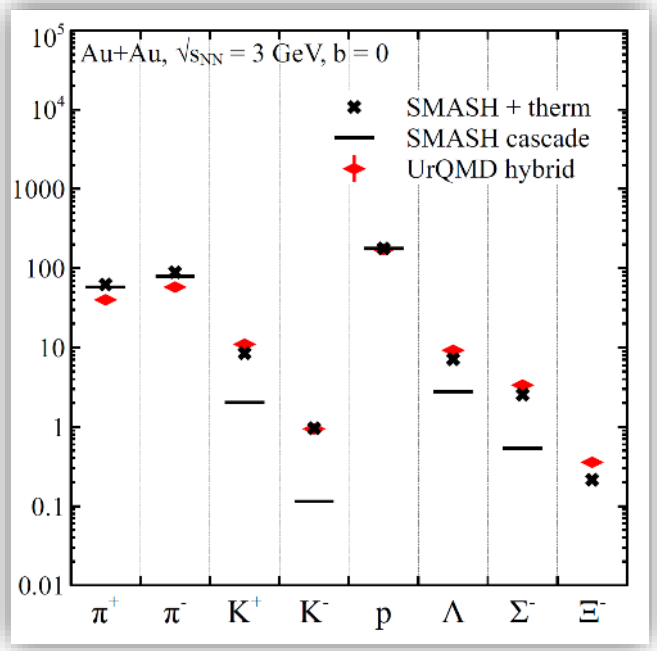

D. Oliinychenko and H. Petersen.
J.Phys. G44 (2017) no.3, 034001

➢ Hagedorn states

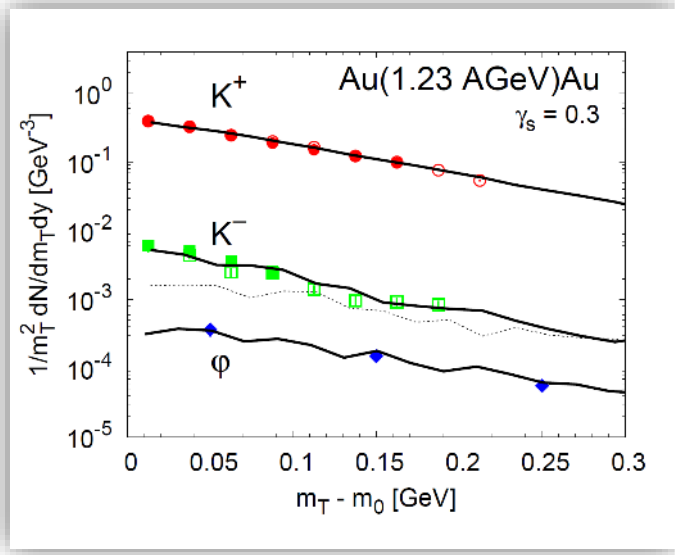

K. Gallmeister, M. Beitel, C. Greiner
arXiv:1712.04018 [hep-ph]

Baryon resonances play a key role!

Can we directly measure resonances and their contributions to hadron production?

g.kornakov@gsi.de

Models for strangeness production below NN threshold

In p + A collisions

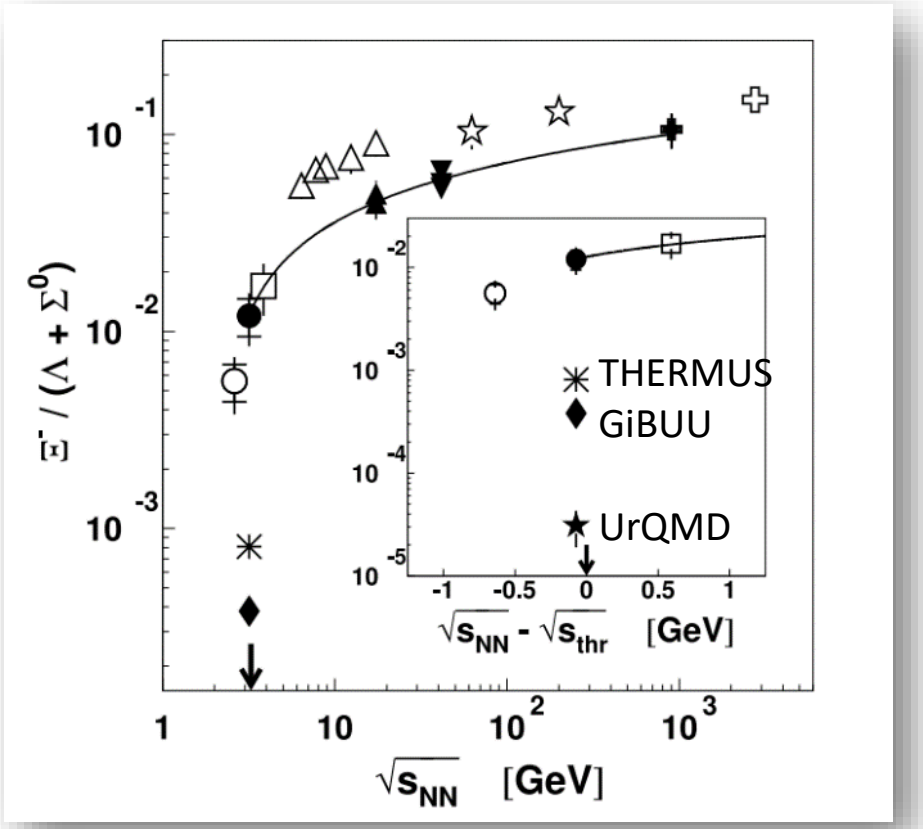

G. Agakishiev et al. (HADES collaboration), Phys. Rev. Lett. 114, 212301 (2015).

Models for strangeness production below NN threshold

In p + A collisions

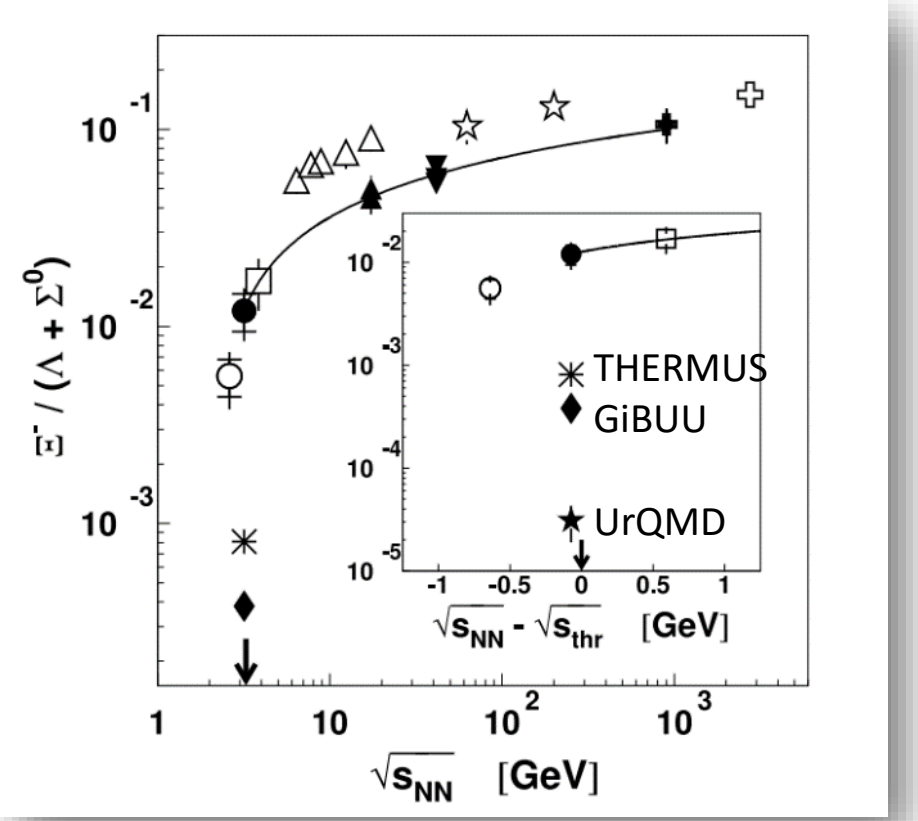

G. Agakishiev et al. (HADES collaboration), Phys. Rev. Lett. 114, 212301 (2015).

M. Zetenyi, G. Wolf
Phys.Lett. B785 (2018) 226-231

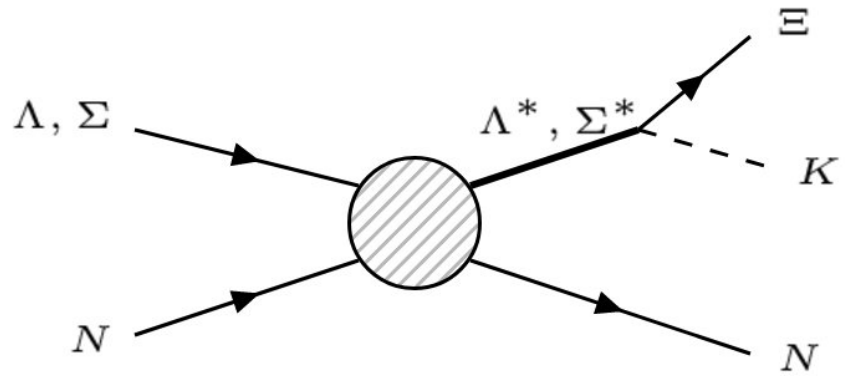

- Two step process:
  - 1st hyperon produced
  - 2nd hyperon scatters on a nucleon
- Strong influence of the angular distributions, anisotropies
- Many uncertainties in production cross-sections of strange resonances and hyperon nucleon-scattering cross-sections

π^- + C/W collisions

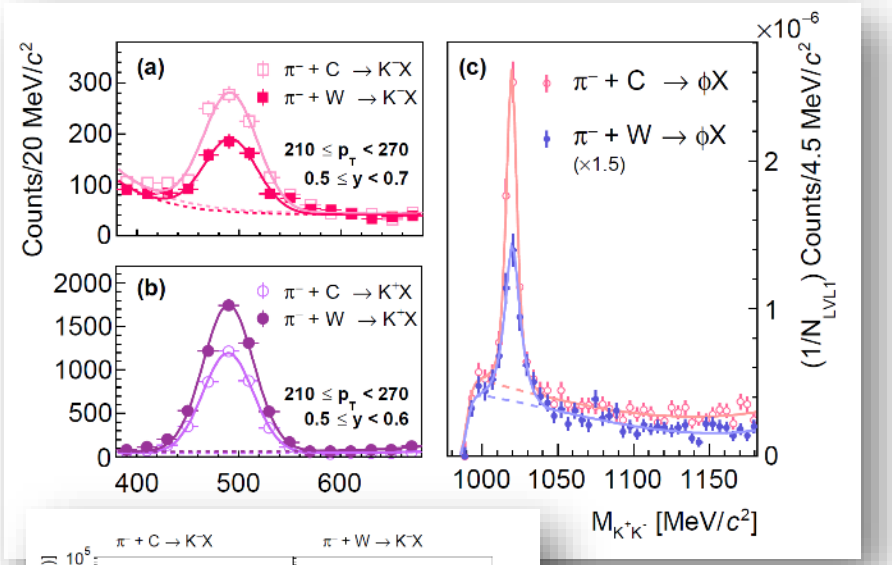

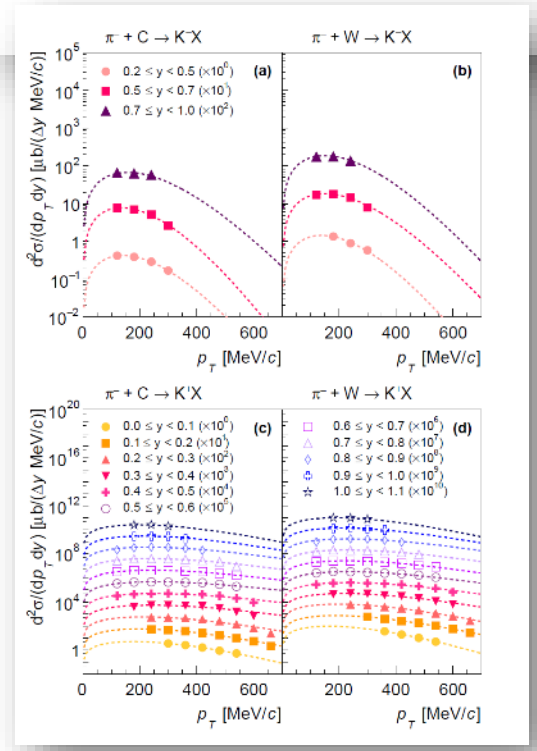

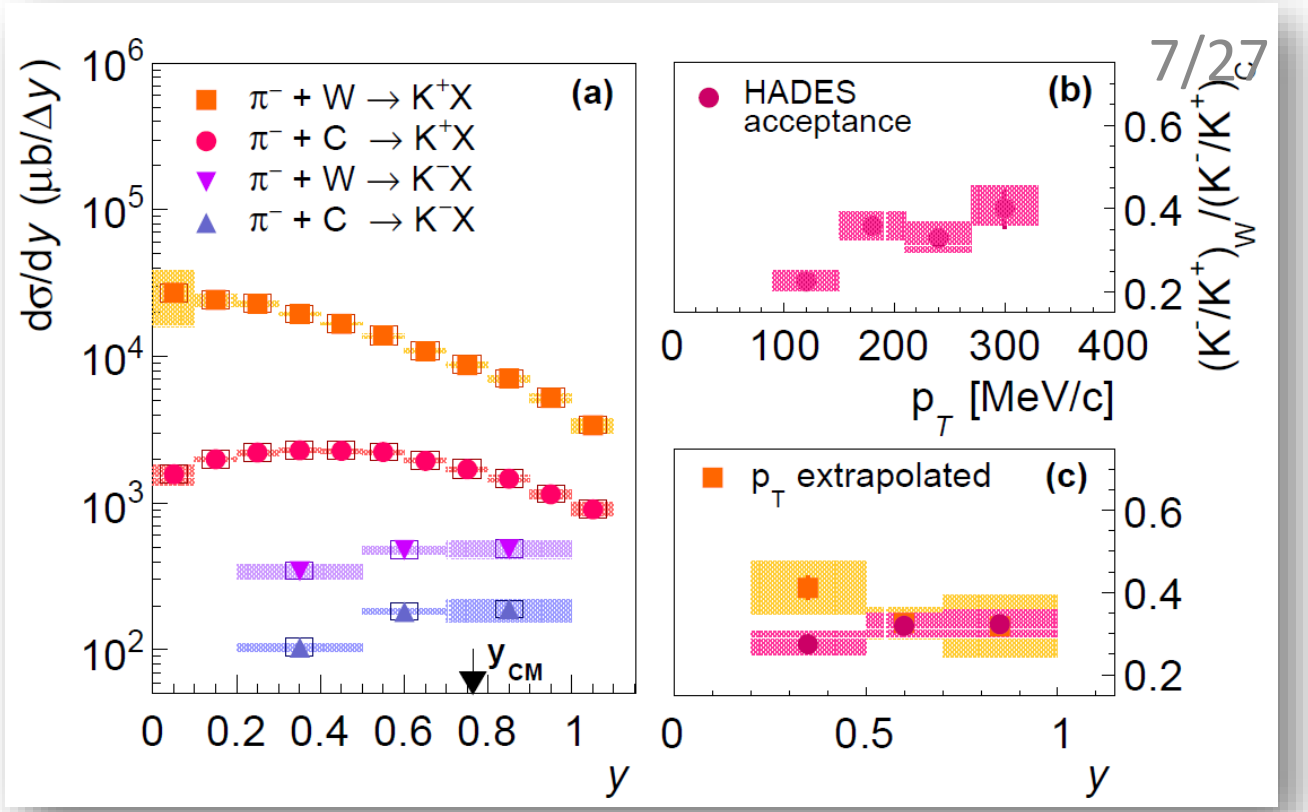

HADES Collab., arXiv:1812.03728 [nucl-ex]

First measurement of kaons and in the same reactions provides experimental evidence of the strong coupling between the and K- dynamics within nuclear matter.

- Strong shift towards backward rapidity of K+, K- is similar in both targets
- Sizable K- absorption in heavy nuclei.

g.kornakov@gsi.de

Au+Au collisions at $\sqrt{s} = 2.42$ GeV

g.kornakov@gsi.de

HADES Au+Au $\sqrt{s}$=2.42 GeV

- **Full azimuthal coverage**, 18-85^{o} polar angle
- **Fast detector**: 1.5 x 10^{6} Au ions/s (8 kHz)
  - 7x10^{9} events recorded

g.kornakov@gsi.de

HADES Au+Au $\sqrt{s}$=2.42 GeV

- **Full azimuthal coverage**, 18-85° polar angle
- **Fast detector**: 1.5 x 10^6 Au ions/s (8 kHz)
  - 7x10^9 events recorded
- Off-line centrality selection:
  - Hit/track multiplicity
  - Forward Wall

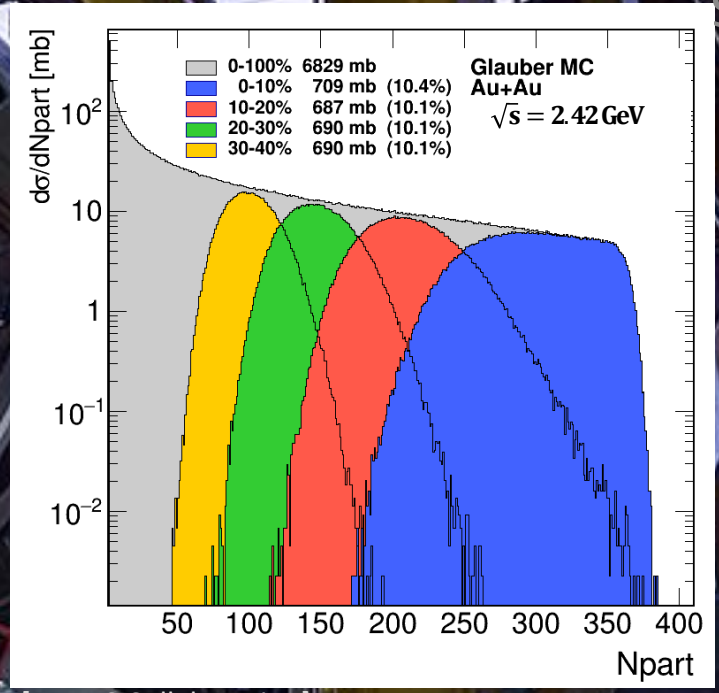

[HADES Collaboration]
arXiv:1712.07993 [nucl-ex]

g.kornakov@gsi.de

HADES Au+Au $\sqrt{s}$=2.42 GeV

- **Full azimuthal coverage**, 18-85° polar angle
- **Fast detector**: 1.5 x 10^6 Au ions/s (8 kHz)
  - 7x10^9 events recorded
- Off-line centrality selection:
  - Hit/track multiplicity
  - Forward Wall
- **High purity** hadron detectors:
  - MDC: momentum ($\Delta P/P<2\%$) and dE/dx
  - TOF (Diamond T_0, RPC and Scintillator Walls)

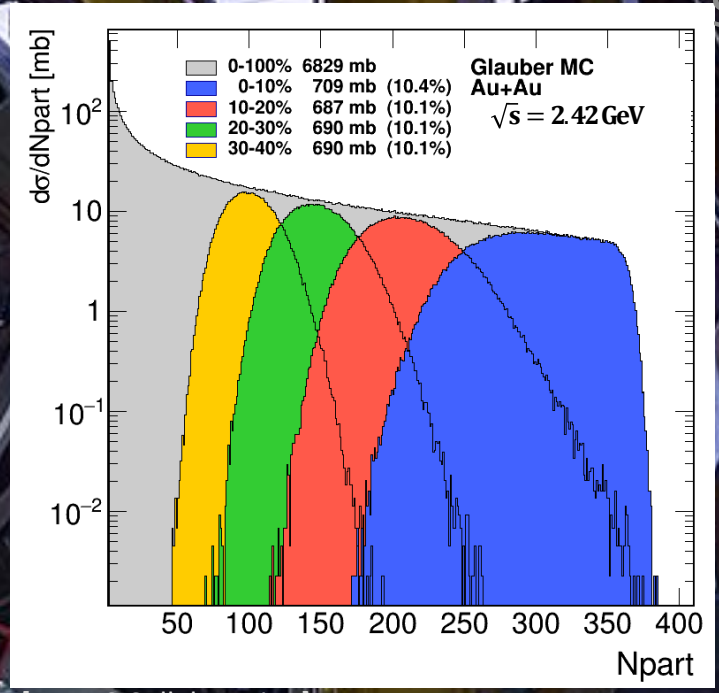

[HADES Collaboration]
arXiv:1712.07993 [nucl-ex]

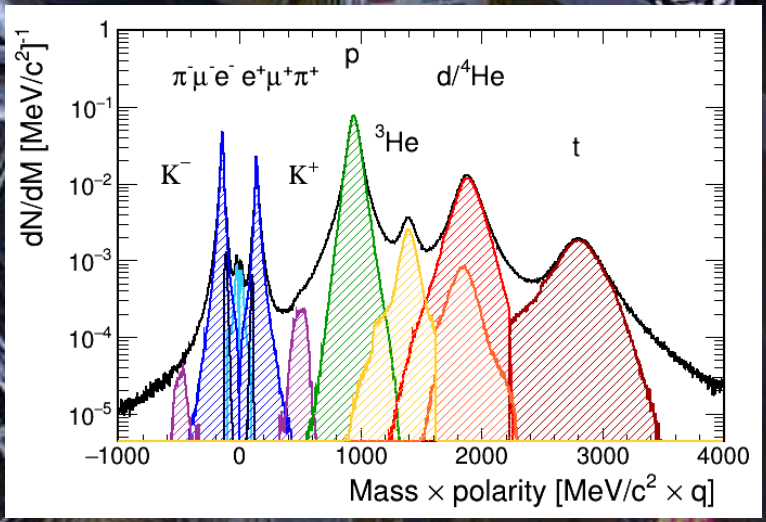

g.kornakov@gsi.de

Centrality dependence charge pion multiplicities

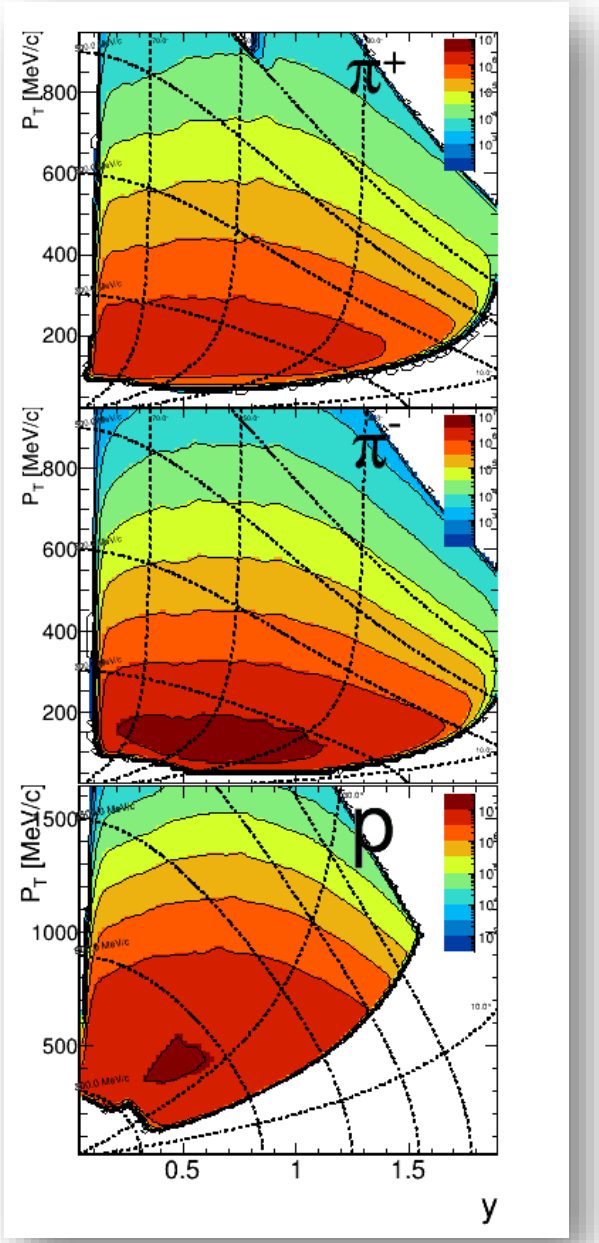

g.kornakov@gsi.de

Centrality dependence charge pion multiplicities

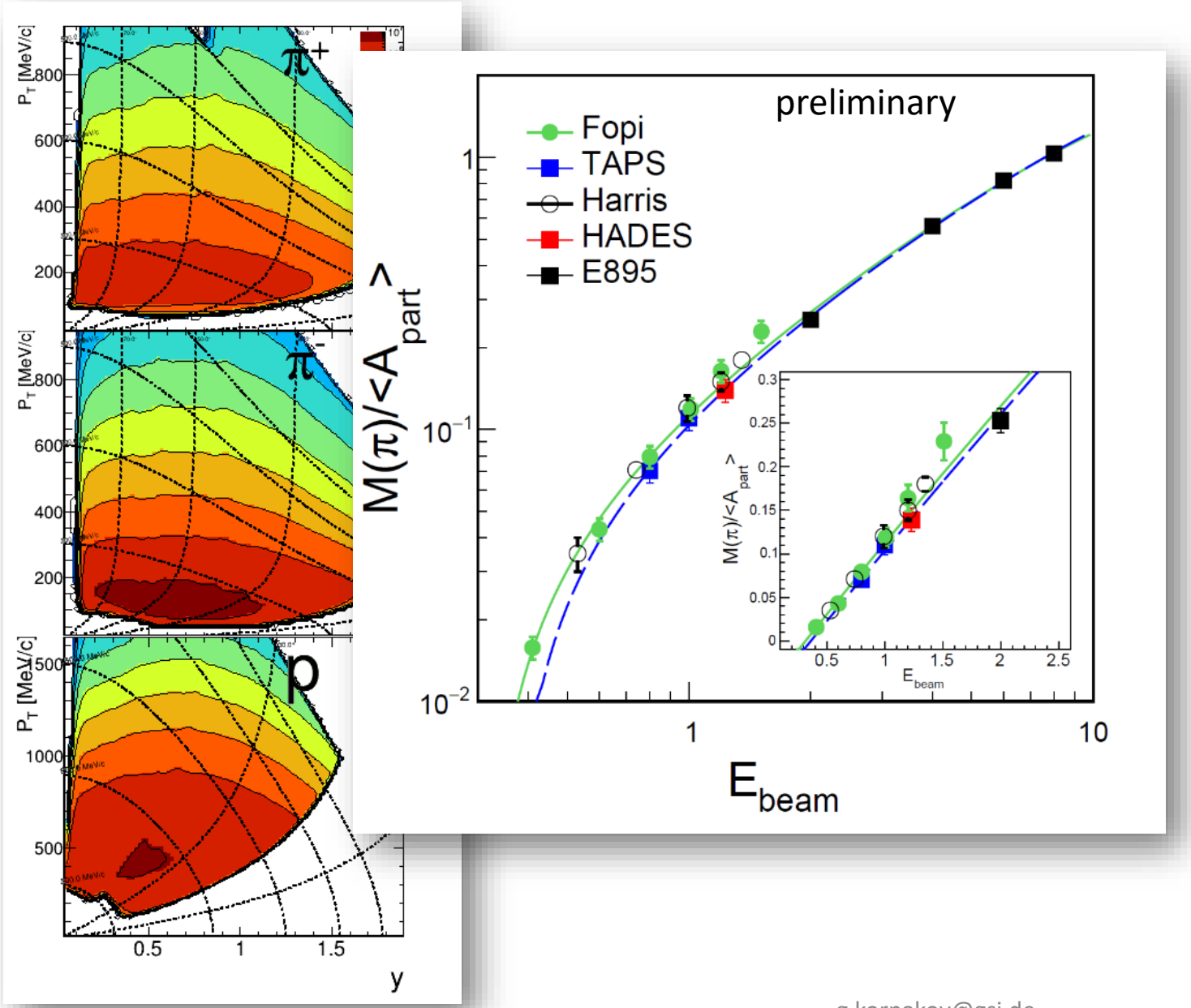

g.kornakov@gsi.de

Centrality dependence charge pion multiplicities

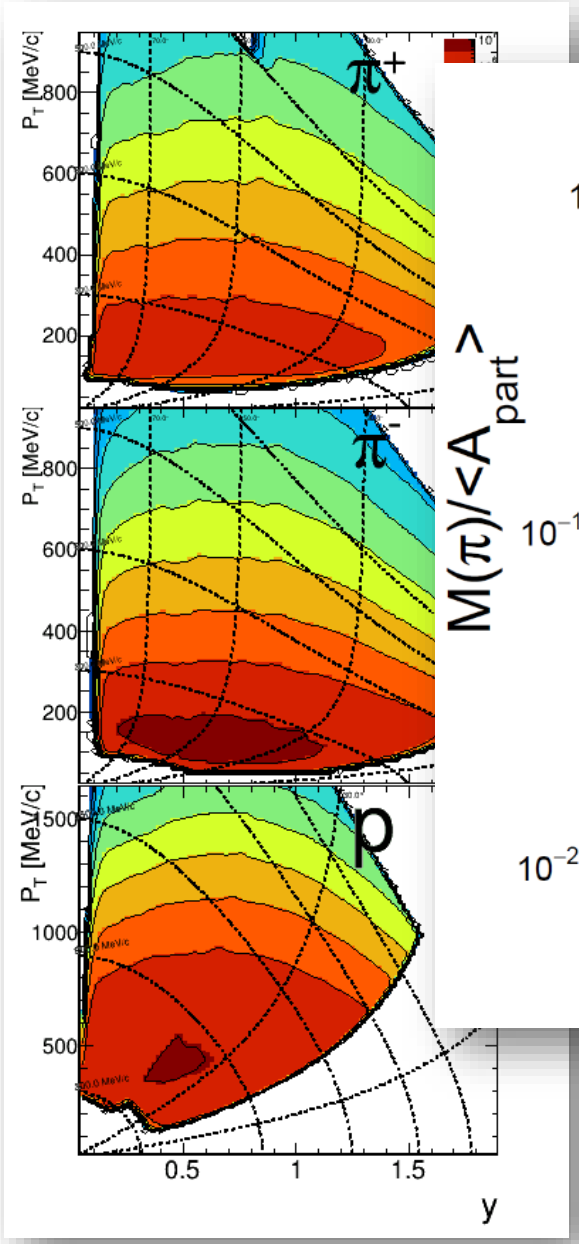

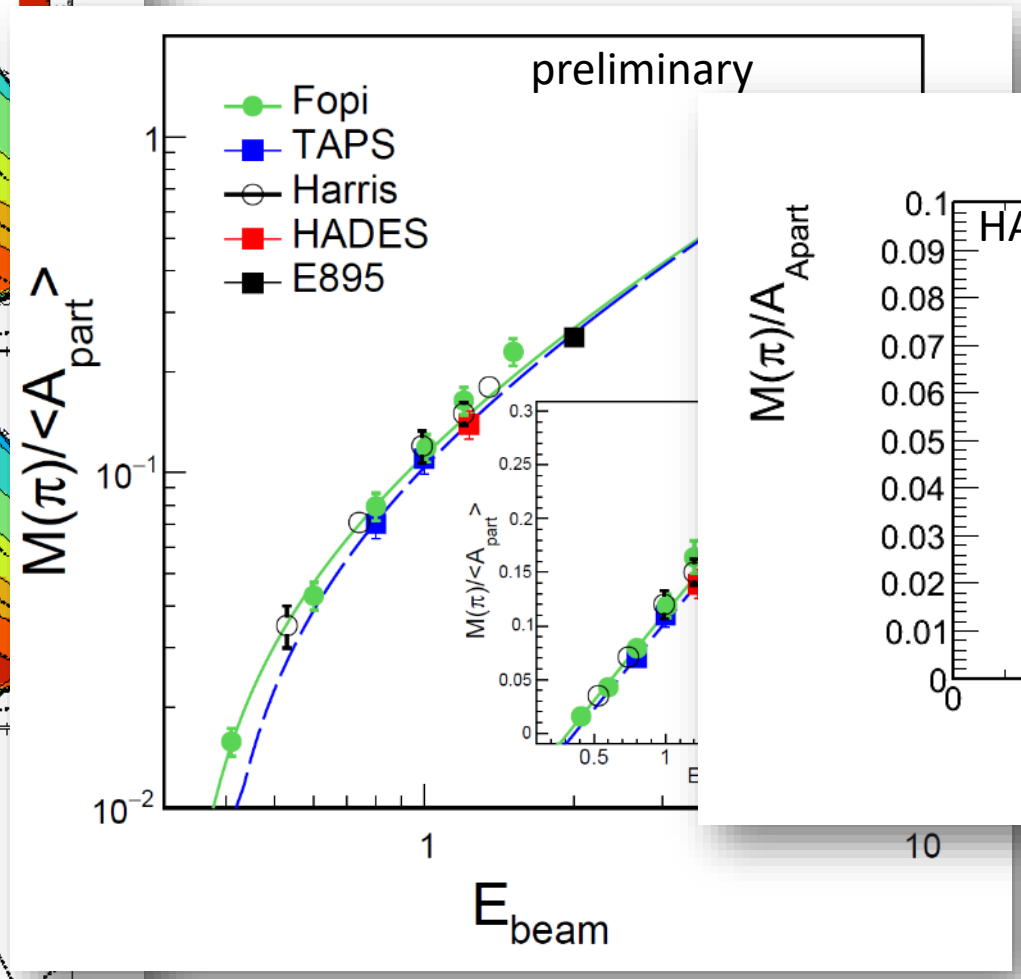

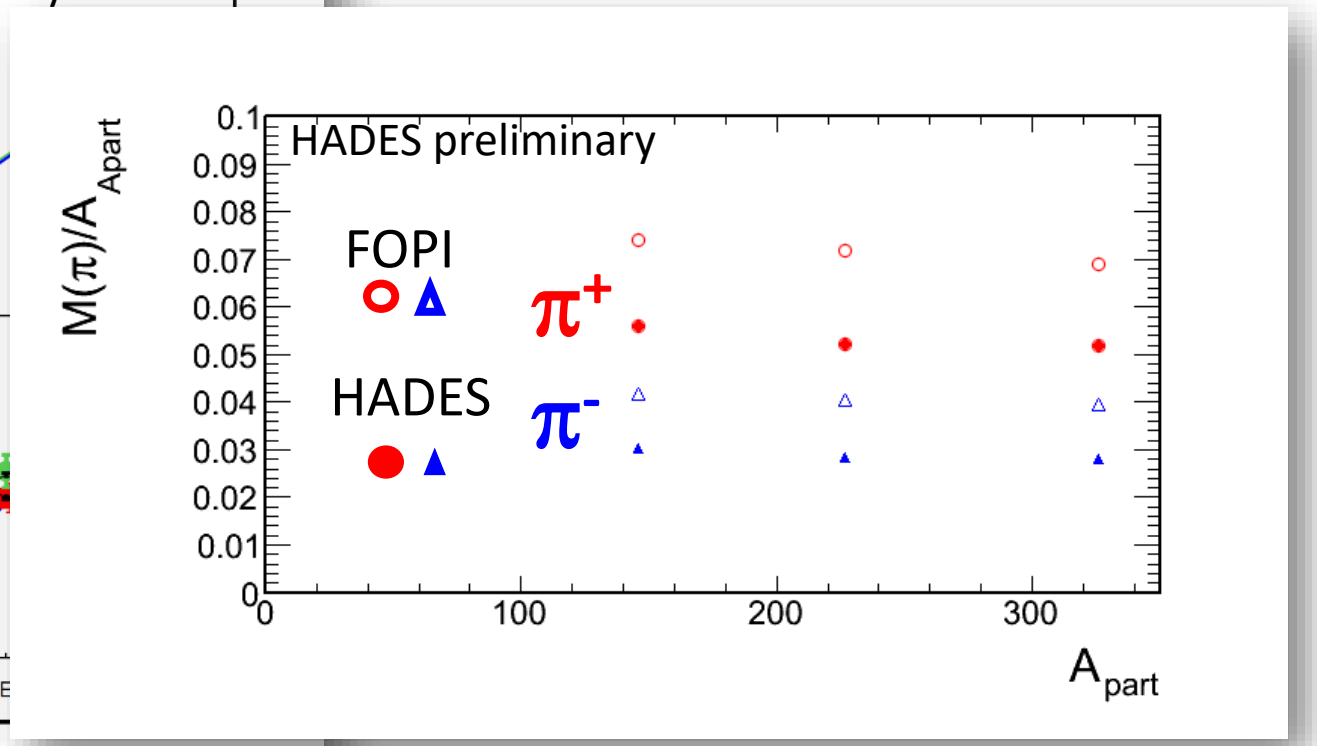

g.kornakov@gsi.de

Centrality dependence charge pion multiplicities

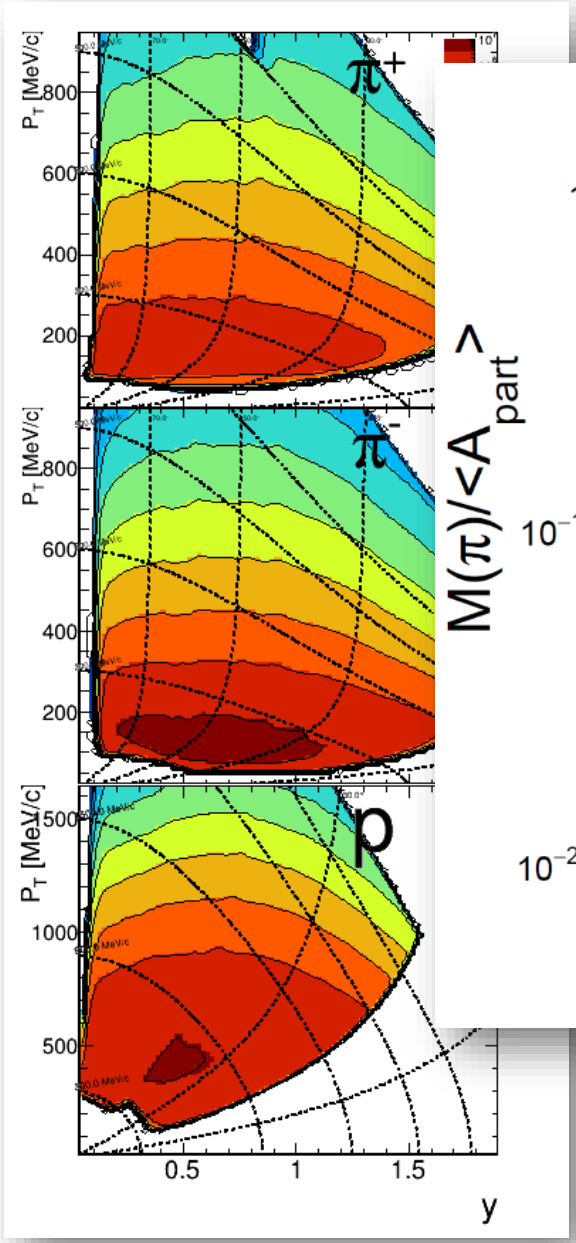

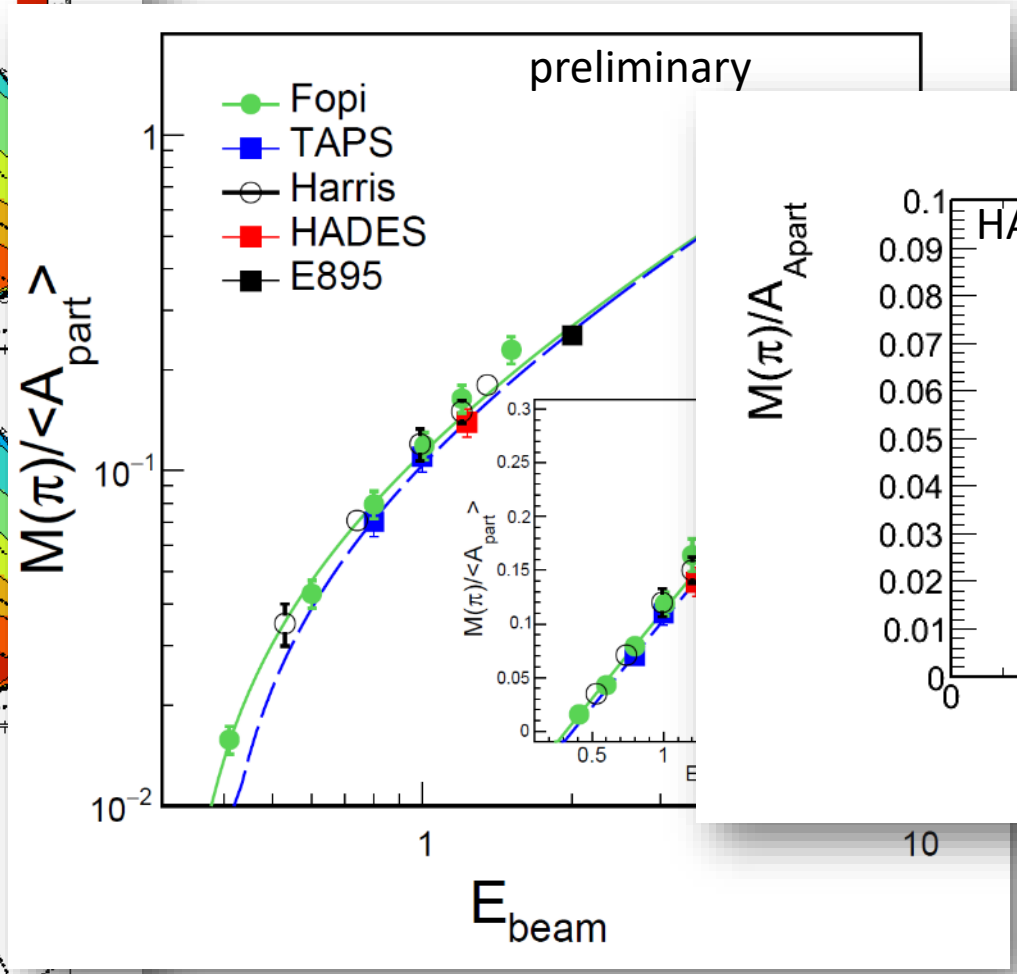

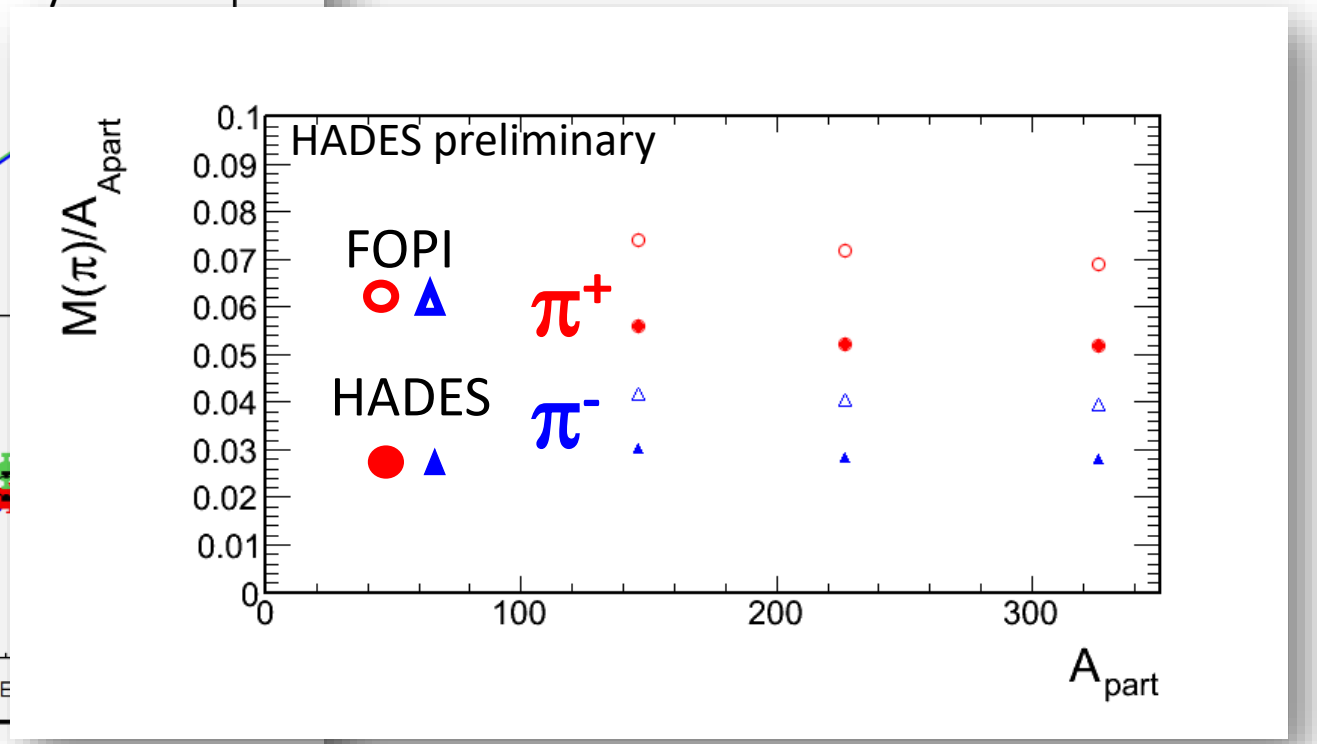

- ~Linear dependence as a function of $\langle A_{part} \rangle$
- Difference in yield by about 25% w.r.t FOPI results

g.kornakov@gsi.de

Charge pion multiplicities: comparison to models

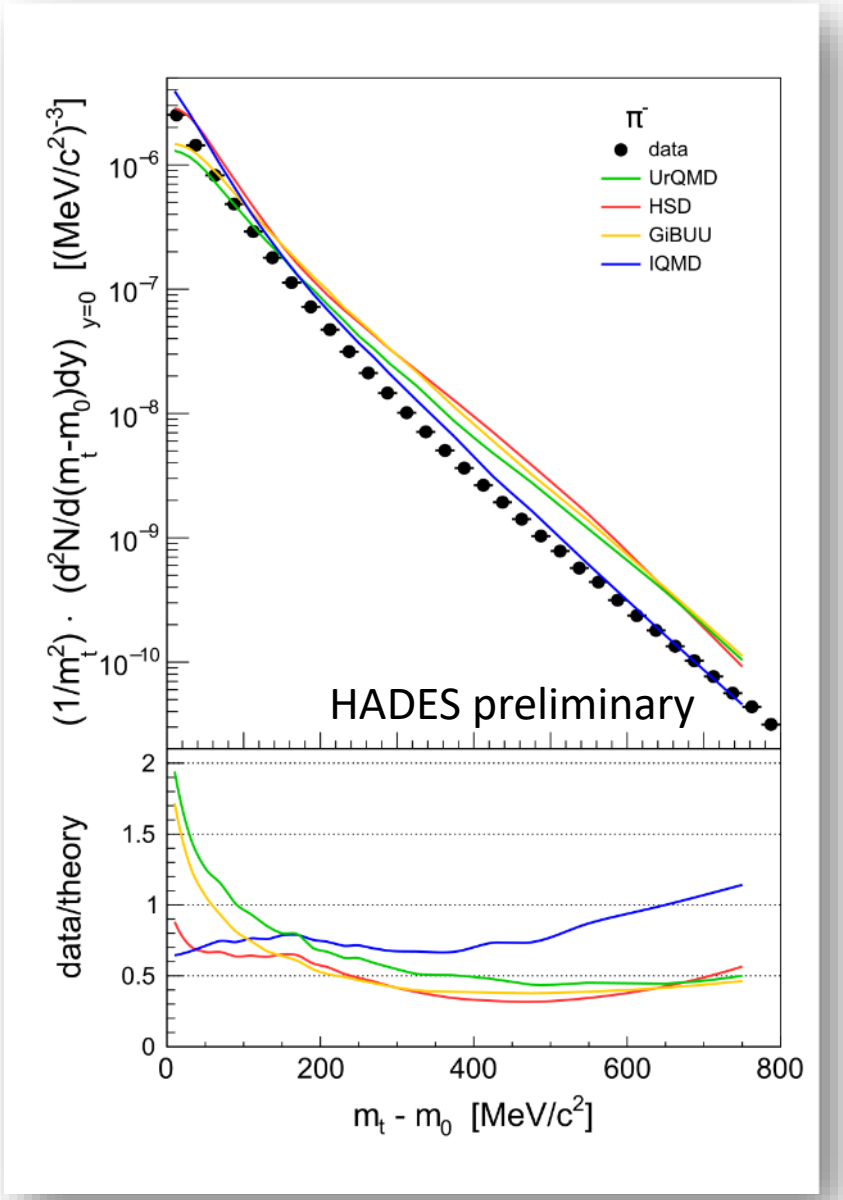

- Au+Au 0-10%
- Mid-rapidity

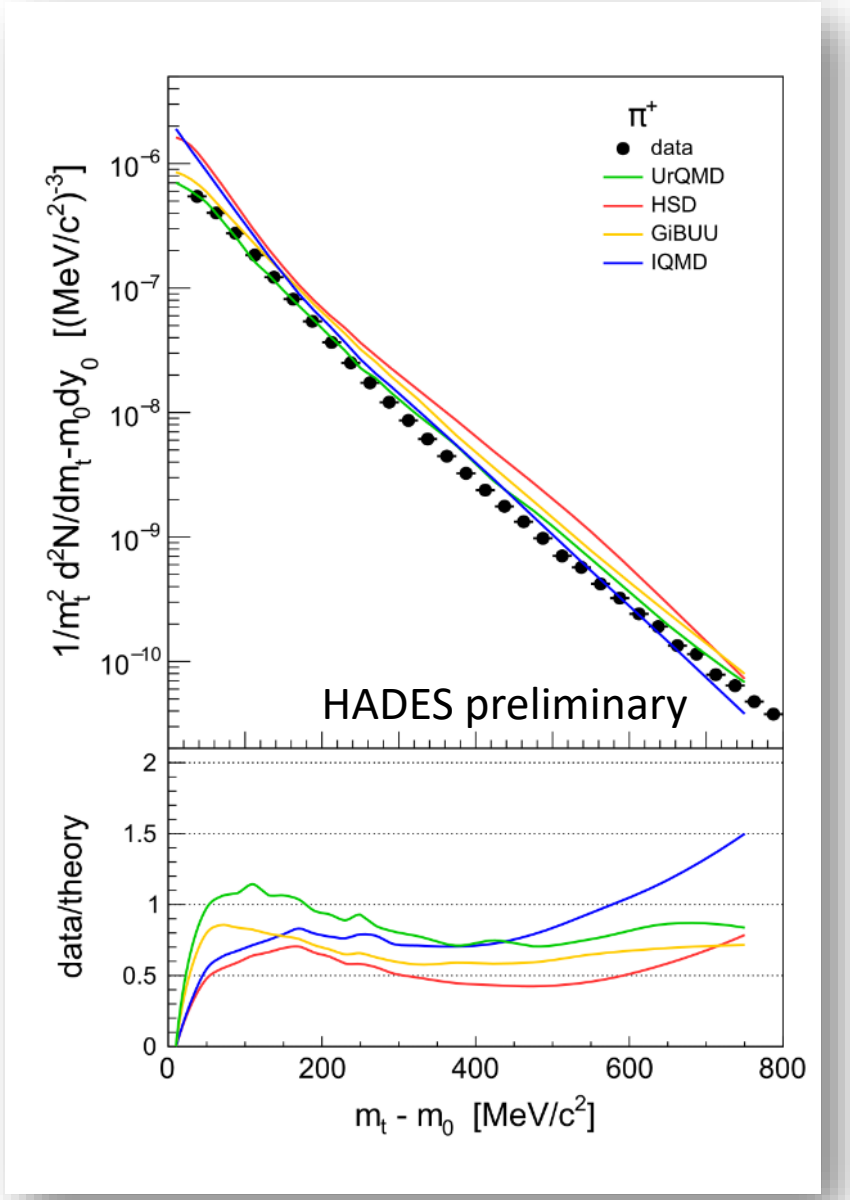

g.kornakov@gsi.de

Charge pion multiplicities: comparison to models

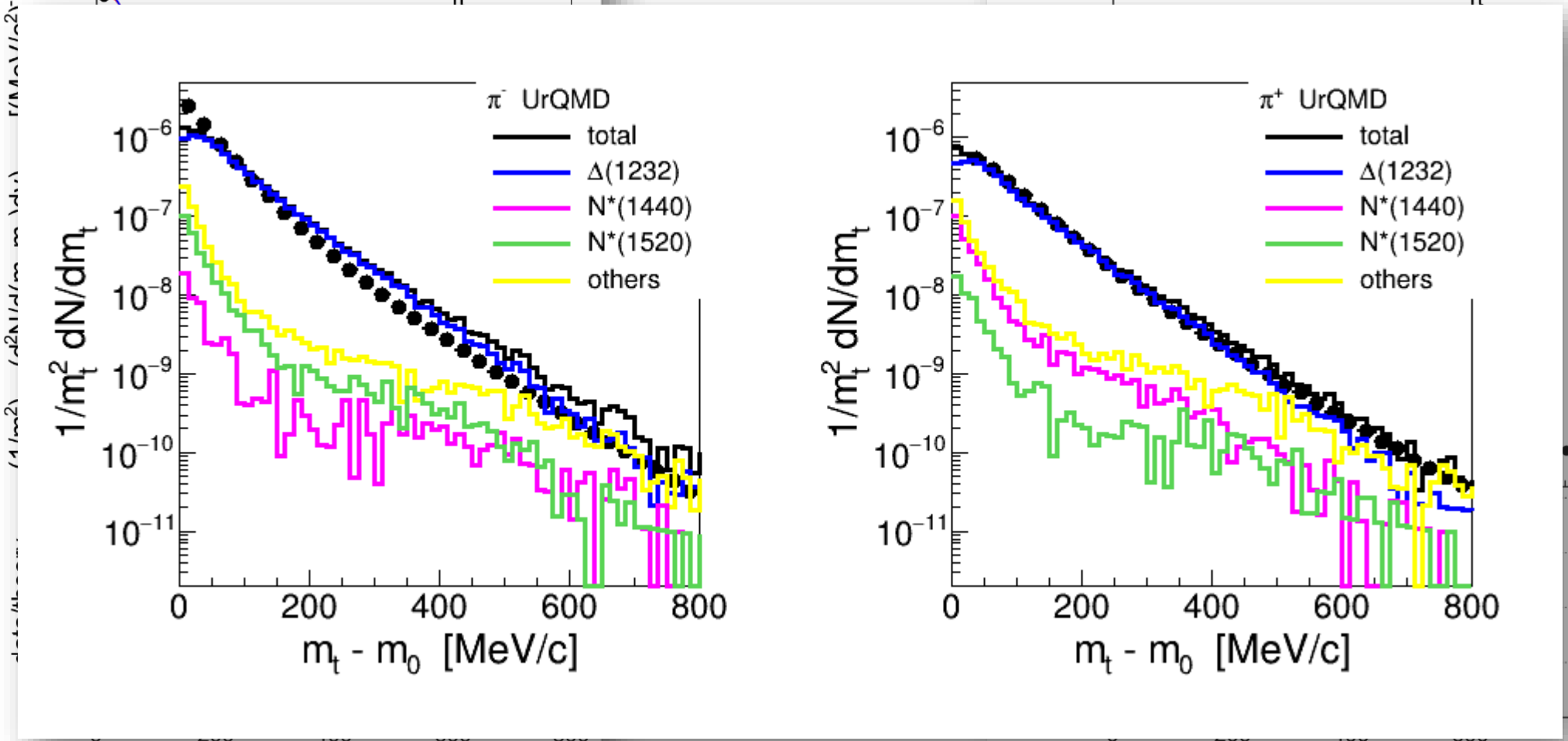

Strangeness measurement: K^0_s and Λ

HADES Collab., arXiv:1812.07304

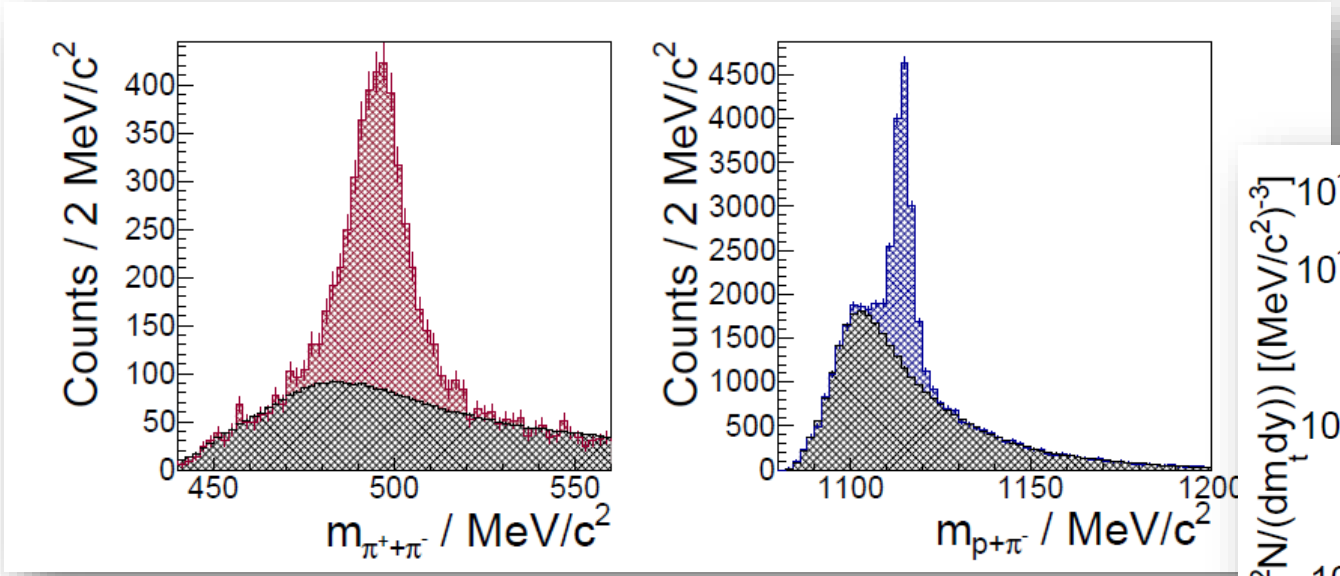

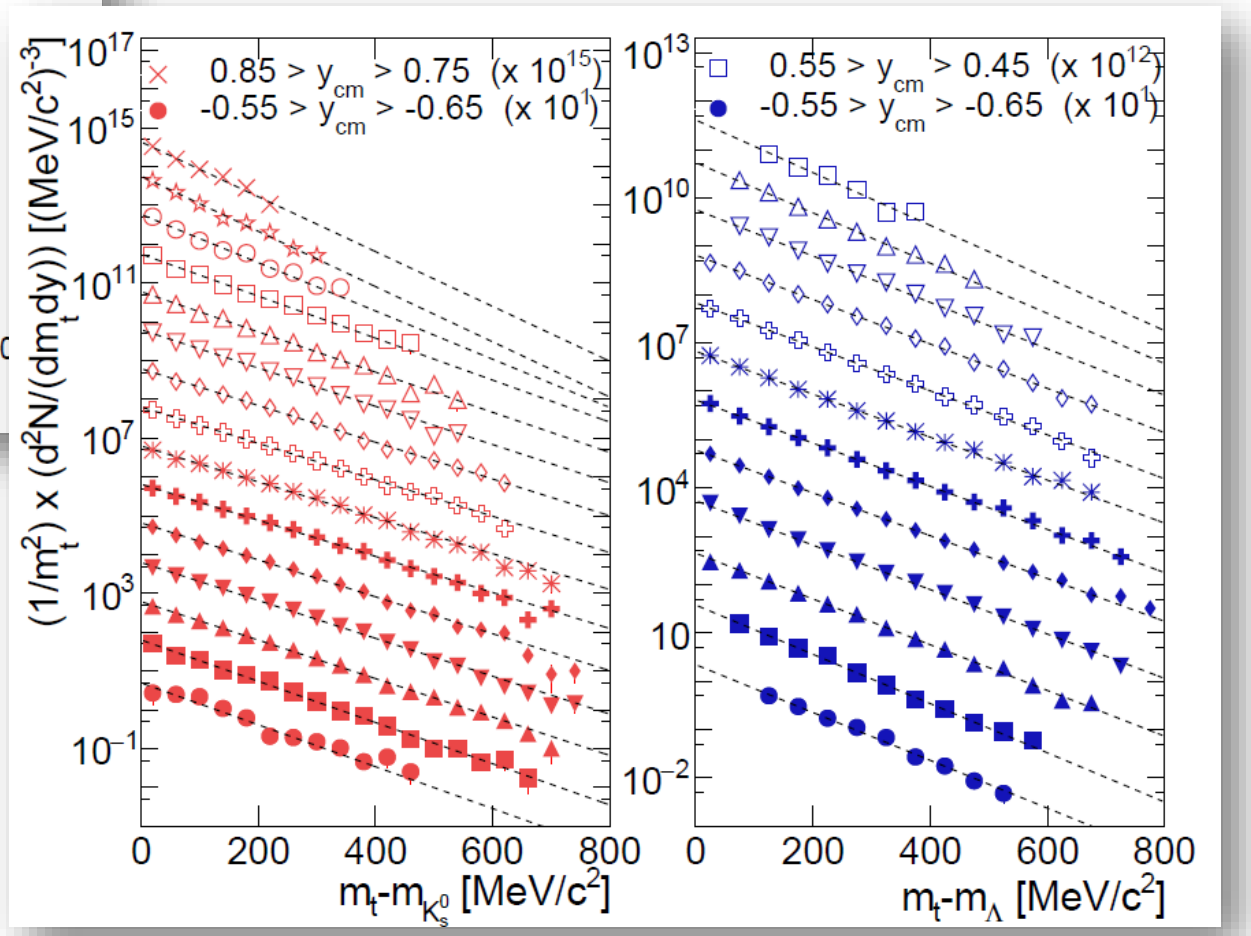

Strangeness measurement: K^0_s , Λ, K^+, K^-, ϕ

HADES Collab., arXiv:1812.07304

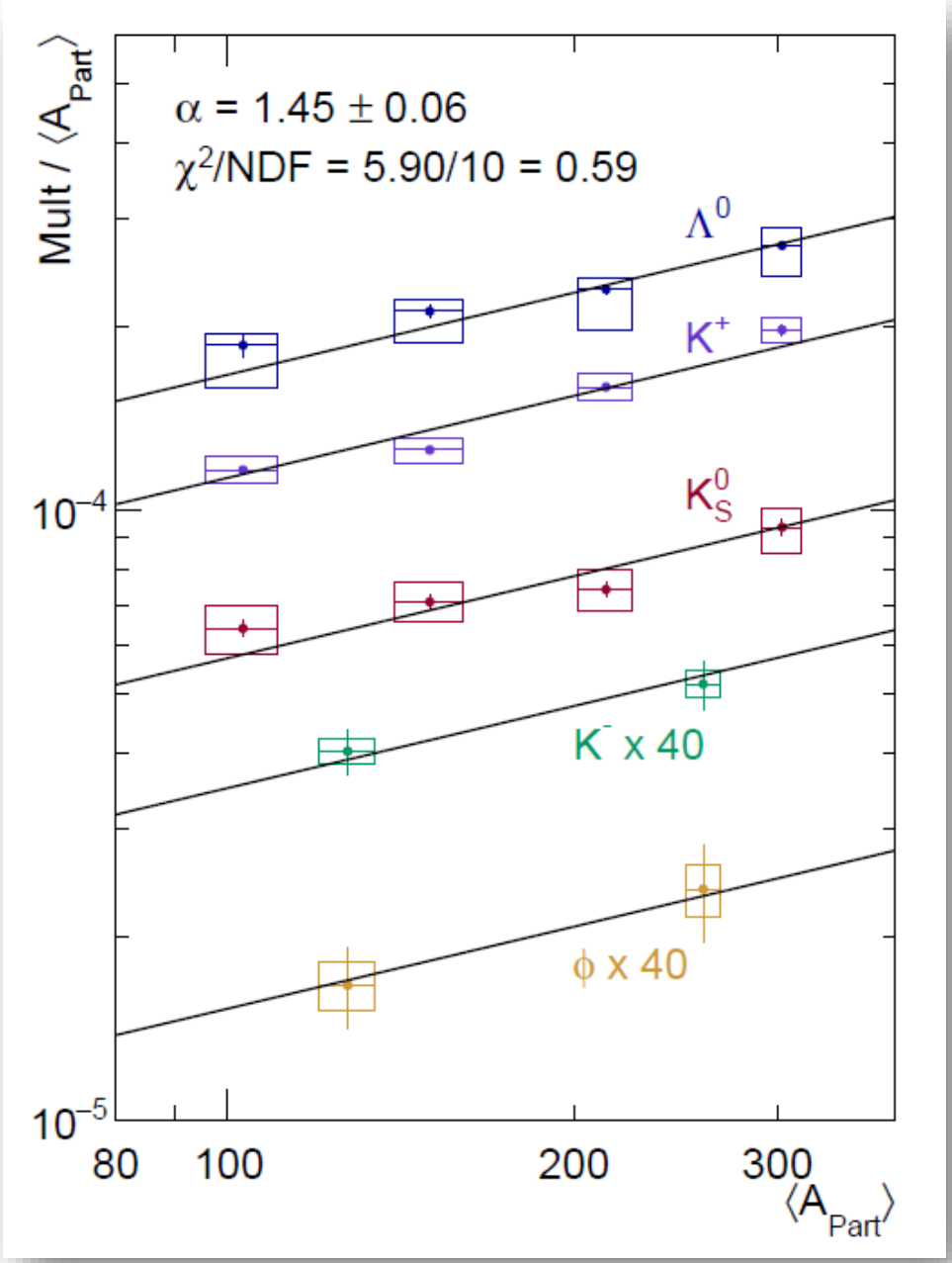

- Universal scaling with A_{part}
- Production in sequential nucleon-nucleon collisions should therefore be revisited.

g.kornakov@gsi.de

Strangeness measurement: K^0_s , Λ, K^+, K^-, ϕ

HADES Collab., arXiv:1812.07304

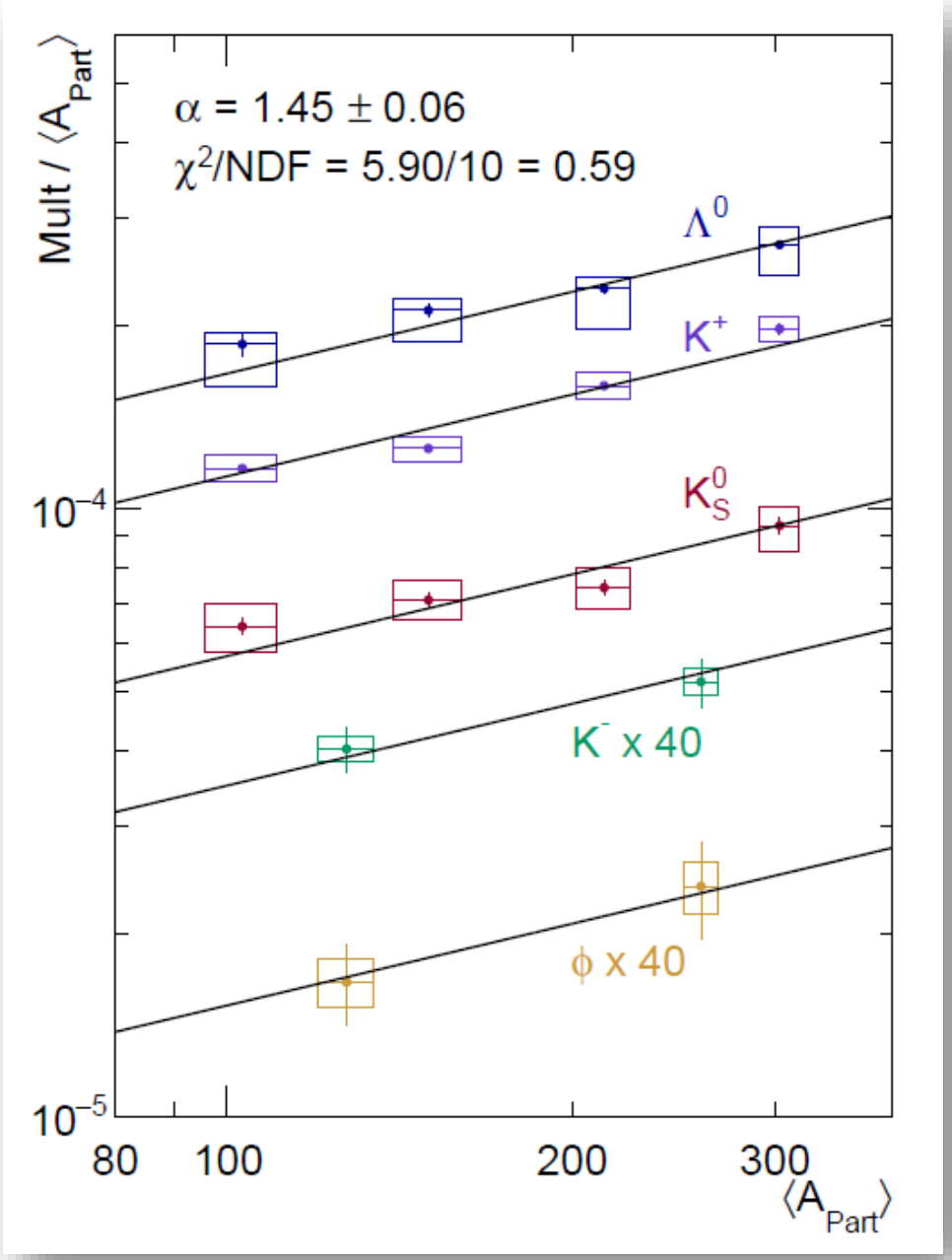

- Universal scaling with A_{part}
- Production in sequential nucleon-nucleon collisions should therefore be revisited.

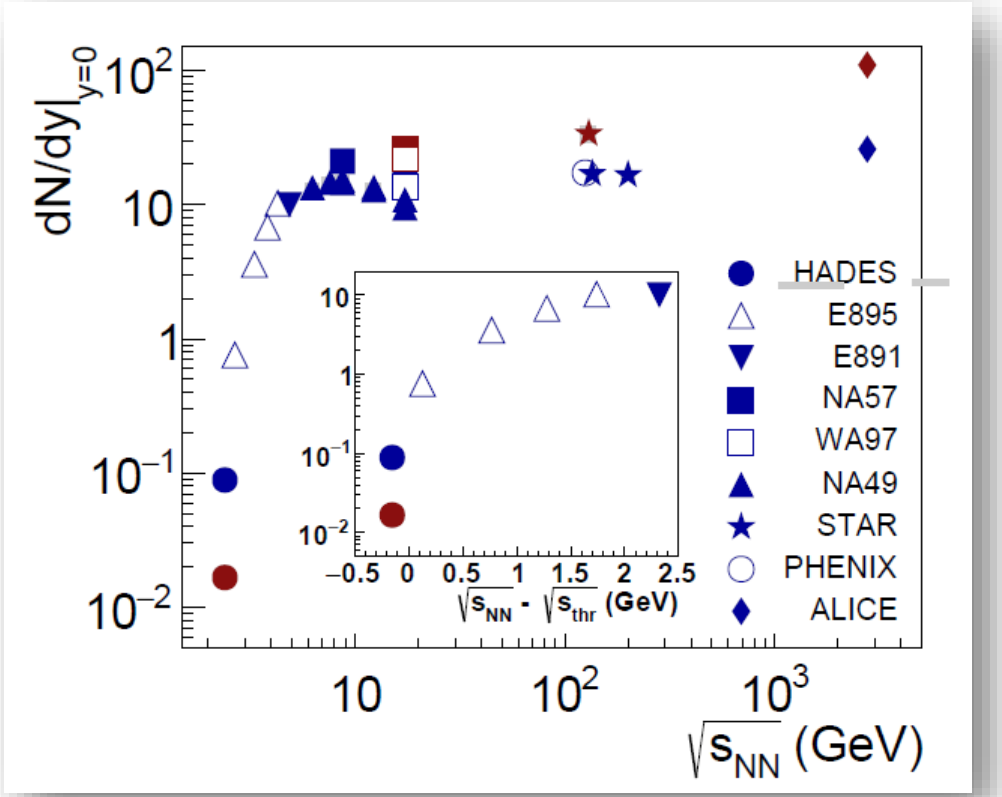

g.kornakov@gsi.de

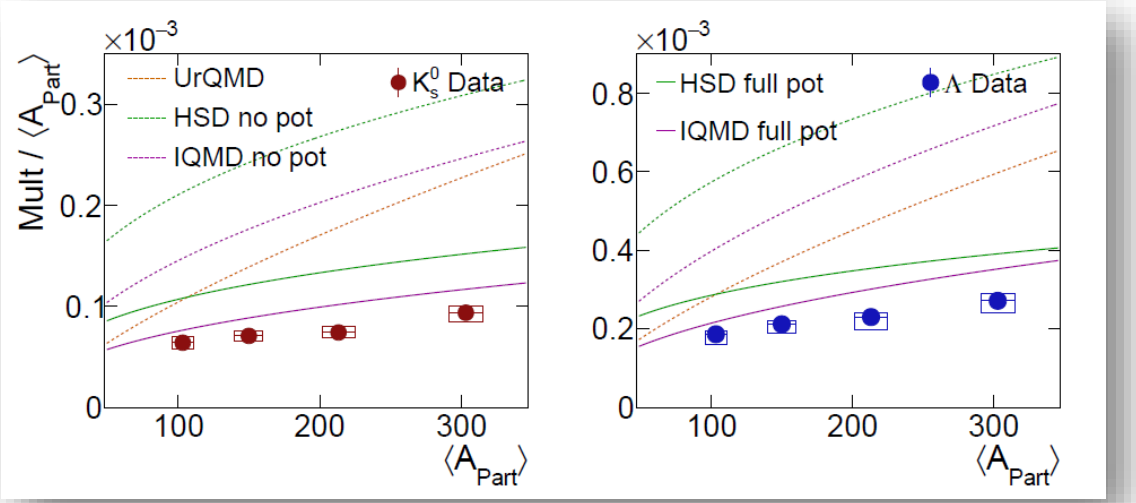

Yields, the centrality **scaling**, ***y*** and $\boldsymbol{p_T}$ spectra compared to transport models does not yet lead to a consistent picture.

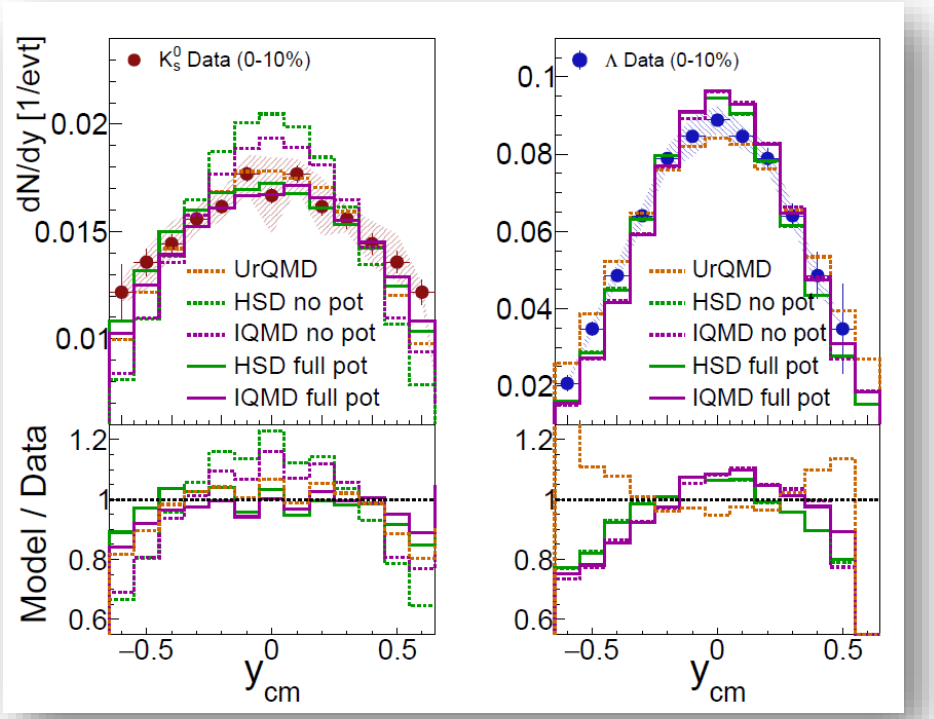

- IQMD + KN repulsive potential → closest to the data (10%)
- HSD & IQMD: Kaon *y* distribution well described including KN repulsive potential.
- UrQMD (intermediate resonances, no potential) describes *y* and p_T, fails to describe the yield and centrality scaling.

g.kornakov@gsi.de

Measuring two particle correlations in πA and AA collisions

g.kornakov@gsi.de

The iterative method

G.K. and T. Galatyuk, arXiv:1808.05466 [physics.data-an].

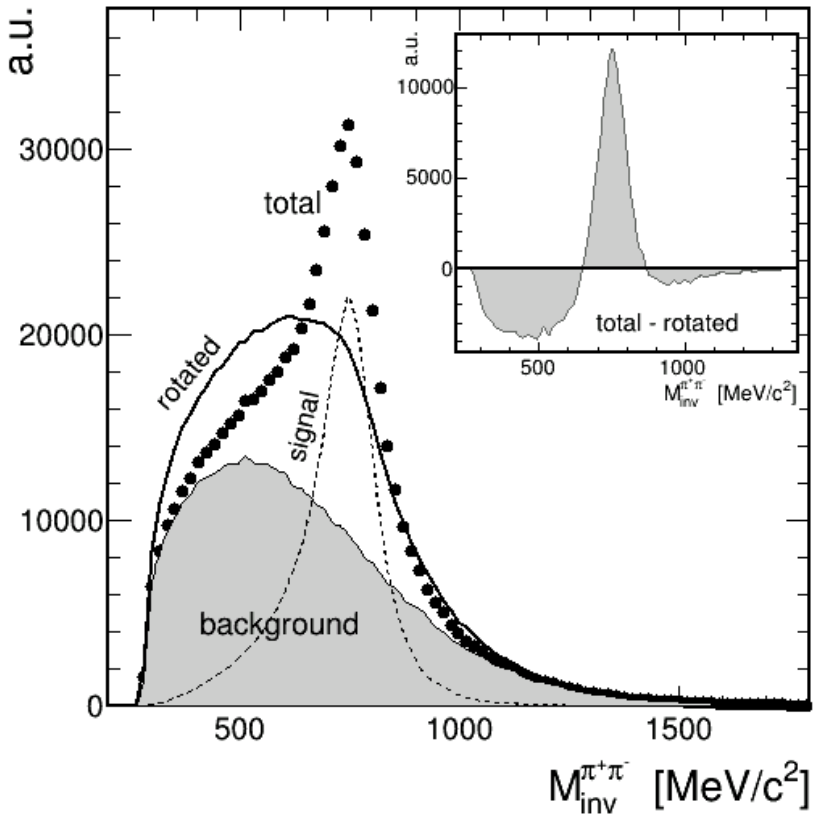

"Signal particles are used to produce the combinatorial background together with uncorrelated particles having, in general, different kinematics."

Unknown signal demands:

- Iterative approach. Every signal hypothesis improves the next reconstruction until convergence.
- Typify the properties of the combinatorial background different from signal: internal symmetries.
- Produce the contribution of the signal particles to the combinatorial background.

Statistical bootstrap: tailoring the distributions

Starting point: random ϕ rotation

Single particle distributions → Time-dependent single particle → Correlation to reaction plane → Pair efficiency scaling

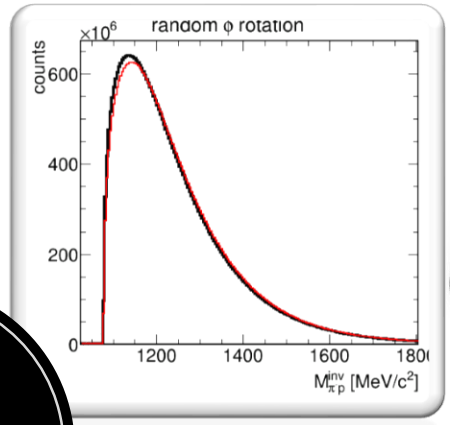

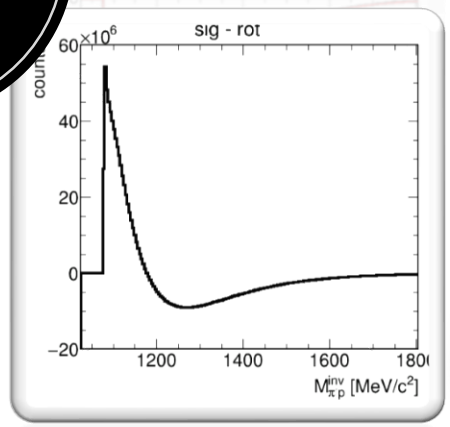

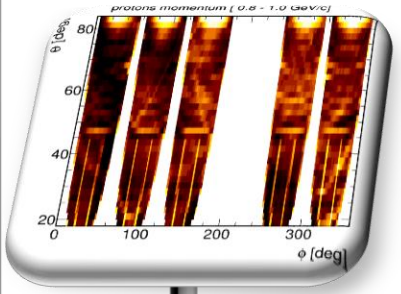

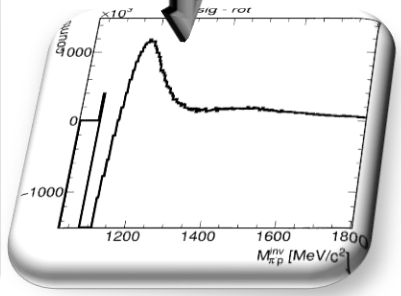

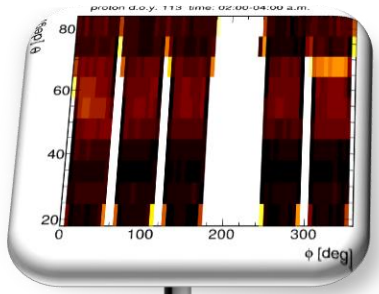

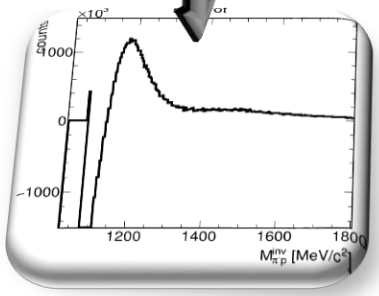

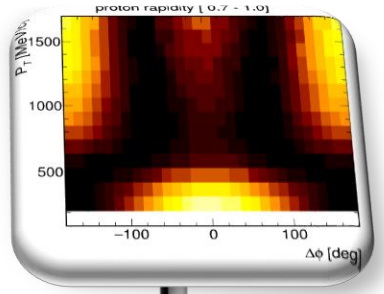

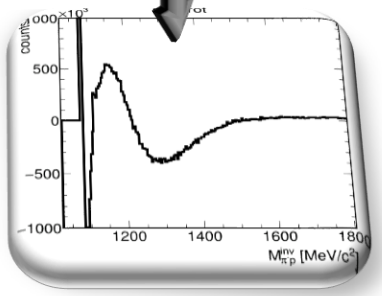

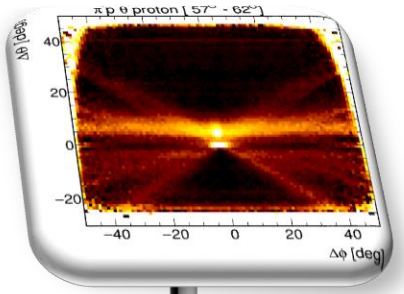

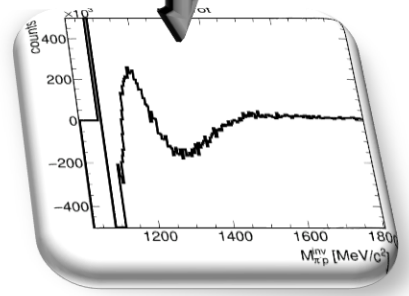

g.kornakov@gsi.de

Inclusive reconstruction: π^-(1.7 GeV/c)+ C

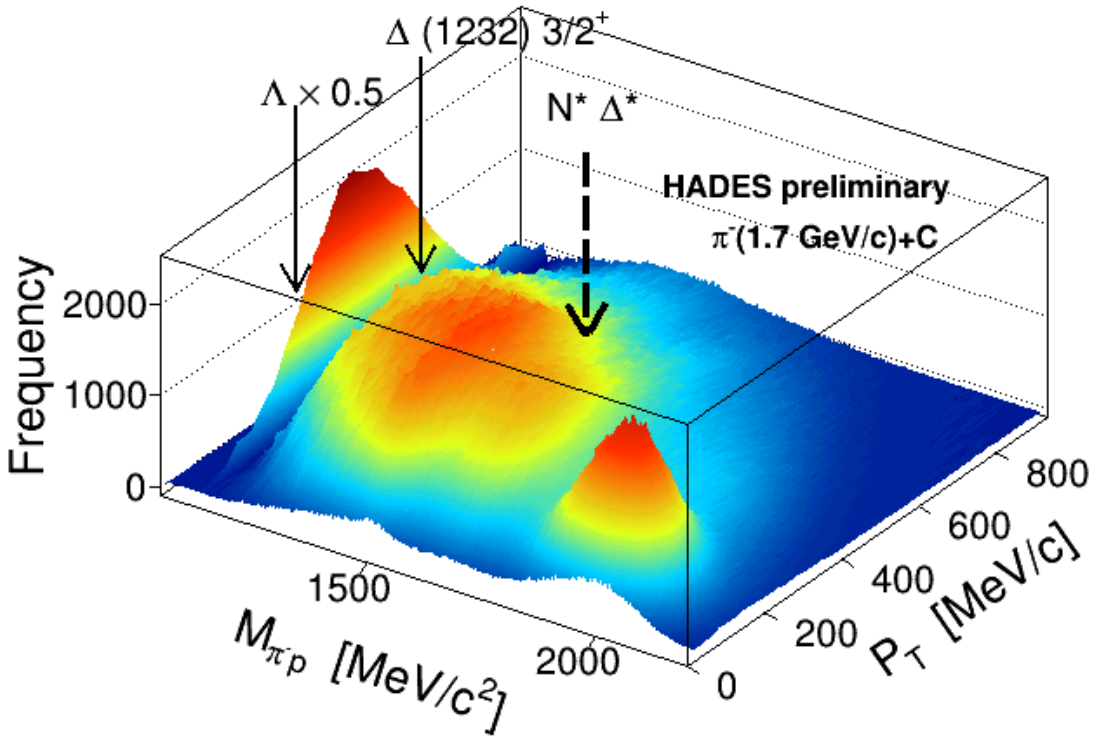

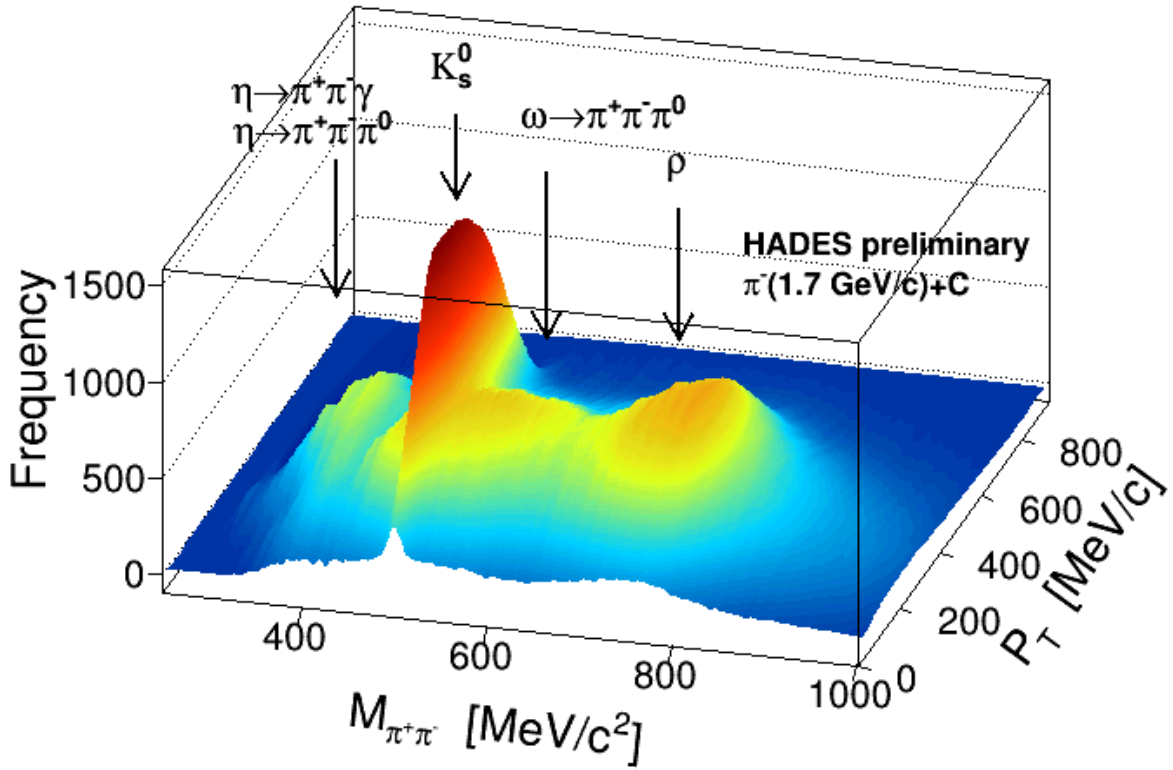

g.kornakov@gsi.de

Inclusive reconstruction: Au+Au at $\sqrt{s_{NN}} = 2.42\ GeV$

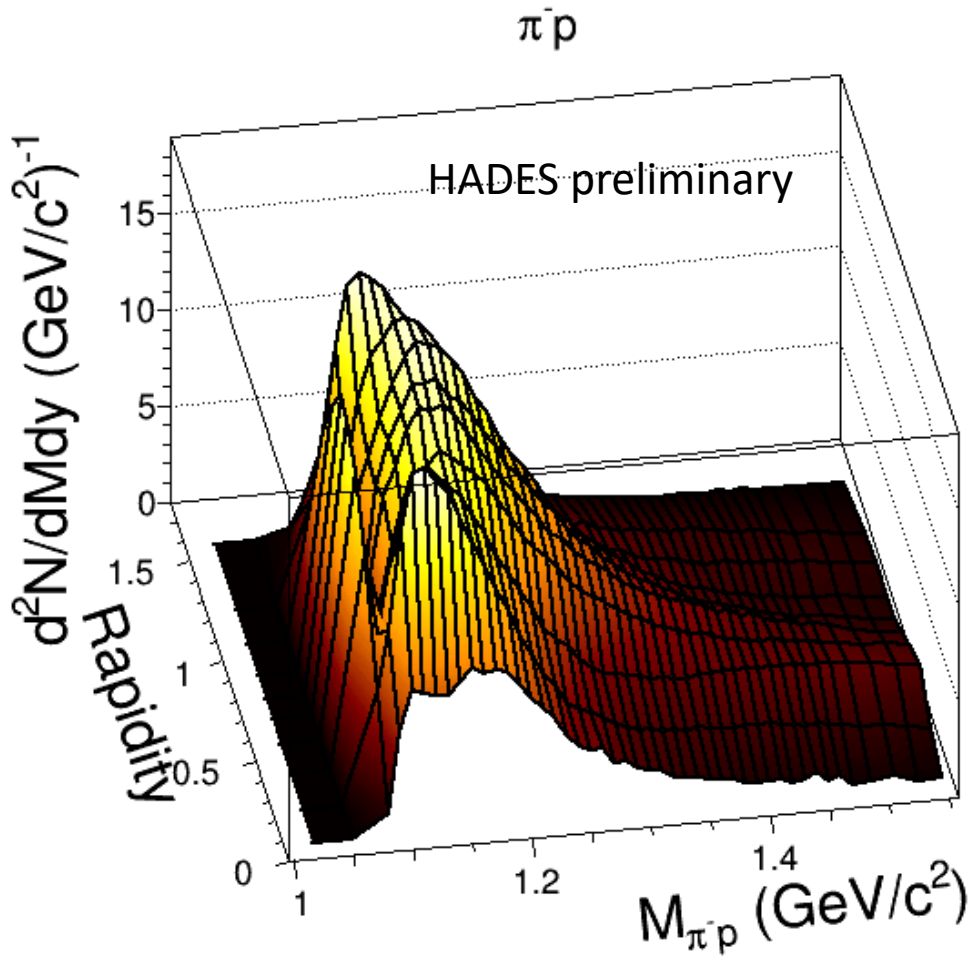

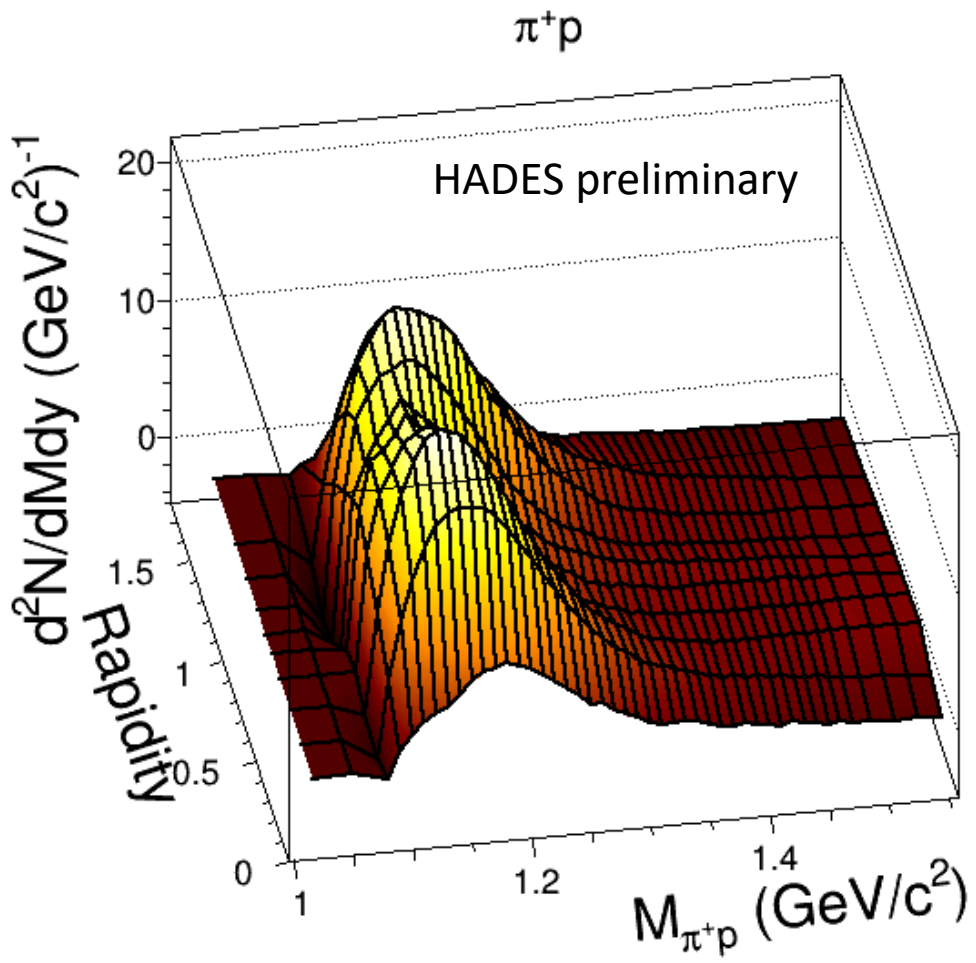

g.kornakov@gsi.de

Inclusive reconstruction: Au+Au at $\sqrt{s_{NN}} = 2.42\ GeV$

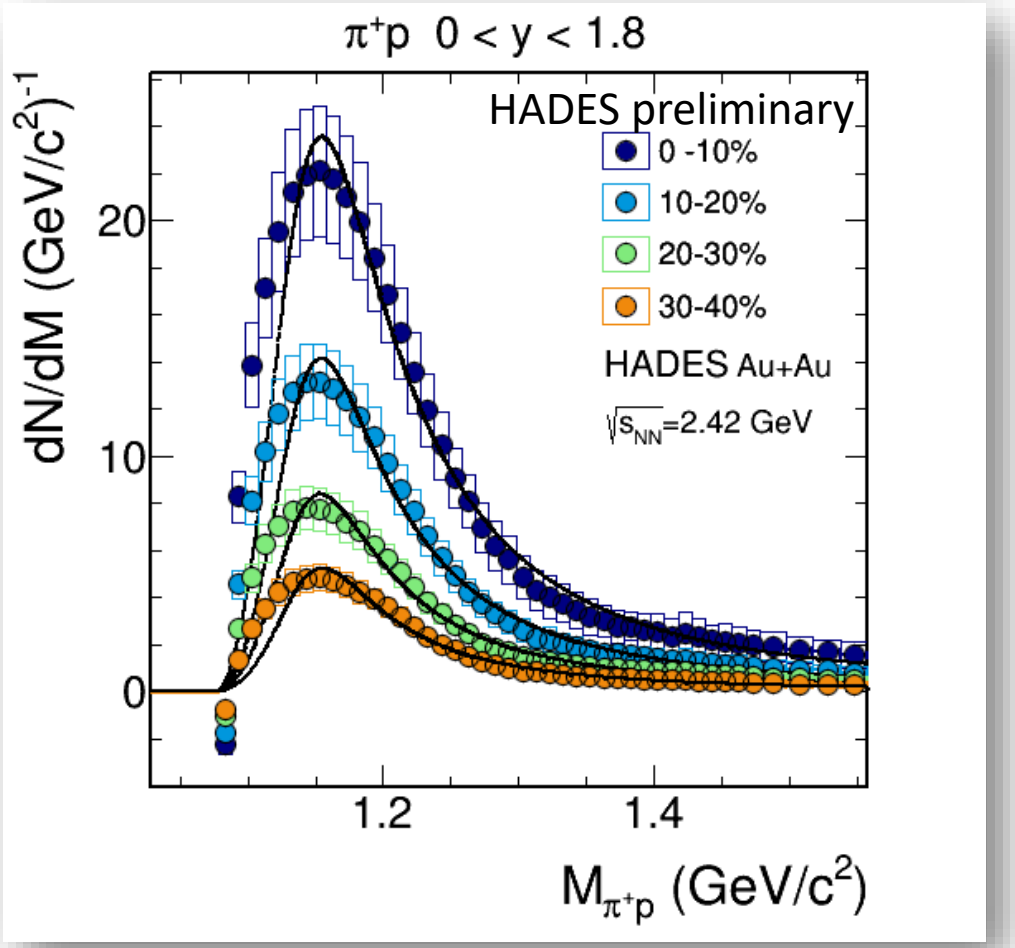

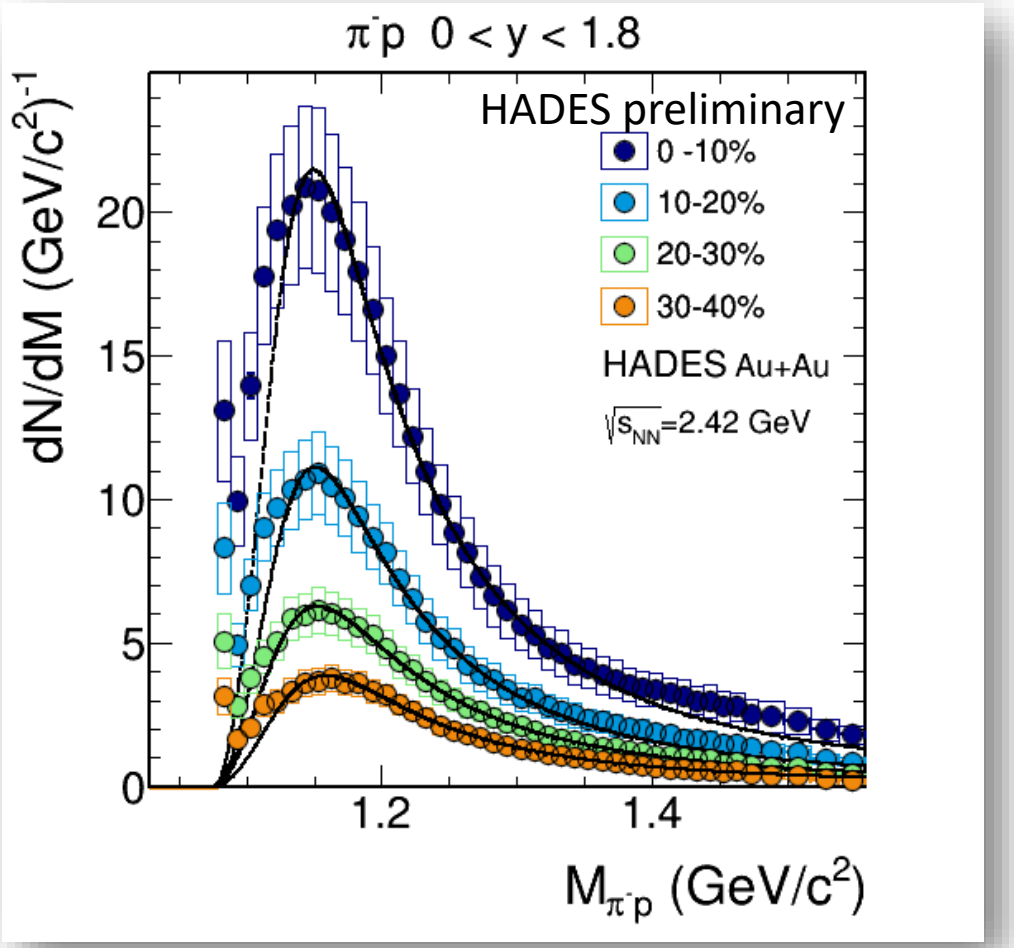

g.kornakov@gsi.de

Inclusive reconstruction: Au+Au at $\sqrt{s_{NN}} = 2.42\ GeV$

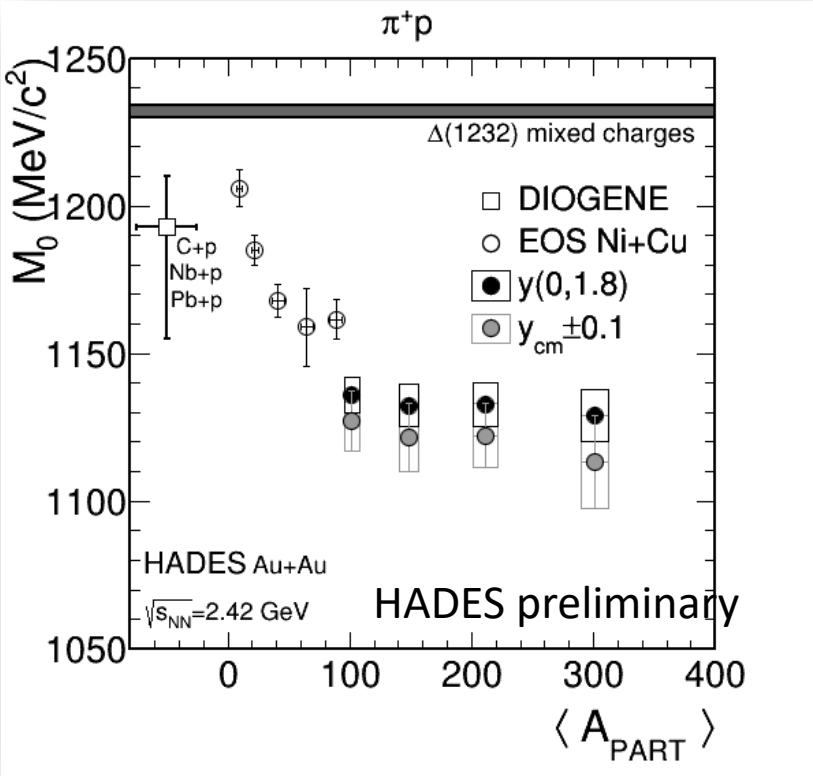

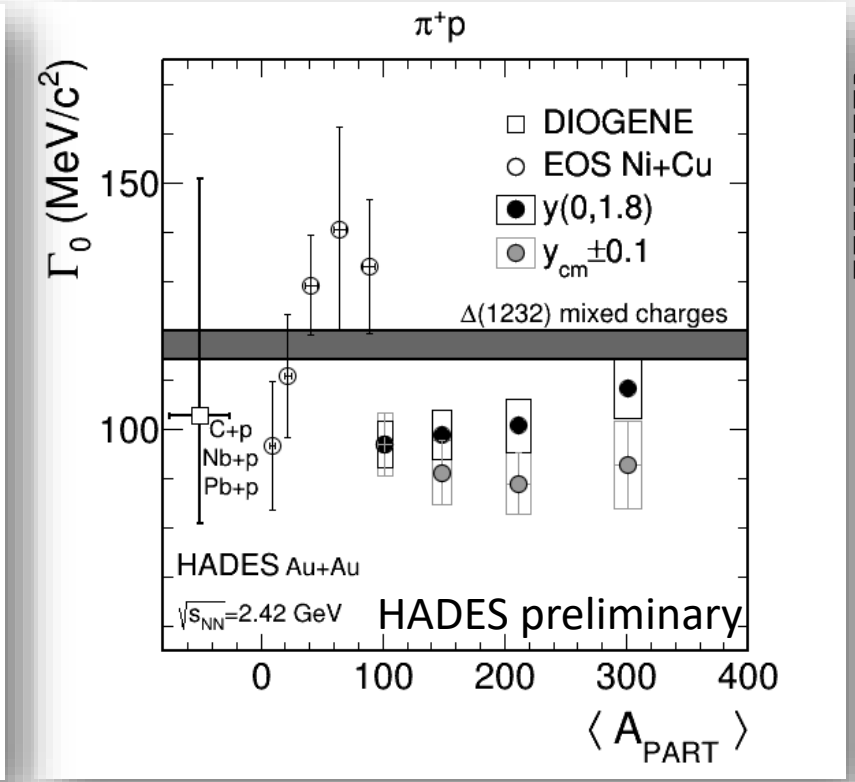

$$\sigma(\mathrm{M}) = a\frac{q^3}{q^3 + 180^3}\frac{1}{4\left(\frac{M - M_0}{\Gamma_0}\right)^2 + 1}$$

$$q = \sqrt{\frac{\left(M^2 - \left(M_p + M_\Pi\right)^2\right)\left(M^2 - \left(M_p - M_\Pi\right)^2\right)}{4M^2}}$$

g.kornakov@gsi.de

[EOS] Phys. Rev. Lett. 79, 4345-4348 (1997), E. L. Hjort et al

Inclusive reconstruction: Au+Au at $\sqrt{s_{NN}} = 2.42\ GeV$

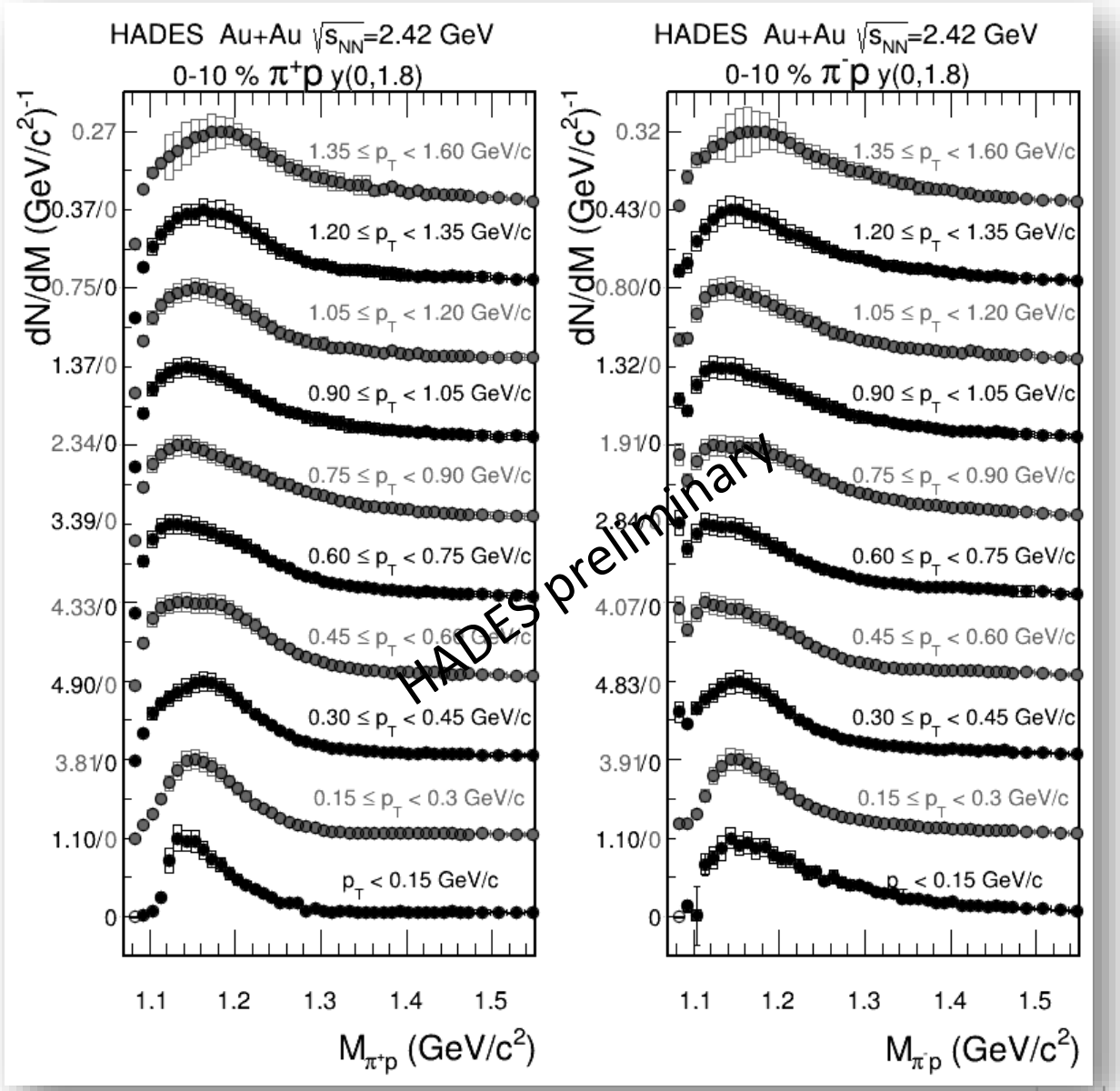

Dependence of the most probable mass with pair p_T

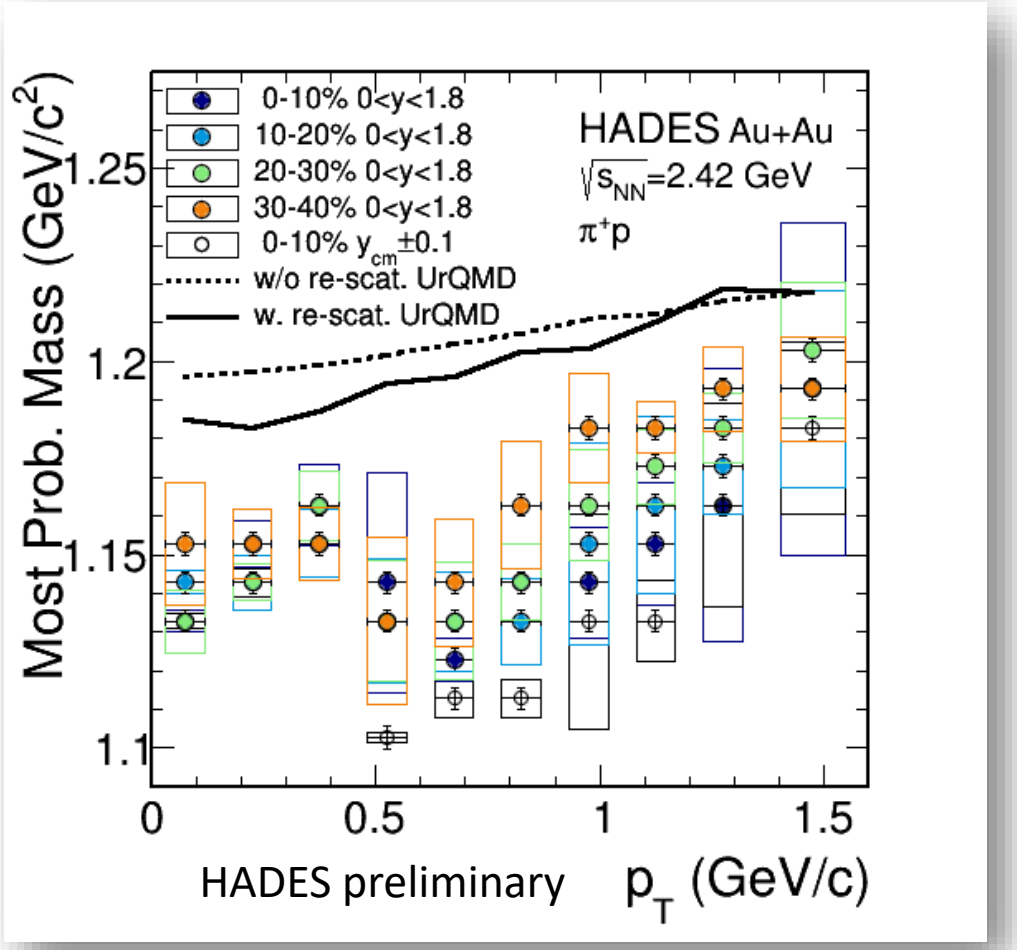

Inclusive reconstruction: Au+Au at $\sqrt{s_{NN}} = 2.42\ GeV$

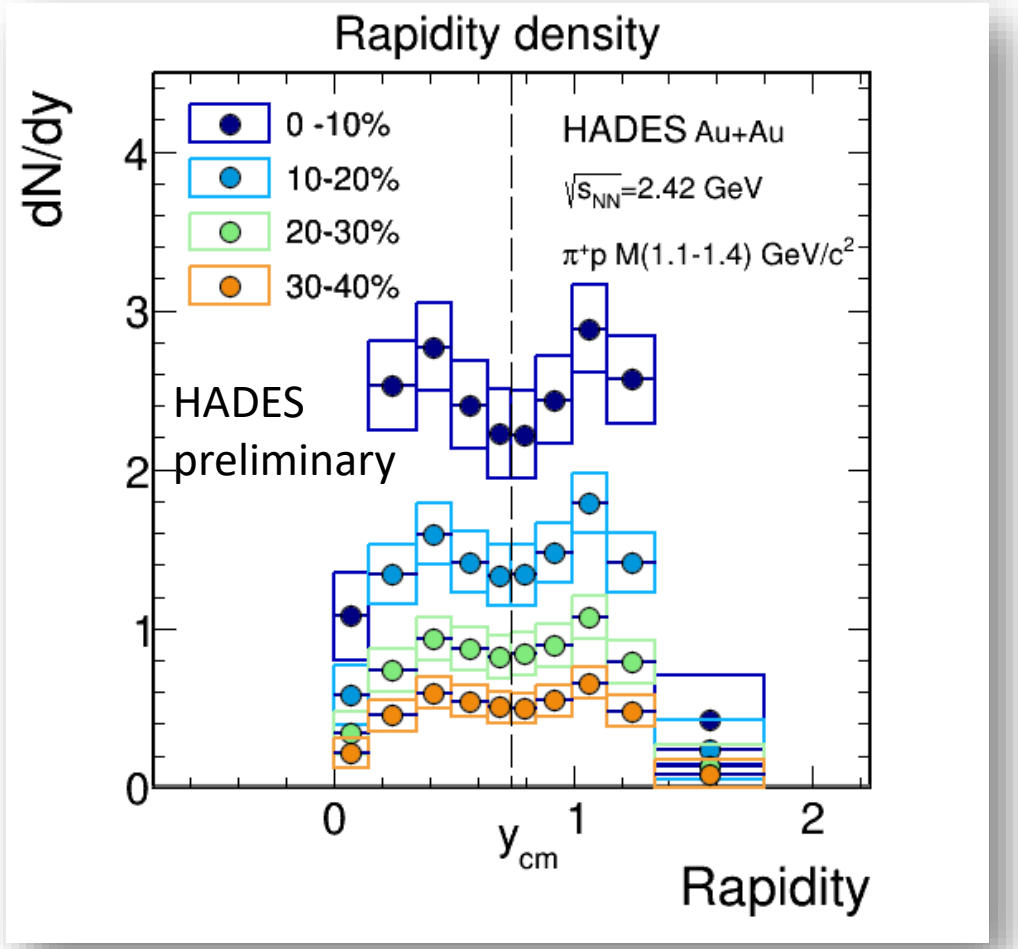

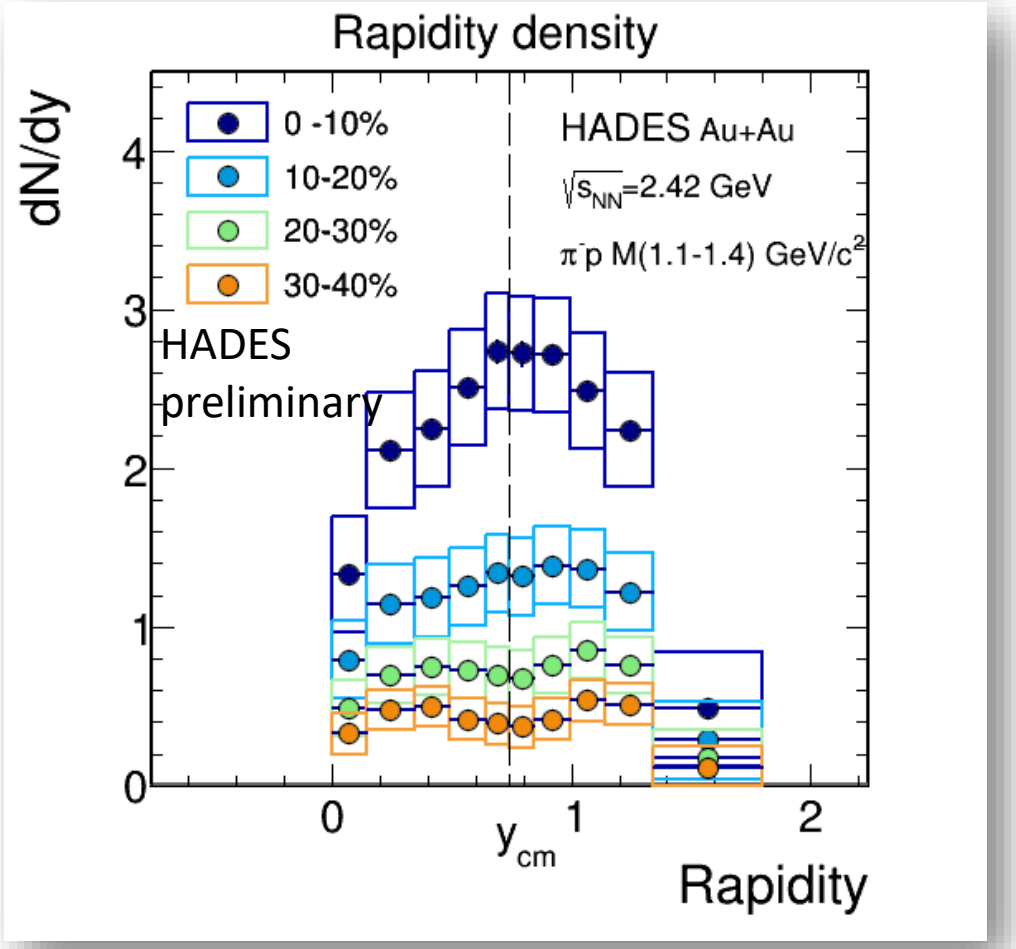

Non –trivial rapidity density distributions:

re-generation vs re-scattering

Role of isospin?

g.kornakov@gsi.de

Inclusive reconstruction: Au+Au at $\sqrt{s_{NN}} = 2.42\ GeV$

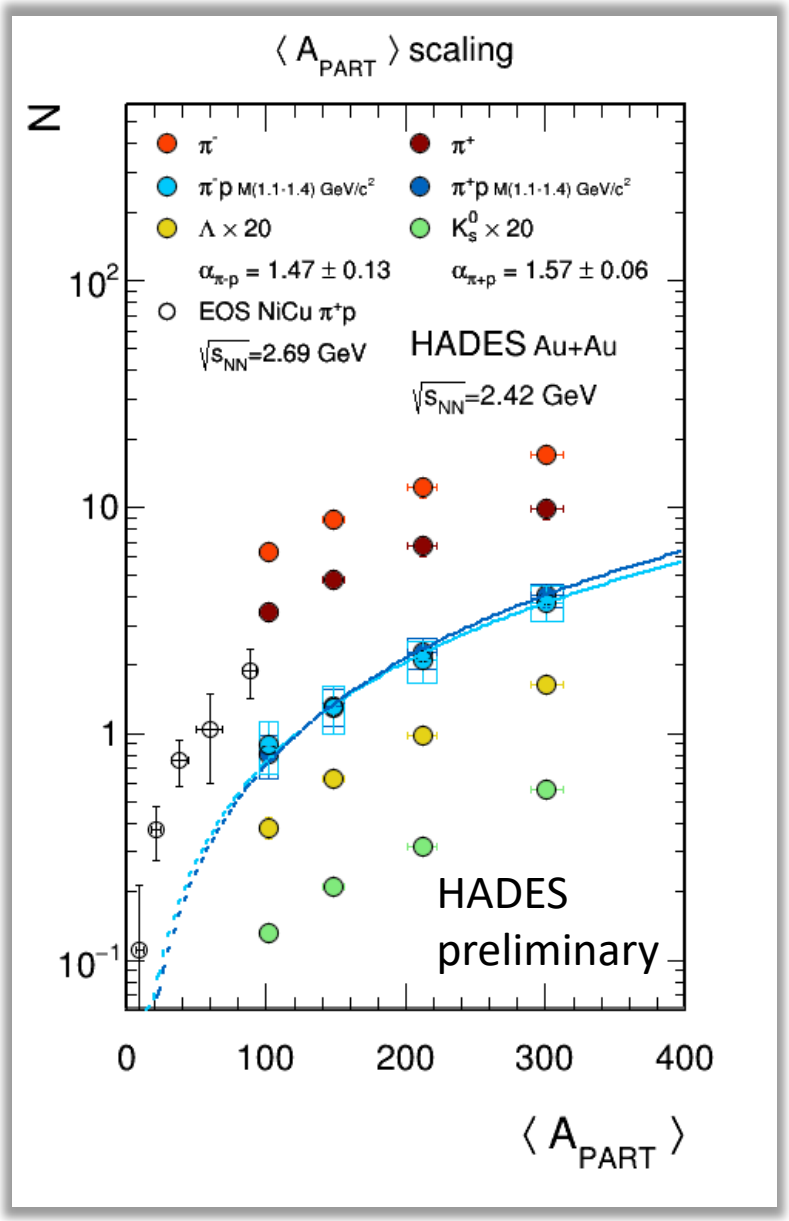

Scaling $N \propto \langle A_{part} \rangle^{\alpha}$ with parameter similar to that of strange hadrons and excess yield of virtual photons!

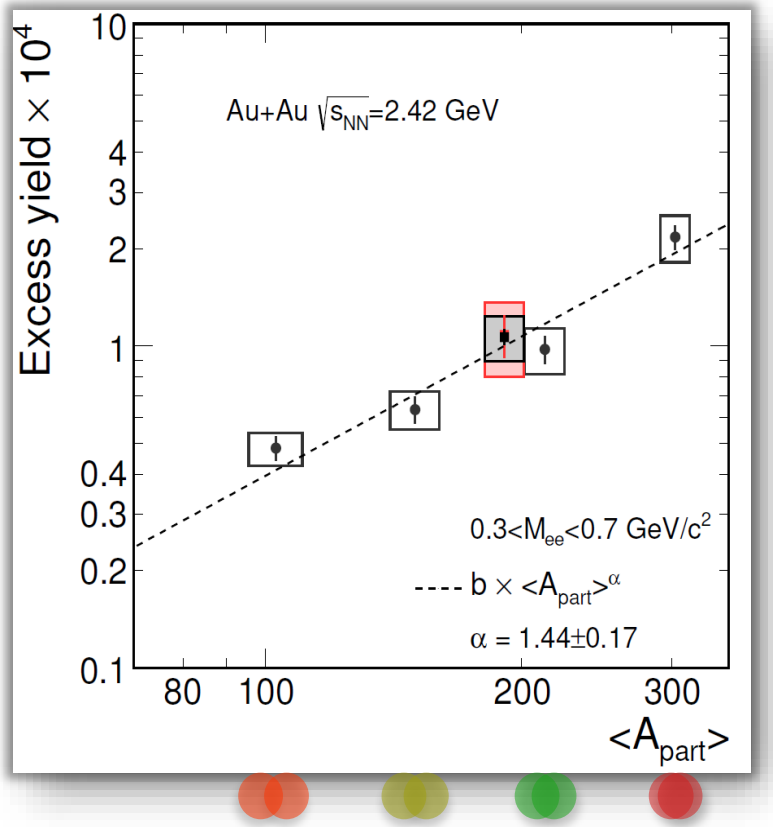

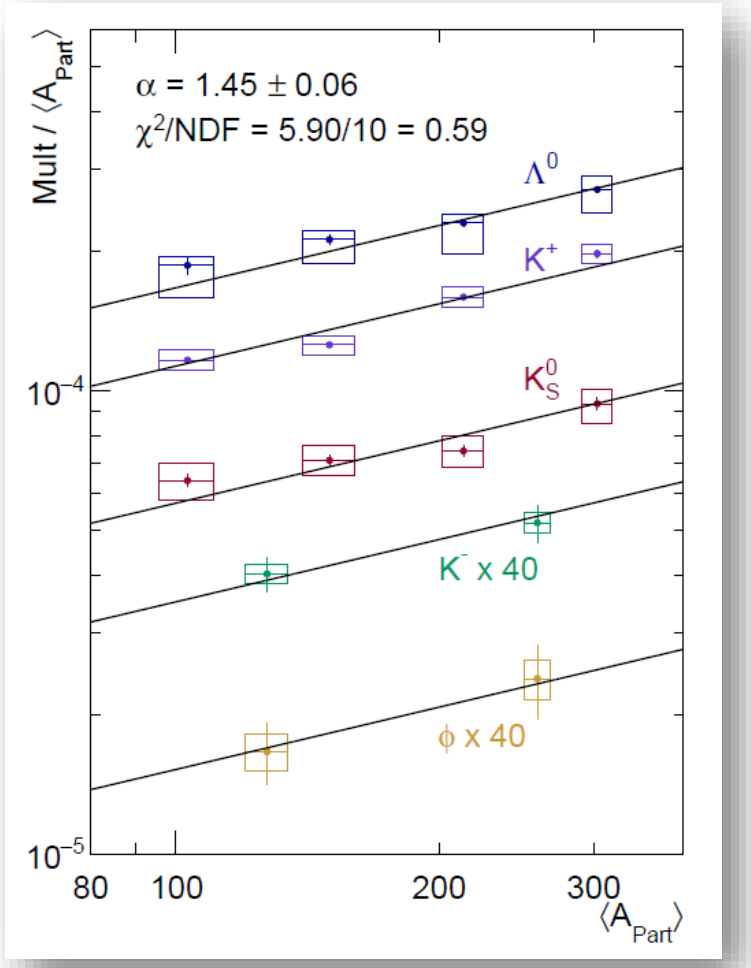

g.kornakov@gsi.de

Production of charged pions from resonances: the most ~~simple~~ abundant mesons

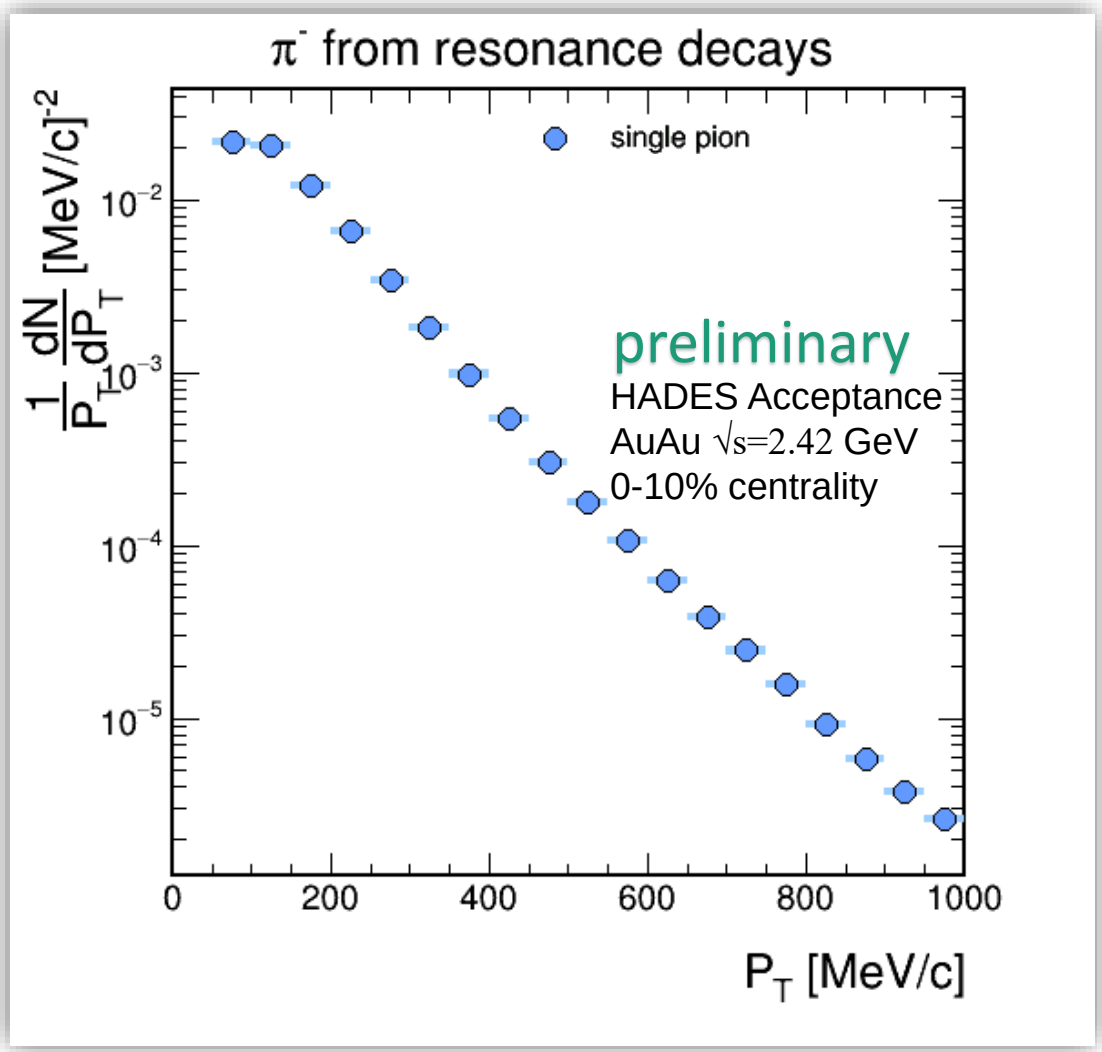

Production of charged pions from resonances: the most ~~simple~~ abundant mesons

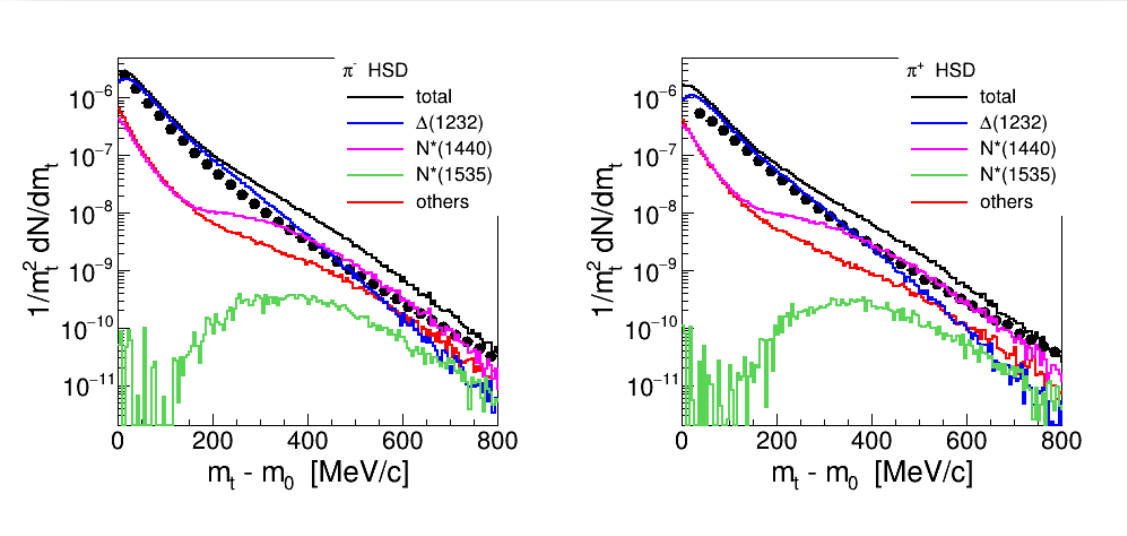

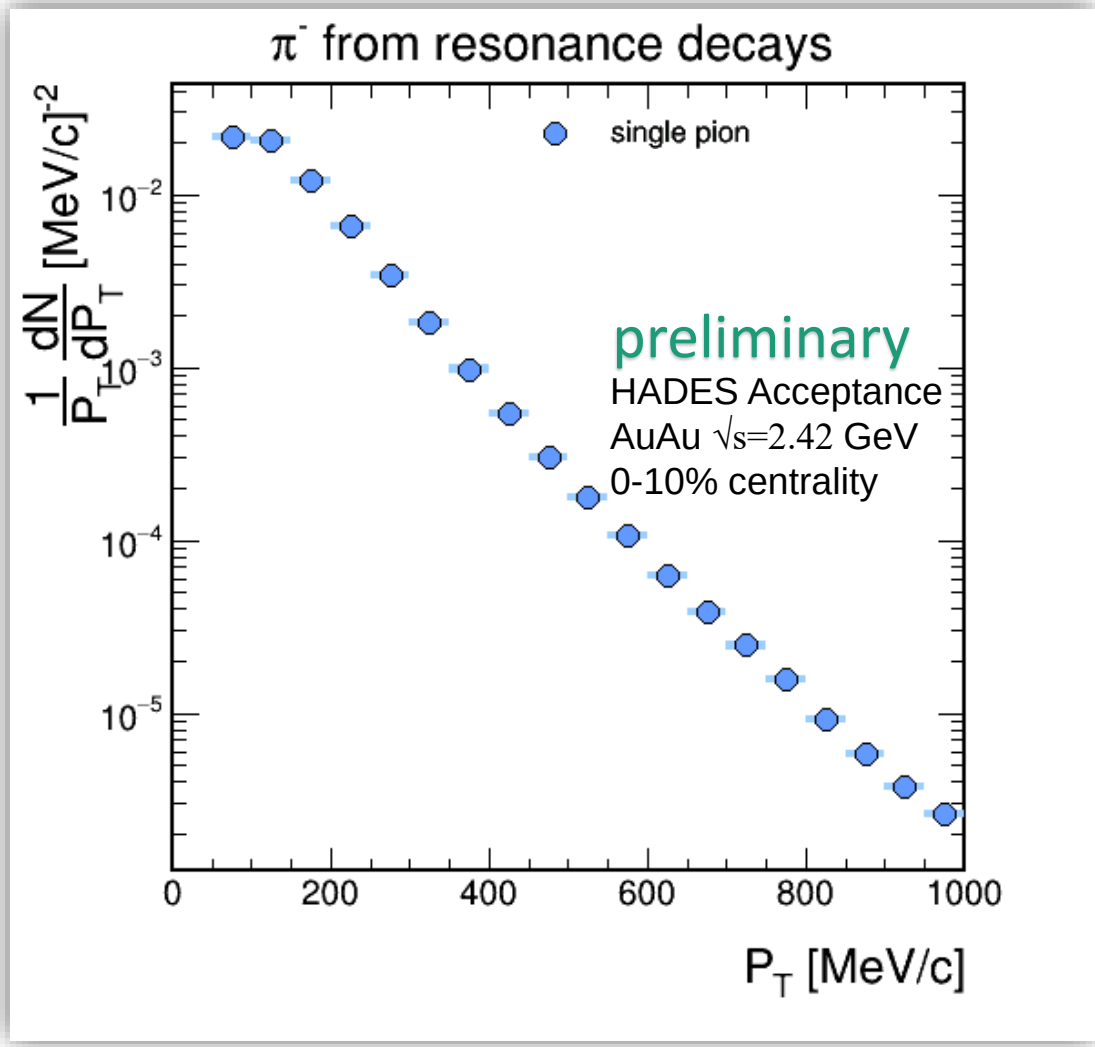

Production of charged pions from resonances: the most ~~simple~~ abundant mesons

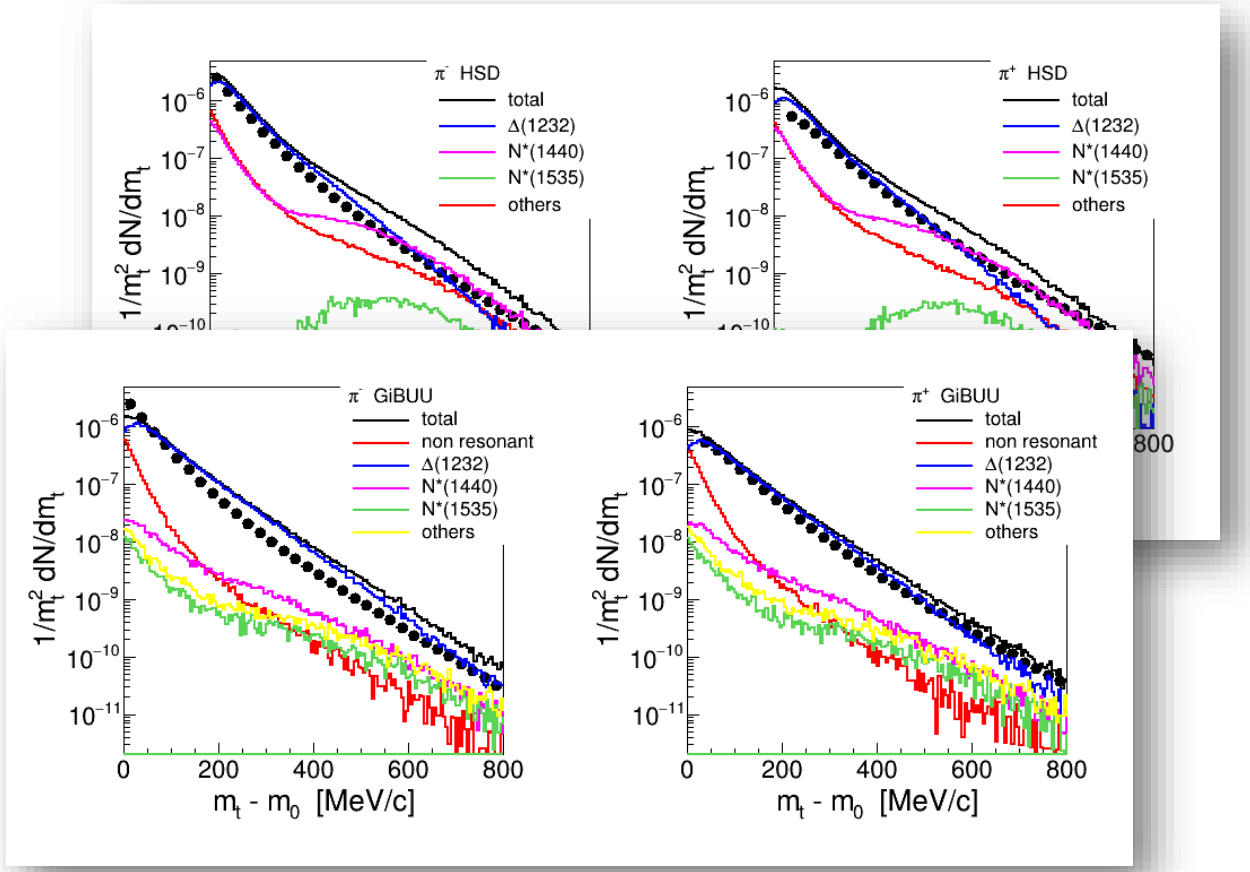

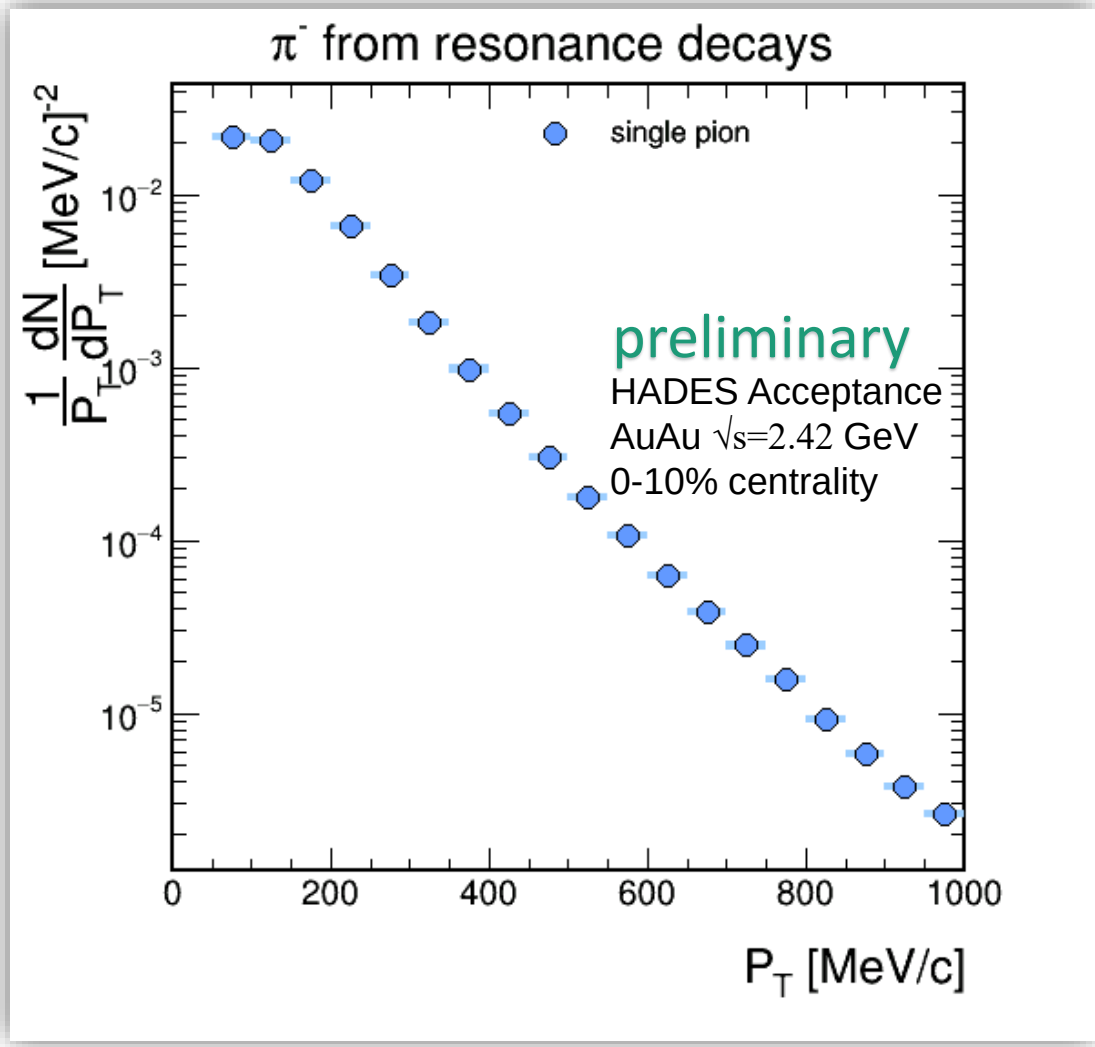

Production of charged pions from resonances: the most ~~simple~~ abundant mesons

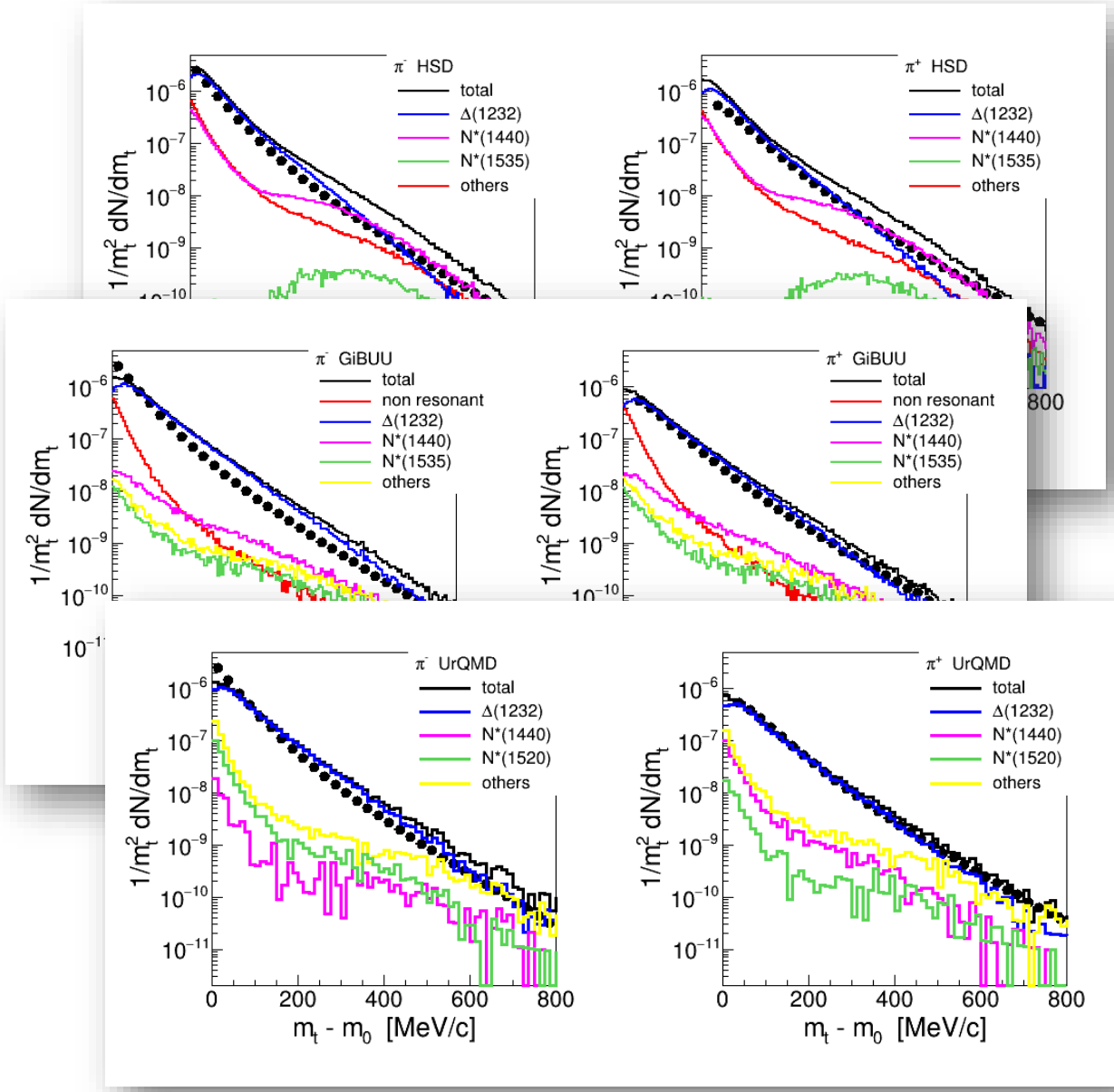

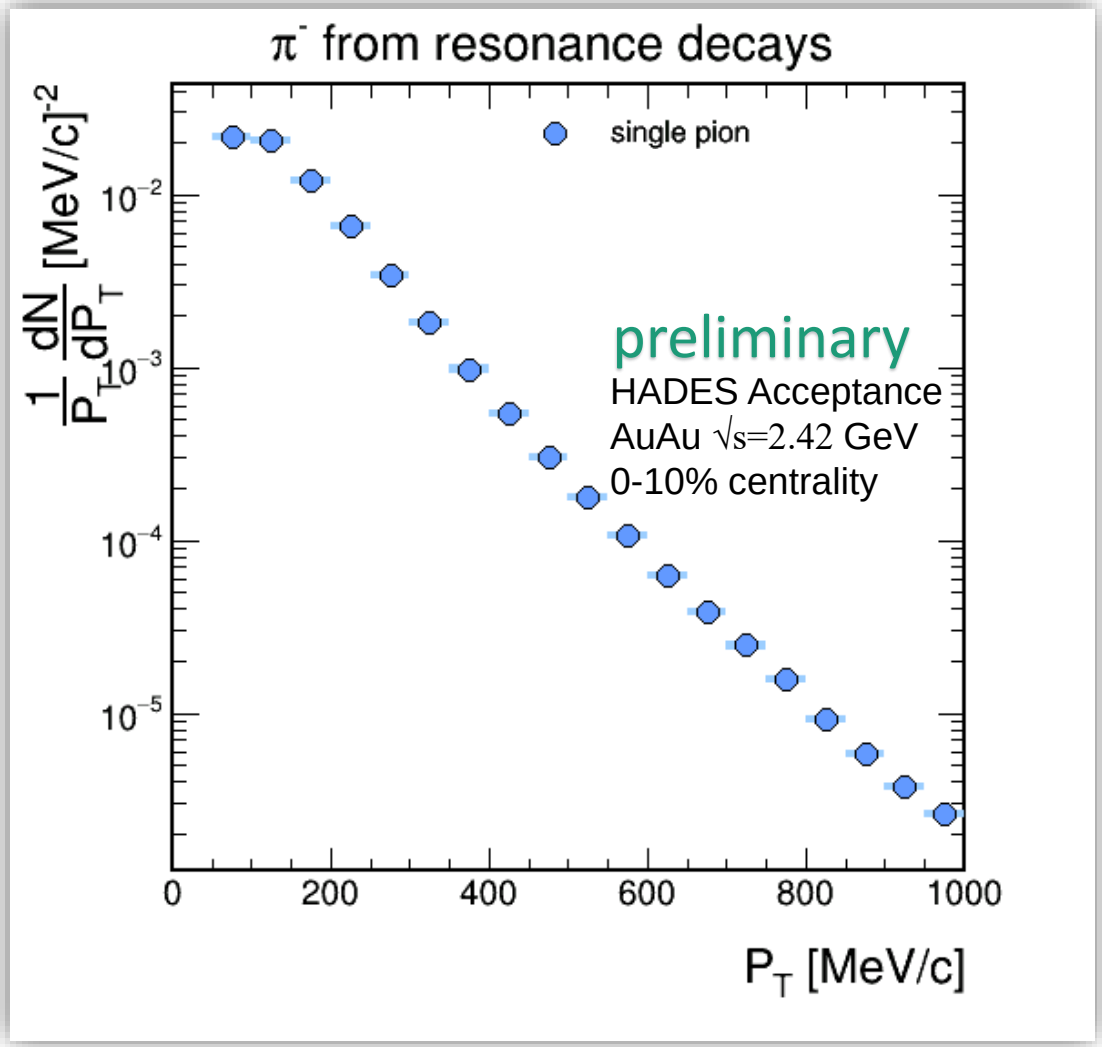

Production of charged pions from resonances: the most ~~simple~~ abundant mesons

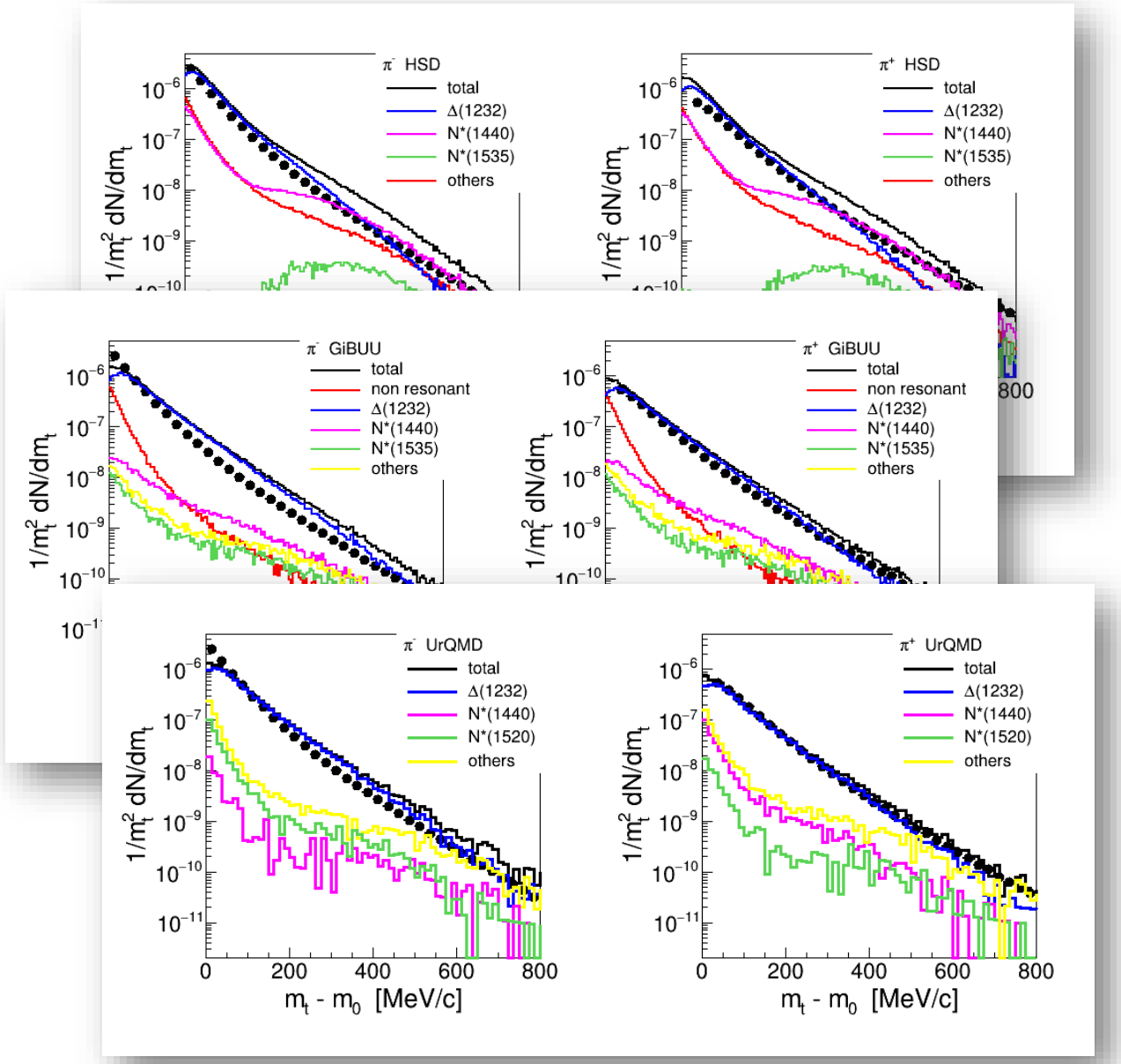

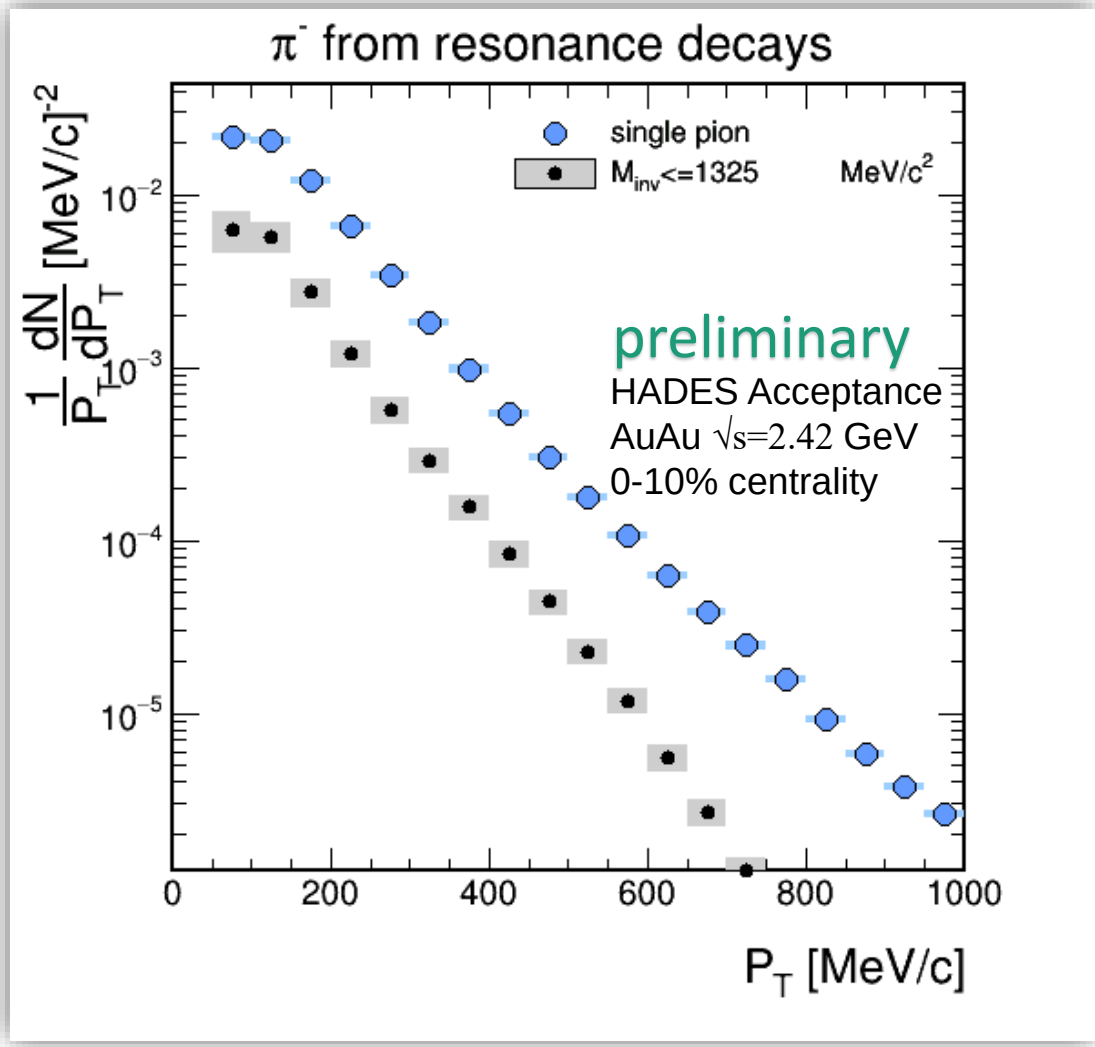

Production of charged pions from resonances: the most ~~simple~~ abundant mesons

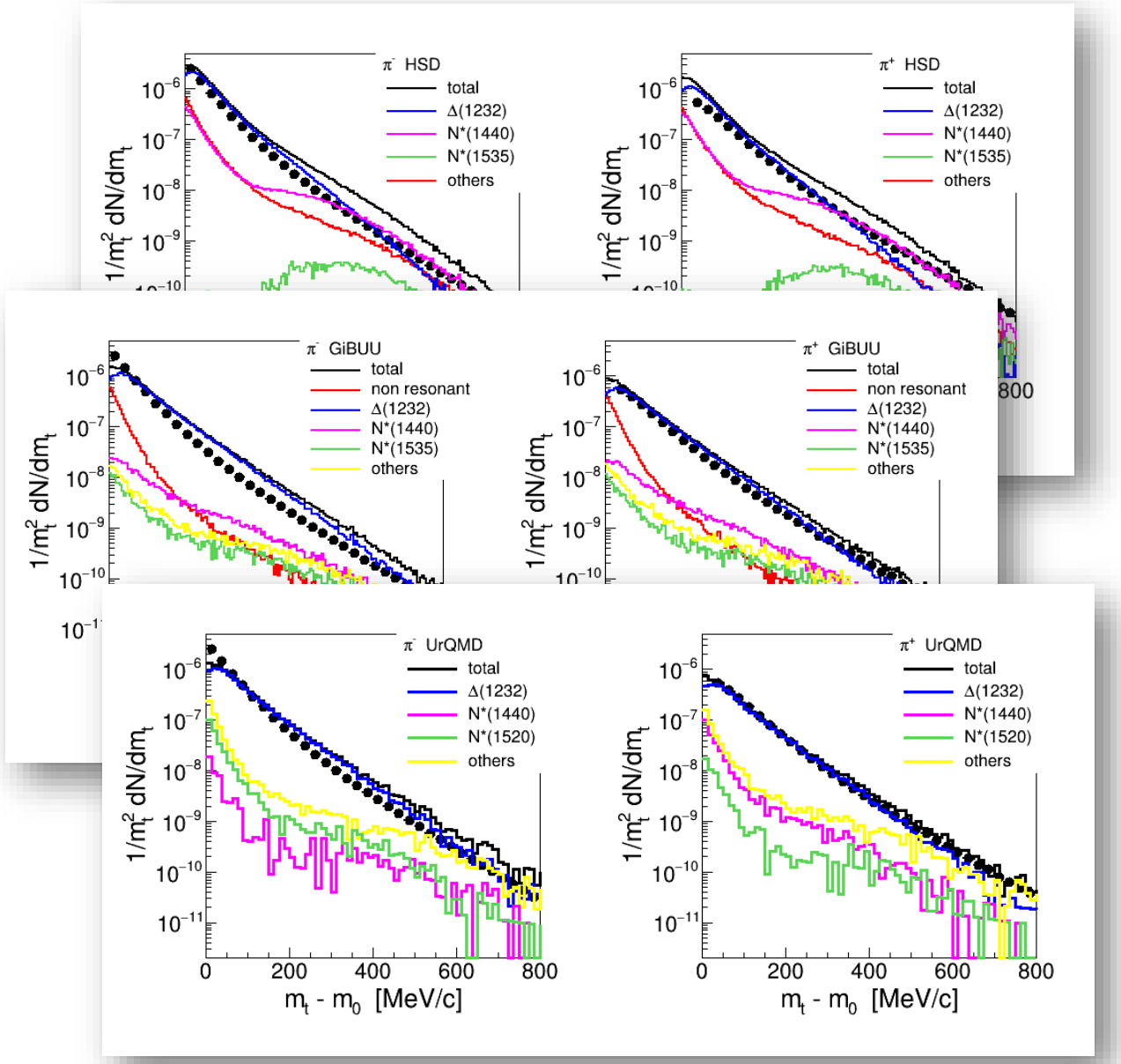

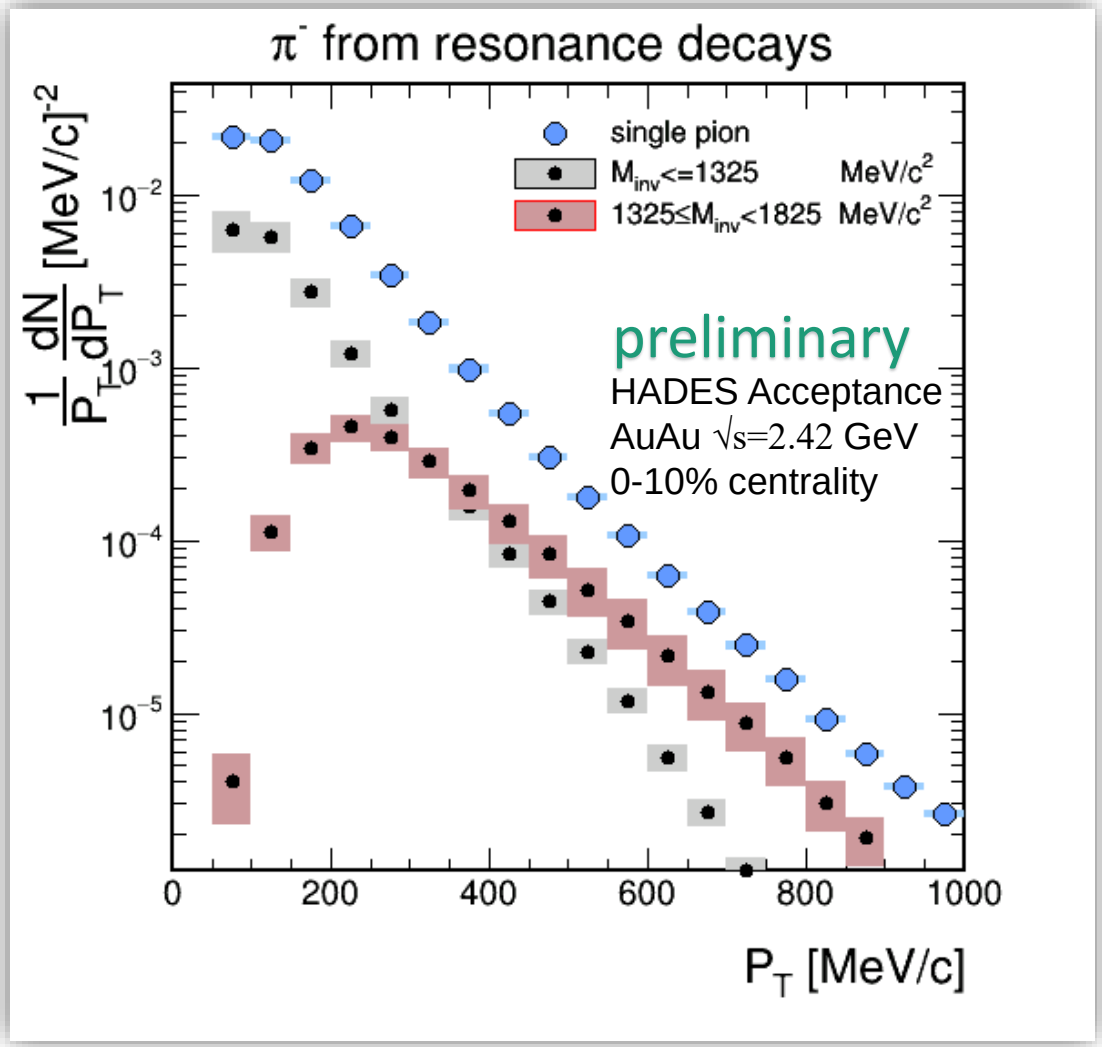

Production of charged pions from resonances: the most ~~simple~~ abundant mesons

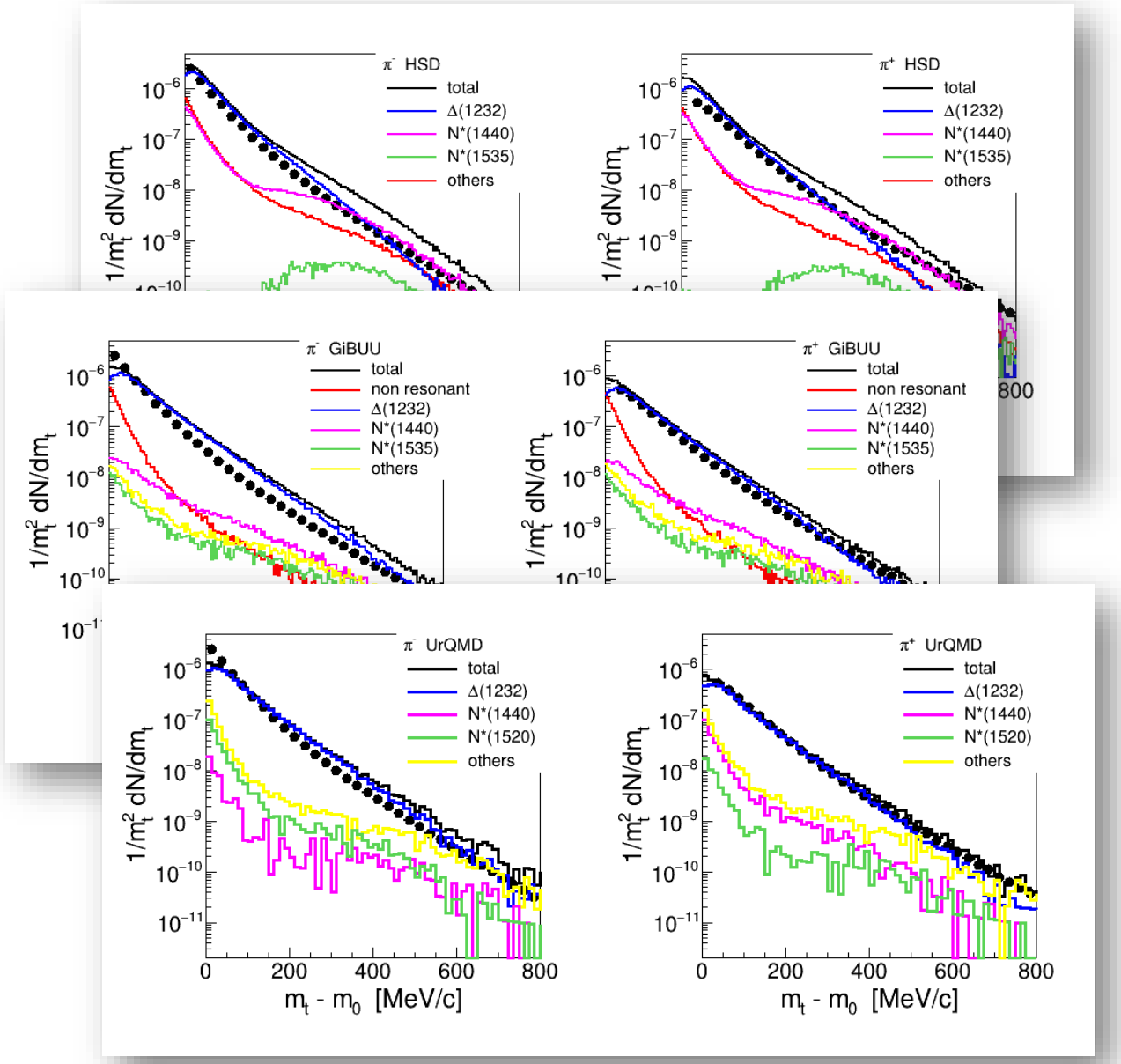

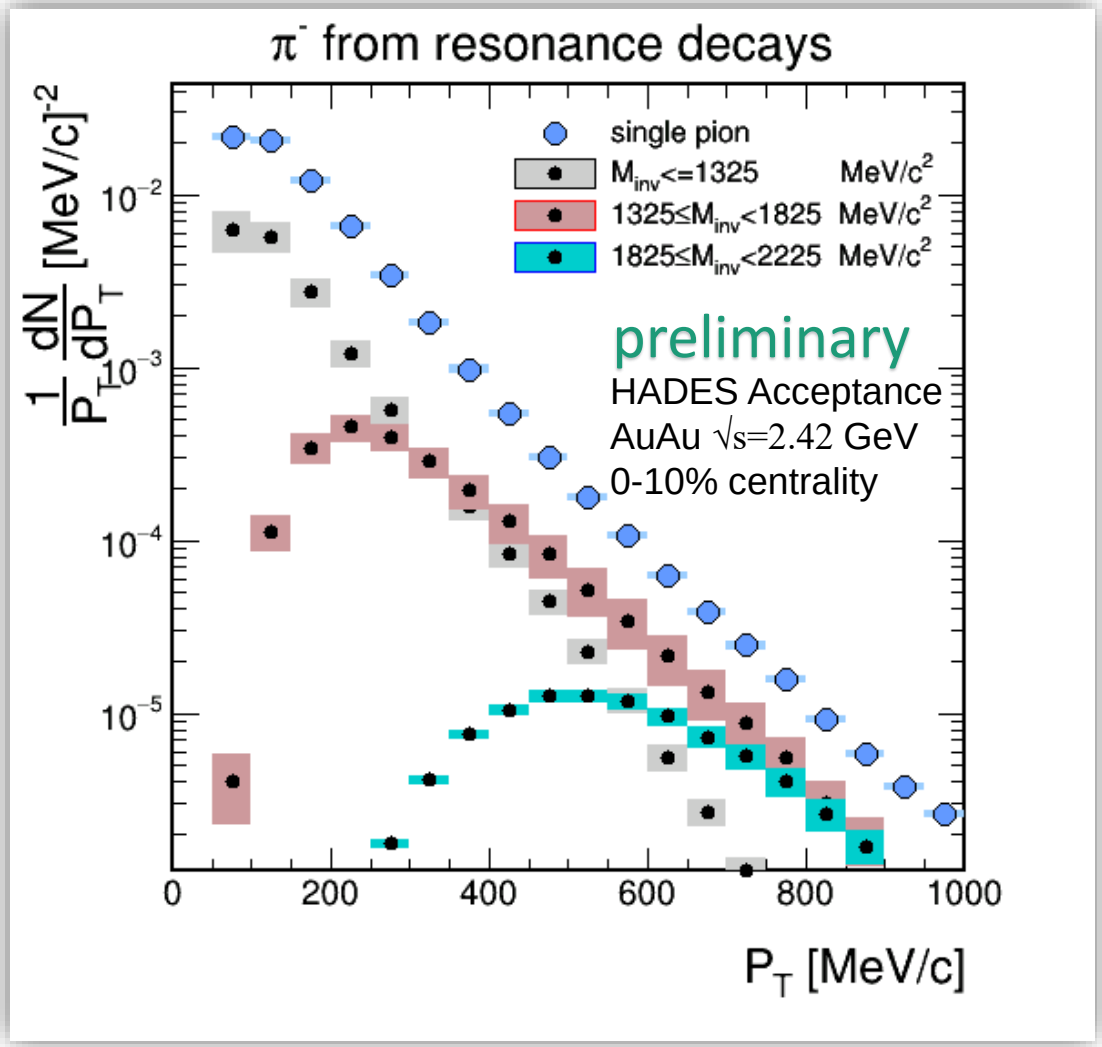

Production of charged pions from resonances: the most ~~simple~~ abundant mesons

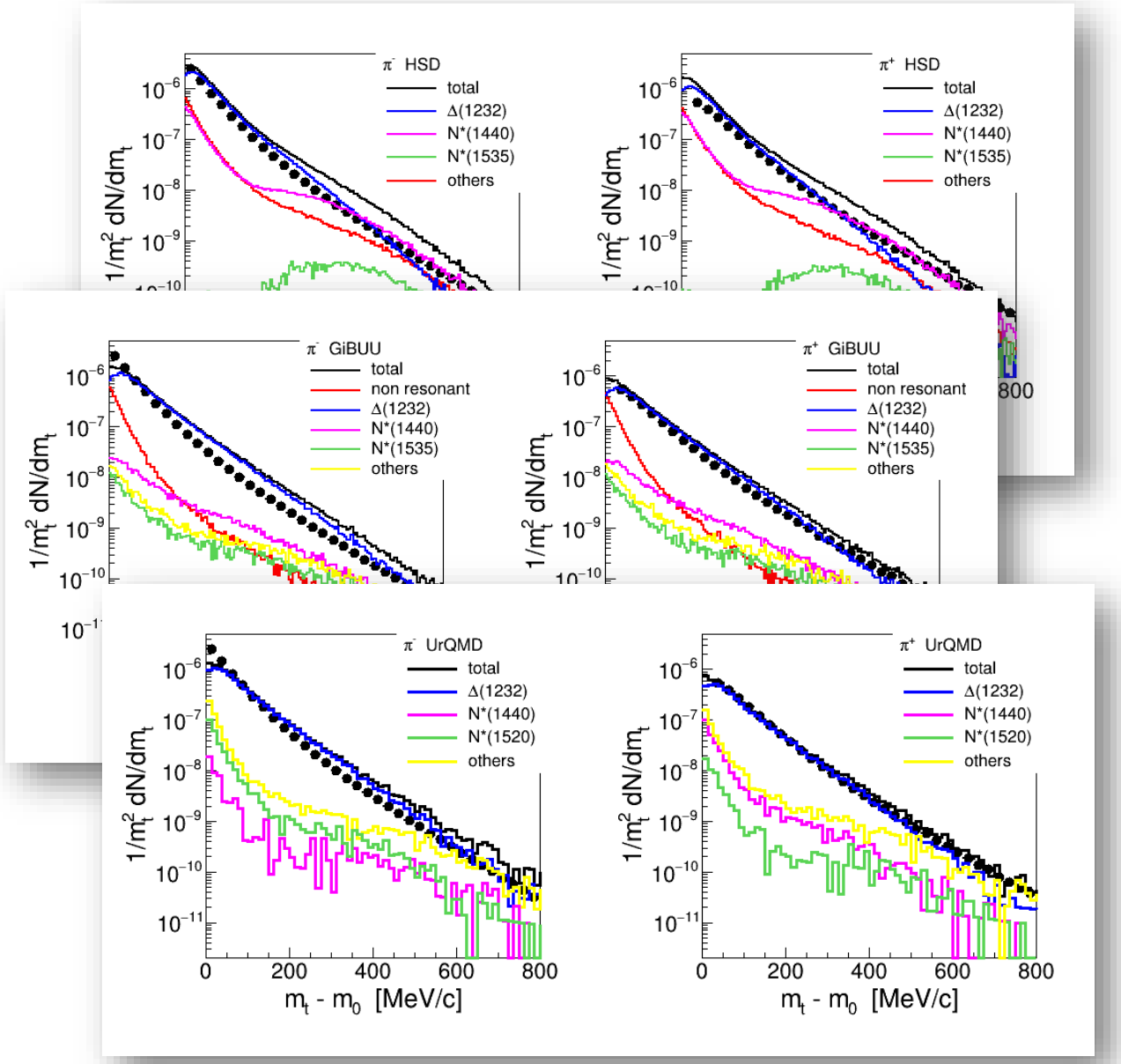

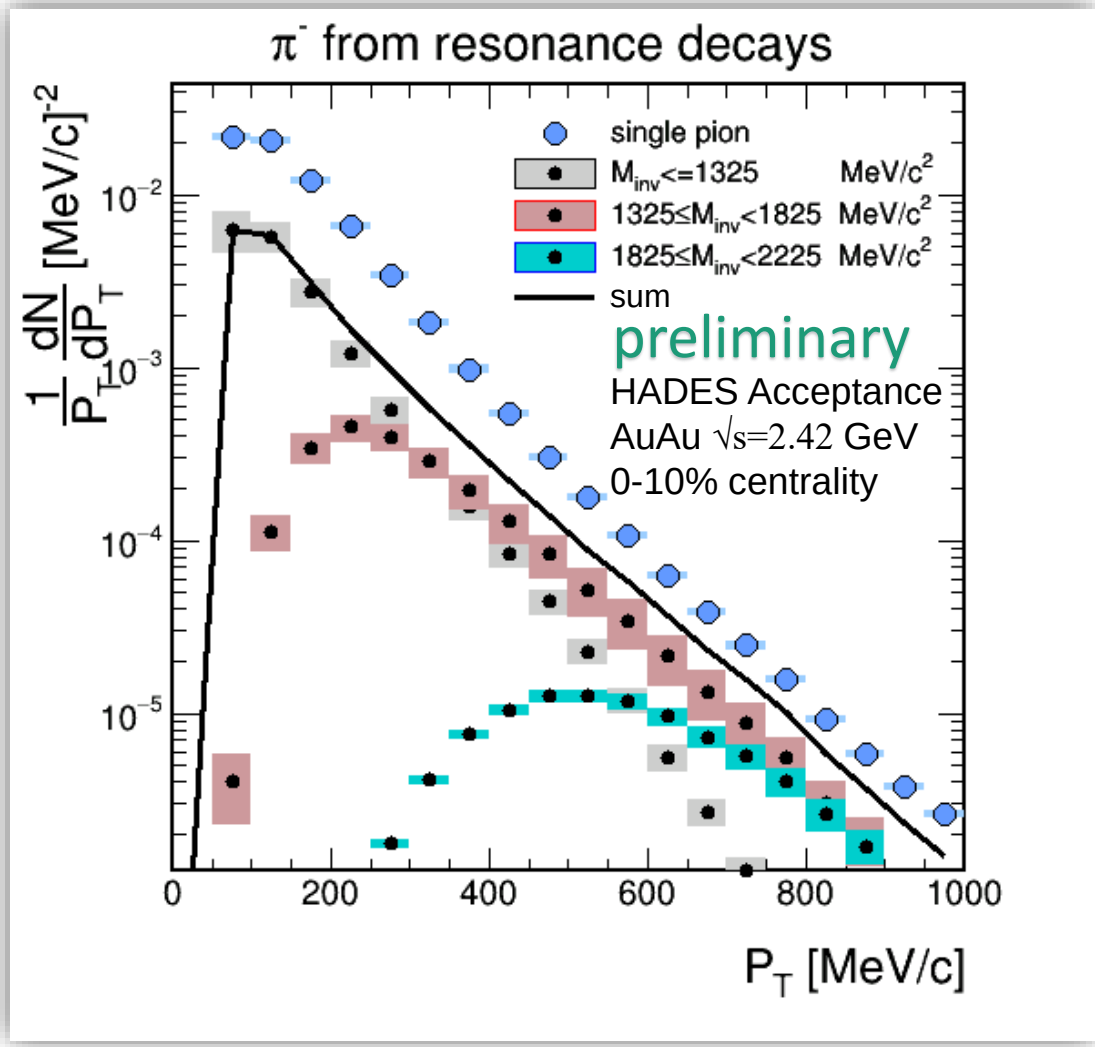

FAIR Phase-0 and beyond

- 2018 Upgrade
  - ECAL
  - MAPMT RICH (with CBM)
- 2019 -202x
  - Ag+Ag =2.6 GeV (March 2019)
  - Pion beam (energy scan)
  - 200 kHz DAQ
  - Forward detector (straw tubes, PANDA)
- FAIR-SIS100
  - Cold matter physics (p+A)
  - A+A
  - Exclusive p+p

g.kornakov@gsi.de

Thank you for your attention!

Strangeness in cold nuclear matter: strong absorption of K-

AuAu:

- **Pions; discrepancies with models, FOPI**
- **Strangeness: universal centrality scaling, from comparison to models not a clear statement**
- **Resonances: a new tool to look into the HIC. Many interesting features in the spectra: rapidity, pT, …**

Backup

Summary

Strangeness in cold nuclear matter: strong absorption of K-

AuAu:

Pions; discrepancies with models, FOPI
Strangeness: universal centrality scaling, from comparison to models not a clear statement
Resonances: a new tool to look into the HIC. Many interesting features in the spectra: rapidity, pT, …

g.kornakov@gsi.de

Two-Pion Intensity Interferometry from Au+Au at $\sqrt{s} = 2.42$ GeV

HADES Collab., arXiv:1811.06213 [nucl-ex]

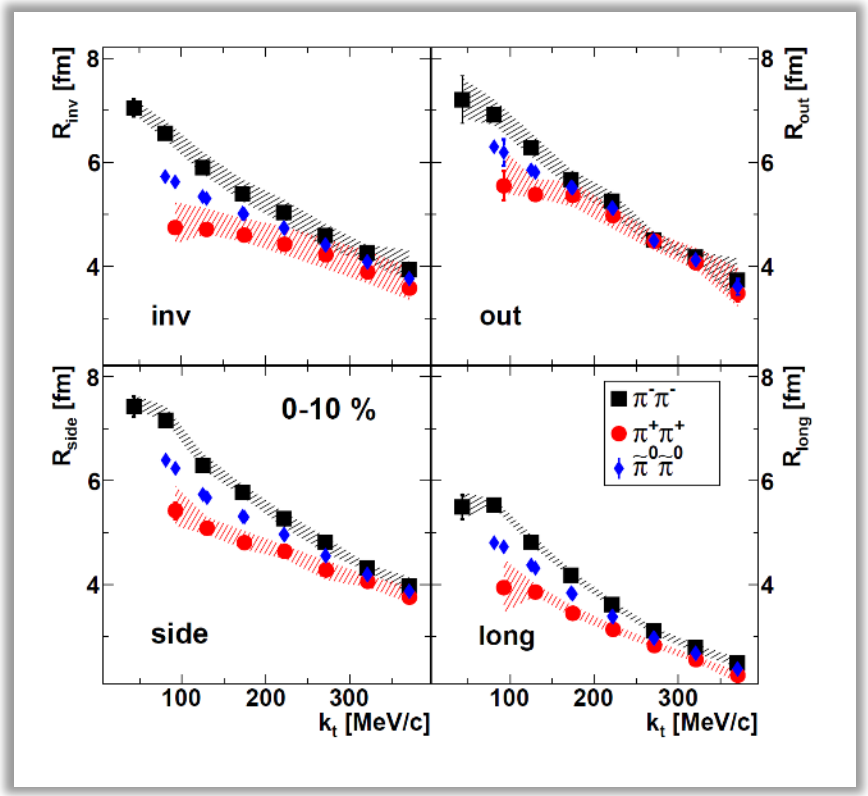

indications for charge-sign dierences reported previously:
E866 R. A. Soltz, M. Baker, J. H. Lee, Nucl. Phys. A 661, 439c (1999)
E877 D. Miskowiec et al., Nucl. Phys. A590, 473c (1995)
opposite eect (!):
NA44 I.G. Bearden et al., Nucl. Phys. A638, 103c (1998)

First time observation of substantial difference between positive and negative pions!

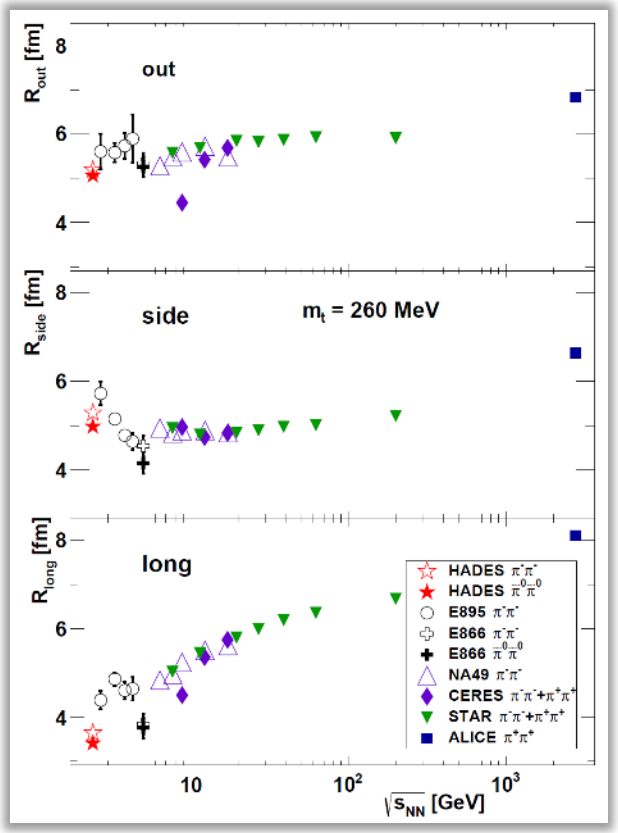

HADES follows trend from STAR/NA49 more than trend from E895

! No new features visible

g.kornakov@gsi.de

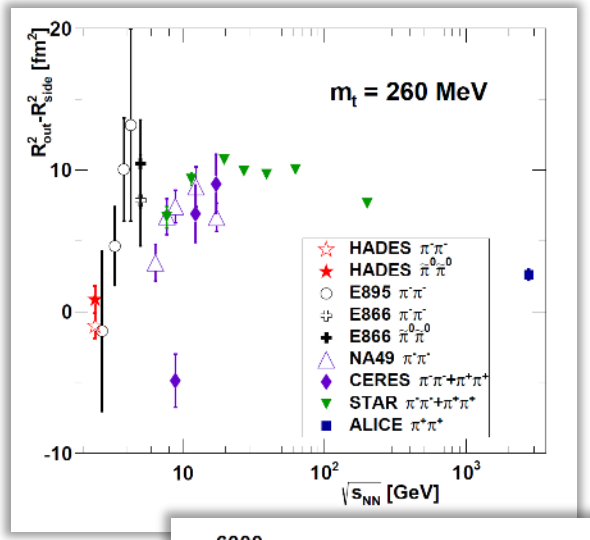

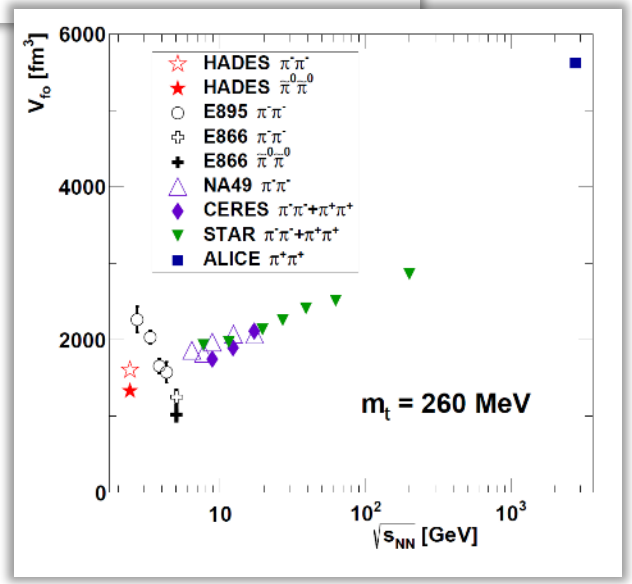

$V_{freezeout(fo)} := (2\pi)^{3/2} R^2_{side} R_{long}$

extrapol. V_{fo} to k_t = 0MeV/c

V_{fo} = 3900 fm^3 ($\pi^0\pi^0$ HADES)

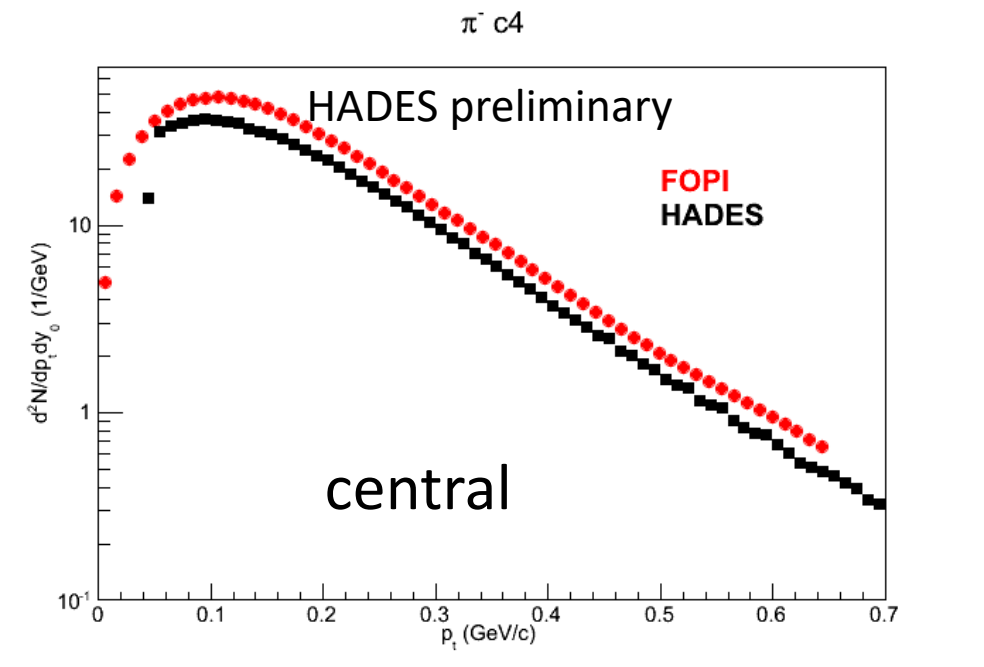

Comprison of p_T-distribution at mid-rapidity

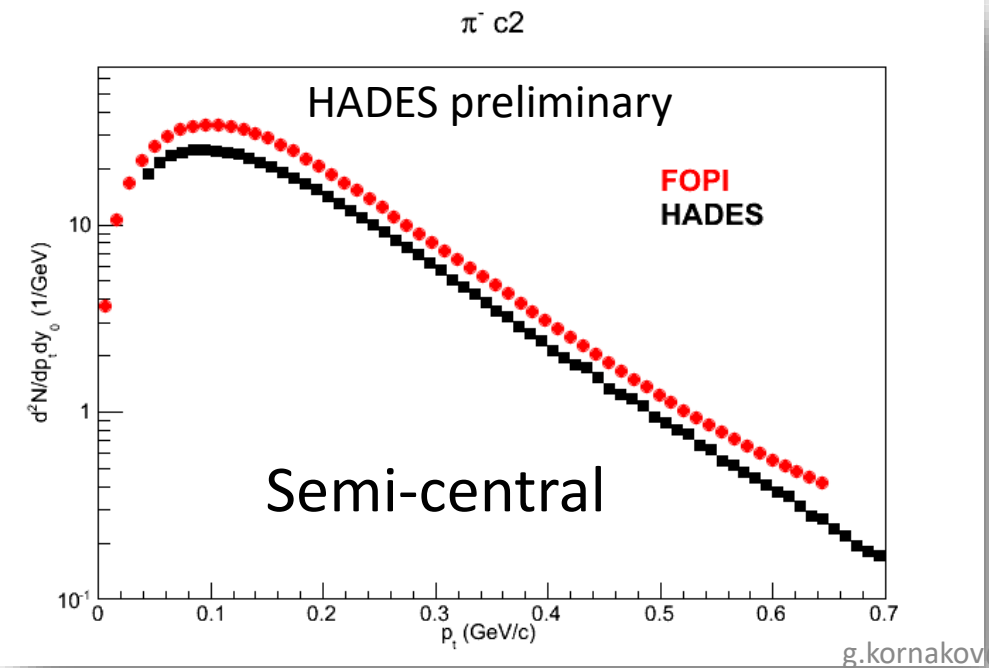

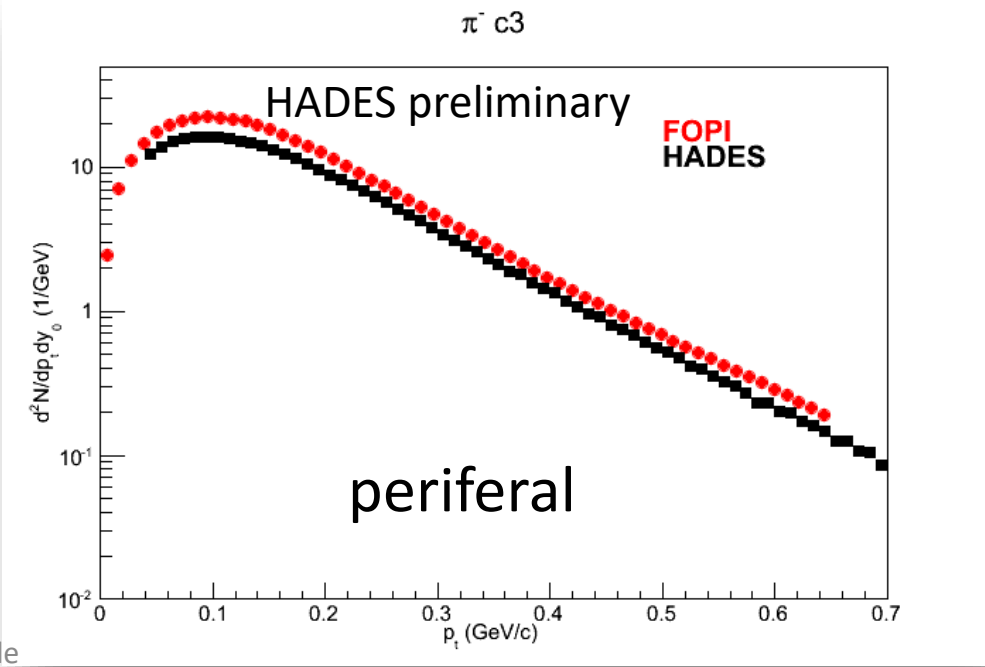

g.kornakov@gsi.de

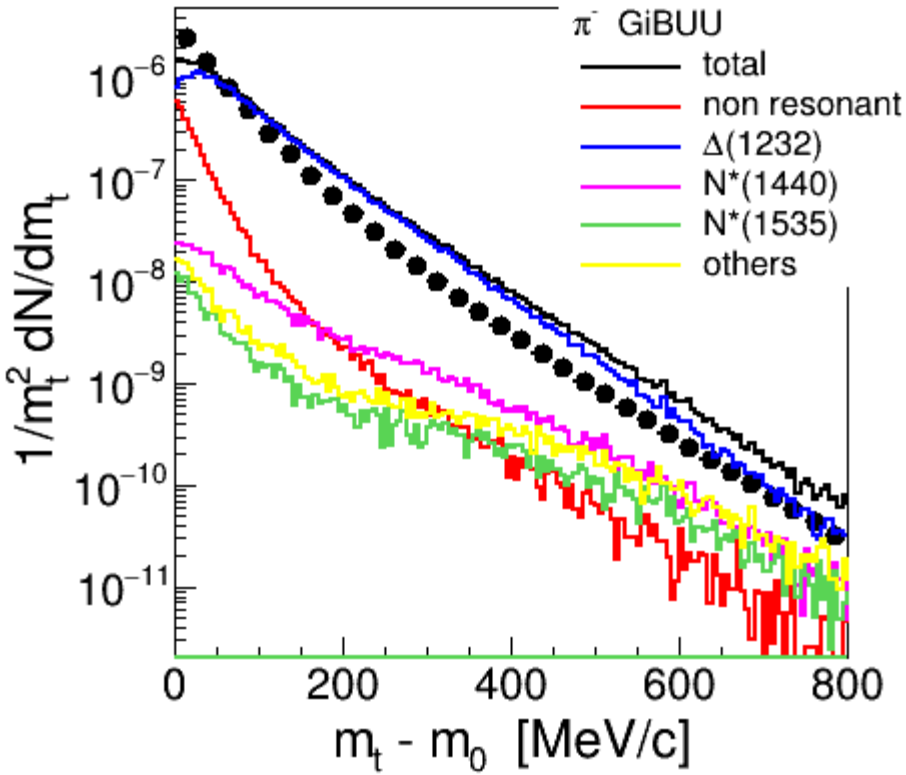

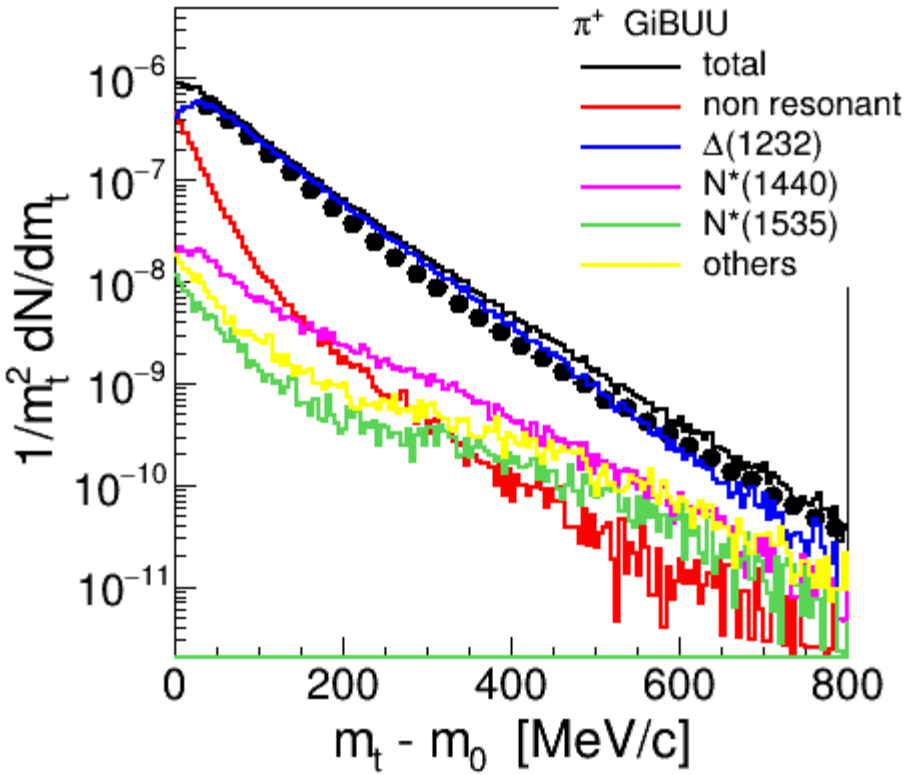

g.kornakov@gsi.de

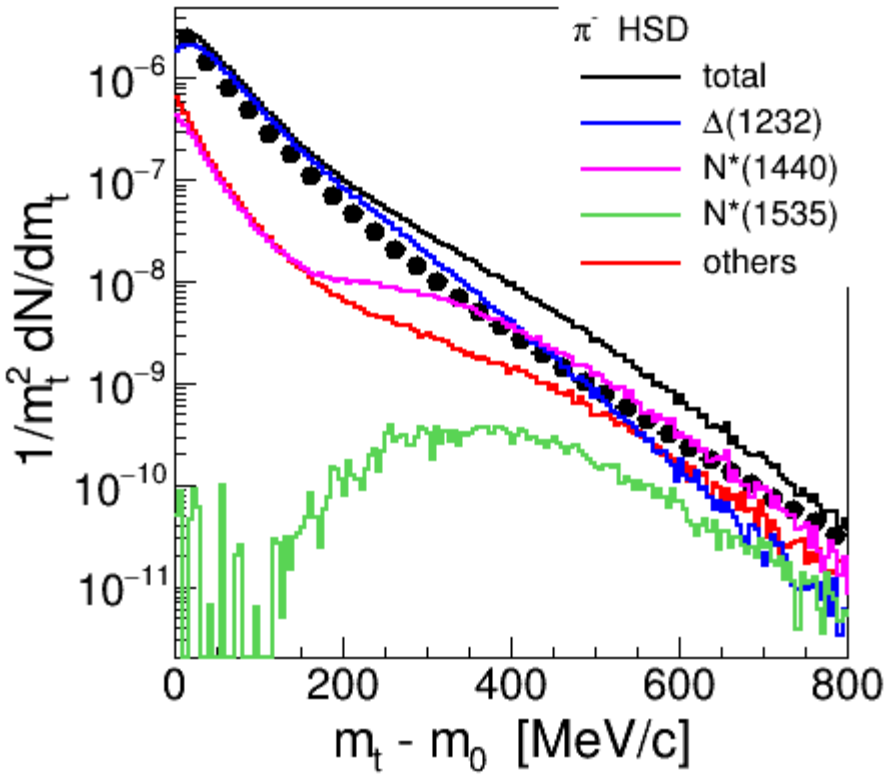

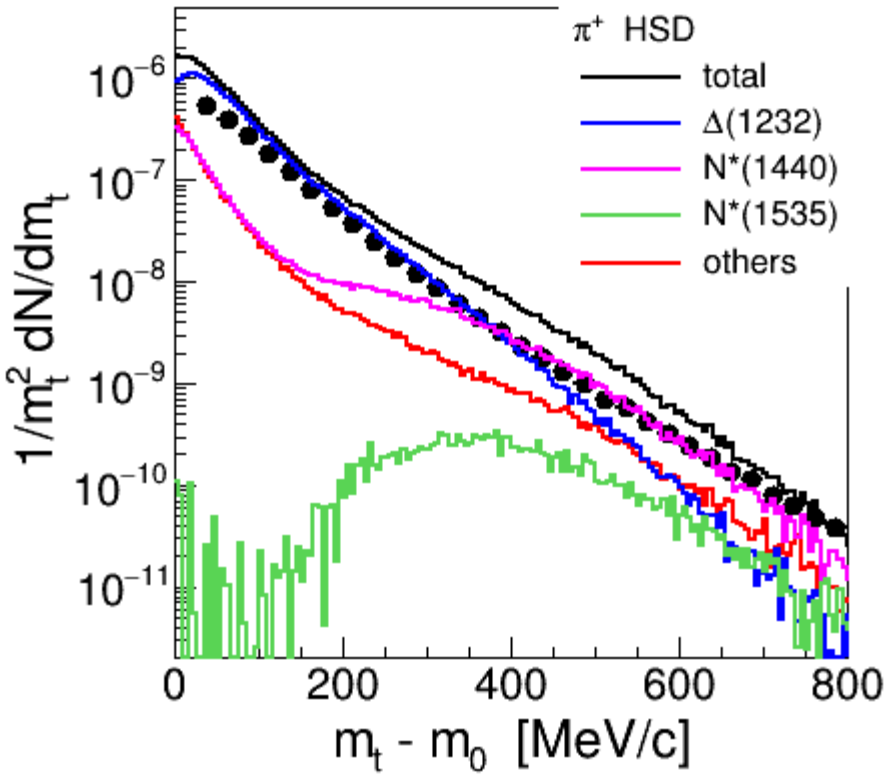

g.kornakov@gsi.de

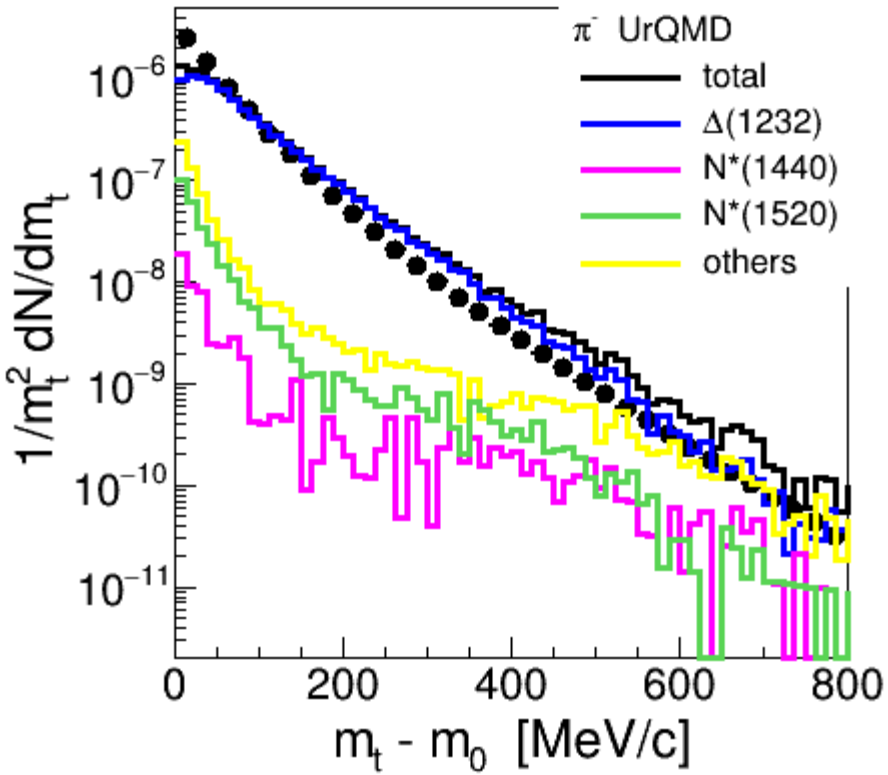
π⁻ UrQMD
total
Δ(1232)
N*(1440)
N*(1520)
others
1/m_t^2 dN/dm_t
m_t - m_0 [MeV/c]

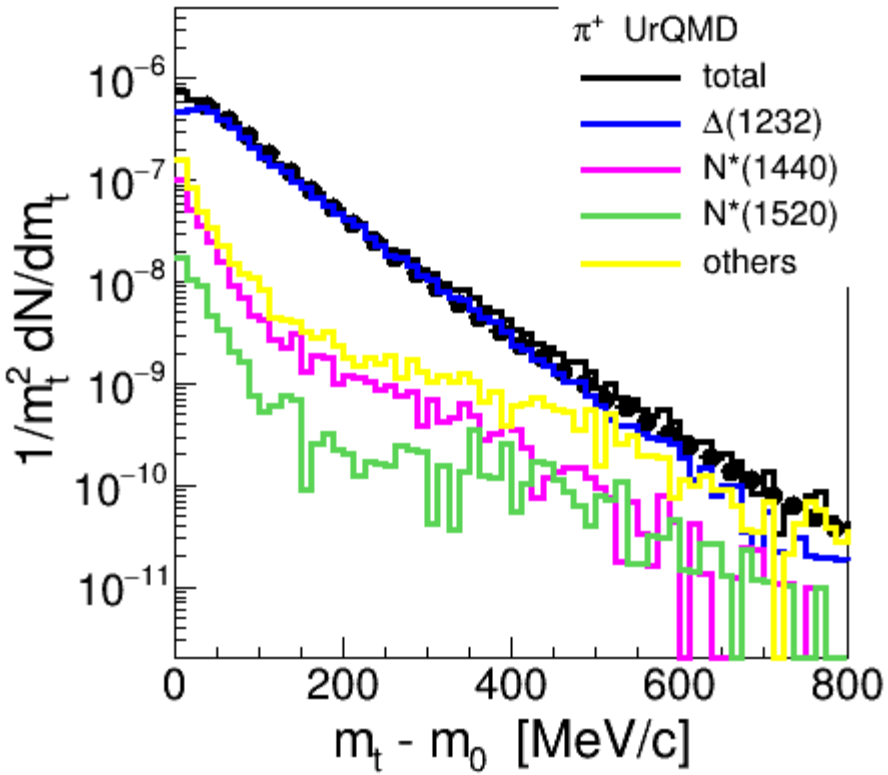
π⁺ UrQMD
total
Δ(1232)
N*(1440)
N*(1520)
others
1/m_t^2 dN/dm_t
m_t - m_0 [MeV/c]

Existing techniques and issues of estimation of combinatorial background

- Monte-Carlo phase-space generators
  - **Inclusive analysis in elementary reactions.**
  - Suitable for low background environments.
- Position-swapping
  - **Suitable for large number of identical particles (di-photon mass at high energies).**
  - Not possible to generalize. Signal particles are used to generate the combinatorial background together with uncorrelated particles having, in general, different kinematics.
- Like-sign
  - **Ideal for unlike-sign analysis (dileptons and dipions) where like-sign combinations are background.**
  - Not possible to generalize.
- Event mixing
  - **Most common technique for inclusive signal extraction. Intuitive implementation.**
  - Arbitrary normalization constants.
  - Strong influence of particle and event class selection used for mixing.
  - Signal particles are used to produce the combinatorial background together with uncorrelated particles having, in general, different kinematics.

The iterative method

- Typify the properties of the combinatorial background: **internal symmetries**
  - Fixed target: CB is invariant under random azimuthal rotations of individual particles.
  - Collider: CB is invariant under random rotations.
- After track rotation the CB remains the same but the signal is decorrelated!

Rotations of particles is technically intuitive and simple.

Collective production properties as flow have to be accounted as well!

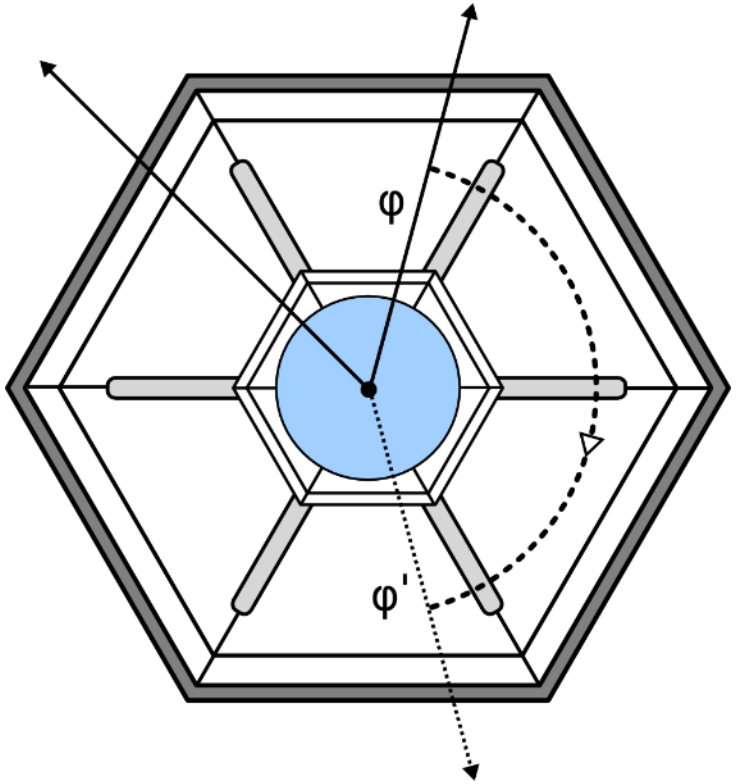

The iterative method

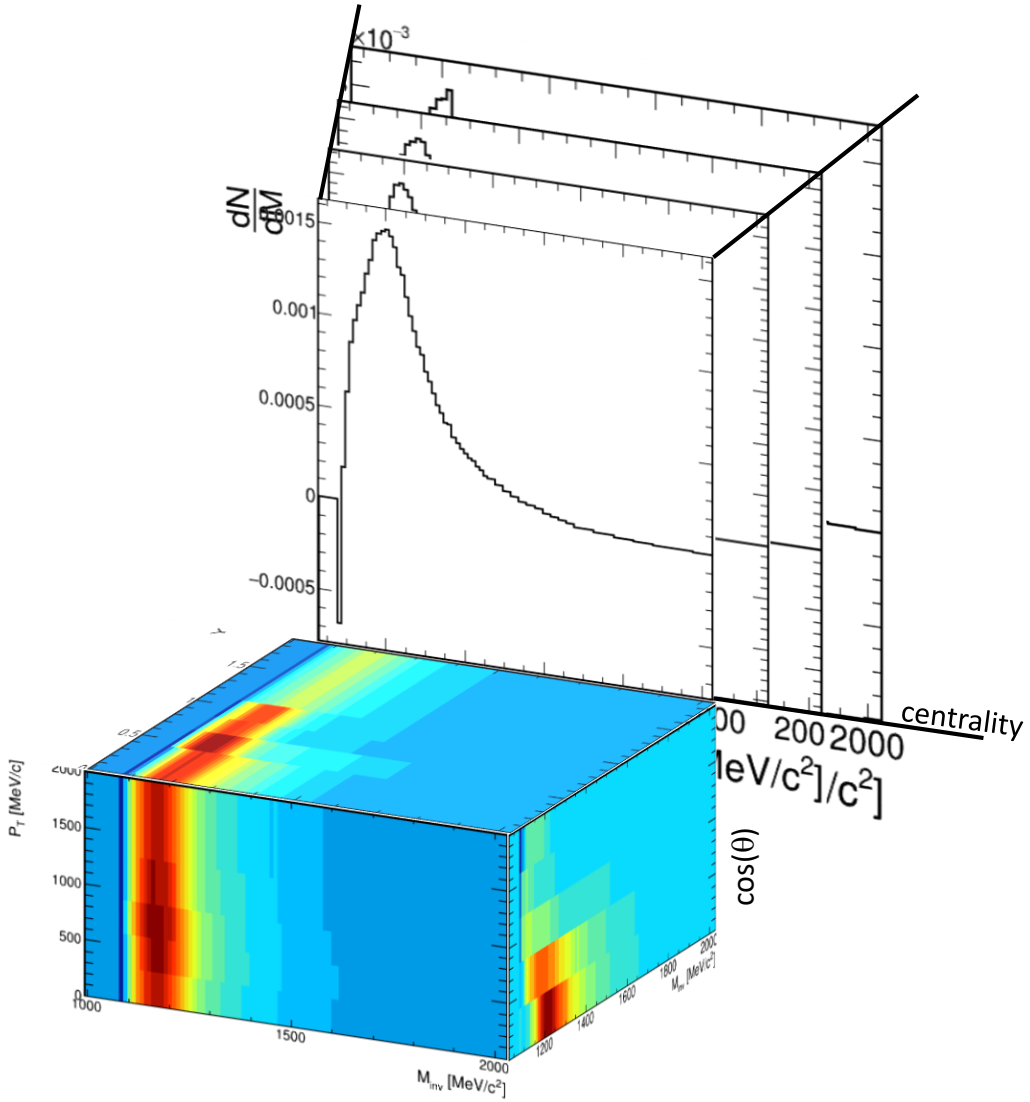

- Produce the contribution of the signal particles to the combinatorial background.
  - To produce the contribution of the signal particles to the CB both four-momentum have to be known.
  - 8D matrix is simplified to a 4D matrix if:
    - Identified particles (fixed M_0) (- 2 d.o.f.)
    - Rotational production symmetry of the mother particle (-1 d.o.f.)
    - No polarization scenario: decay rotational symmetry (- 1 d.o.f.)
  - Mass – pair P_T – pair Y – decay angle (Helicity, Gottfried-Jackson.. frames) constraints completely the kinematics of daughter particles.

Real data

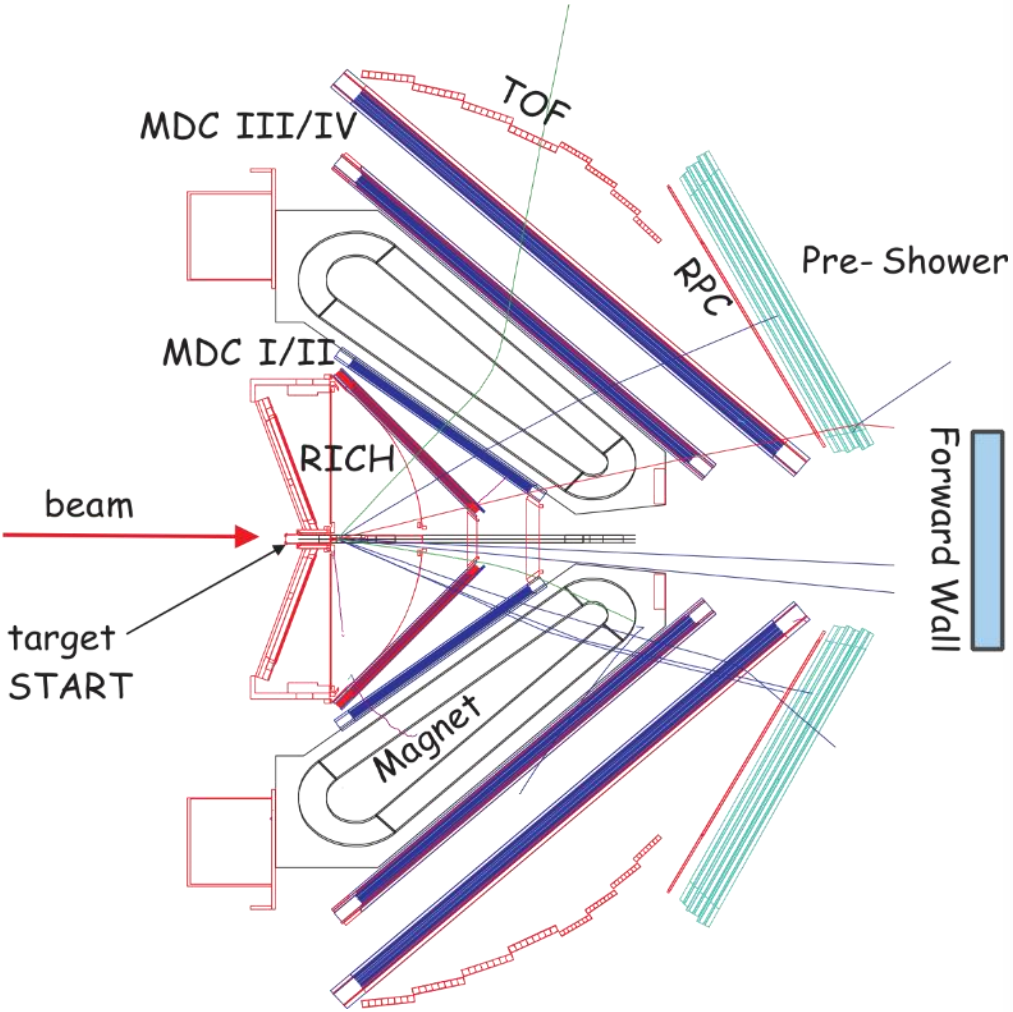

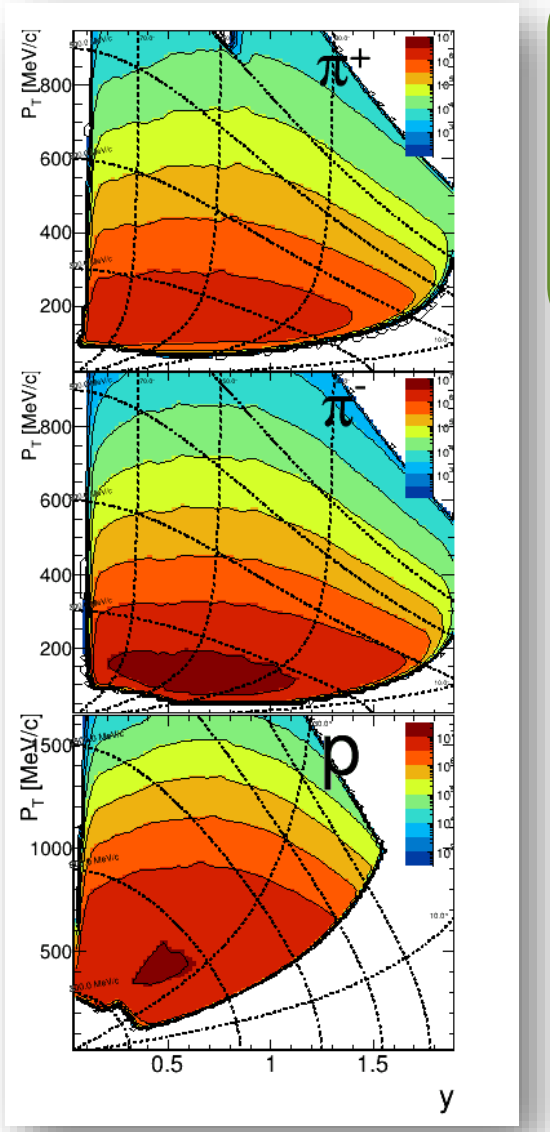

Event selection:

- Multiplicity trigger 0-40%
- Pile-up rejection
- 4 equal centrality classes
- Reaction plane

Particle selection:

- 2.5 sigma selection (combined b-p and dE/dx-p)
- Maximum and minimum PT (left Fig.)
- low theta 15°, max theta 85°)

TOF

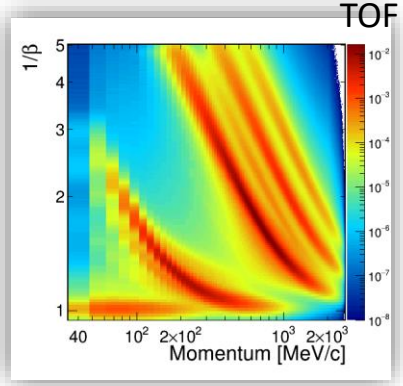

RPC

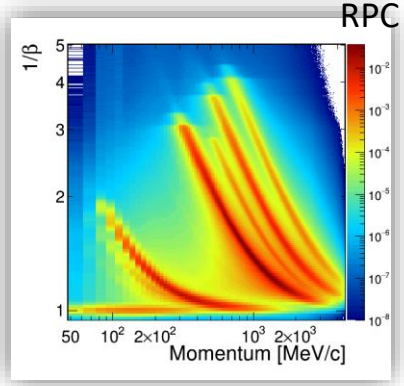

The iterative method

$$\mathcal{T} = \mathcal{B} + \mathcal{S}$$ Total = background plus signal

Let $\hat{\mathcal{U}}$ Be the uncorrelator (rotator)

Then, $$\mathcal{B} = \hat{\mathcal{U}}(\mathcal{B})$$

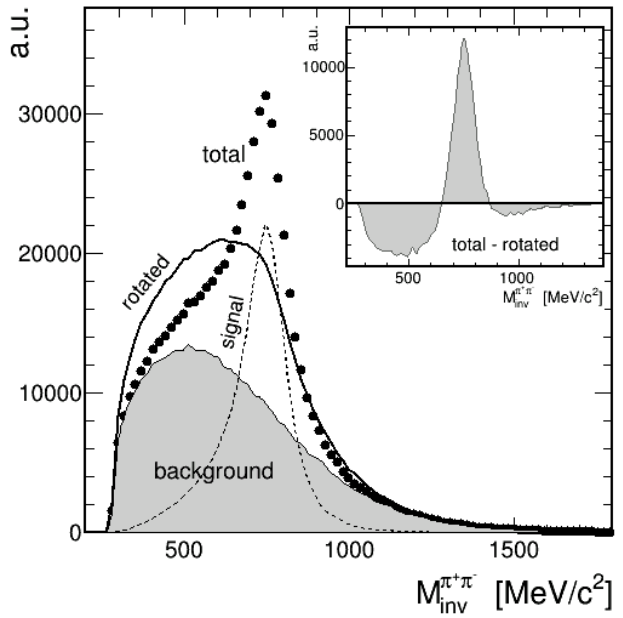

Then,any difference from the transformation of the total spectrum is due to signal

$$\mathcal{T} - \hat{\mathcal{U}}(\mathcal{T}) = \mathcal{S} - \hat{\mathcal{U}}(\mathcal{S})$$

The iterative method

Then the first iterative solution will be:

$$\mathcal{S}^1 = \mathcal{T} - (\hat{\mathcal{U}}(\mathcal{T}) - \hat{\mathcal{U}}(\mathcal{S}^0))$$

Ideally, iterator stops when:

$$\mathcal{S}^{k+1} = \mathcal{S}^k$$

And the iterative solution can be written:

$$\mathcal{S}^{k+1} = \max\{\mathcal{T} - (\hat{\mathcal{U}}(\mathcal{T}) - \hat{\mathcal{U}}(\mathcal{S}^k)), 0\}$$

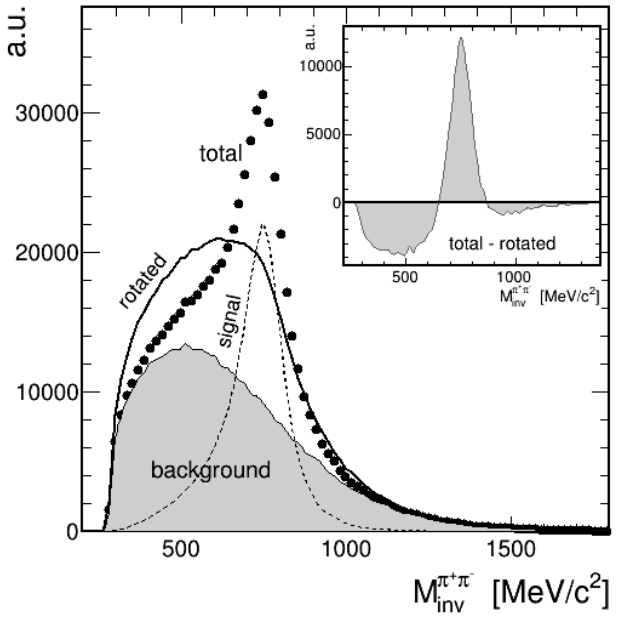

Test on simulation

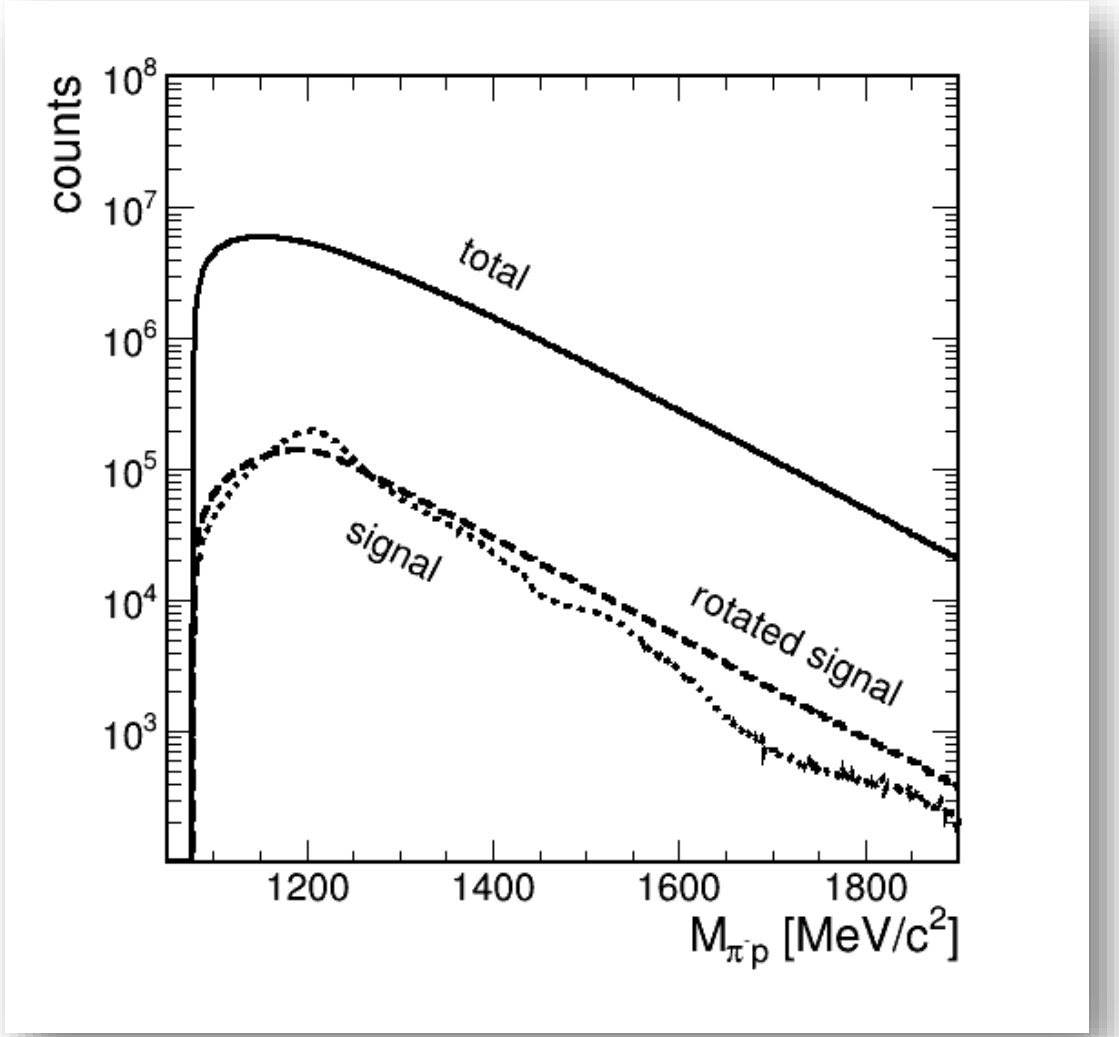

Validation of the method with simulated* resonance cocktail

* I. Frohlich et al. arXiv:0708.2382 [nucl-ex]

	N/Nprot	Channels	Γ/Γ_i
$\Delta(1232)^0$	5 %	π^-p	1
$N(1440)^0$	2 %	π^-p, pρ^-,$\Delta^+\pi^-$	0.62/0.02/0.36
$N(1535)^0$	1.5 %	π^-p, pρ^-,$\Delta^+\pi^-$	0.70/0.06/0.23
$\Delta(1620)^0$	1 %	π^-p, pρ^-,$\Delta^+\pi^-$	0.18/0.12/0.70
$\Delta(1920)^0$	0.5 %	π^-p, pρ^-,$\Delta^+\pi^-$	0.7/0.2/0.1
p	20		
π^-	10 %		

Test on simulation

$$\mathcal{T} - \hat{\mathcal{U}}(\mathcal{T}) = \mathcal{S} - \hat{\mathcal{U}}(\mathcal{S})$$

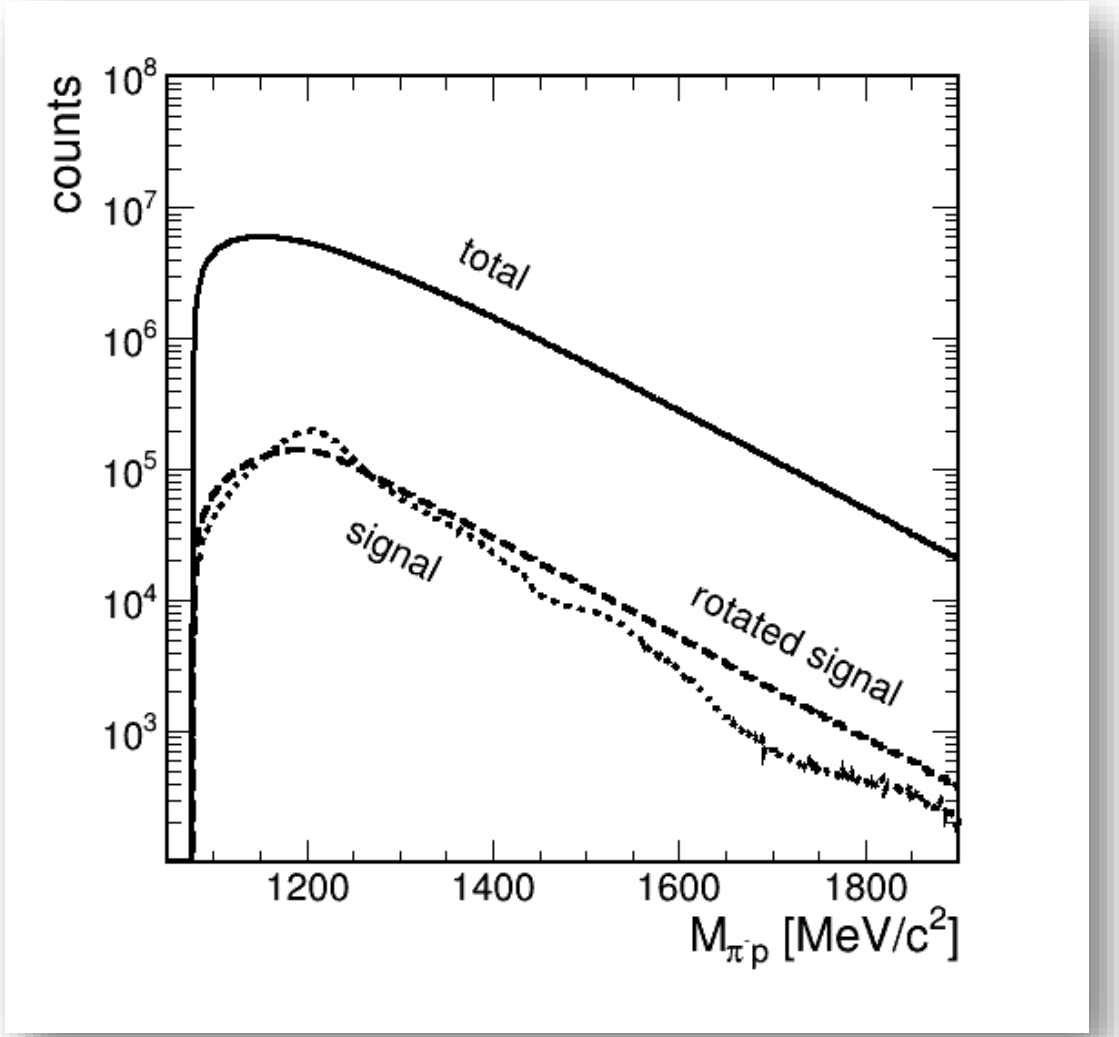

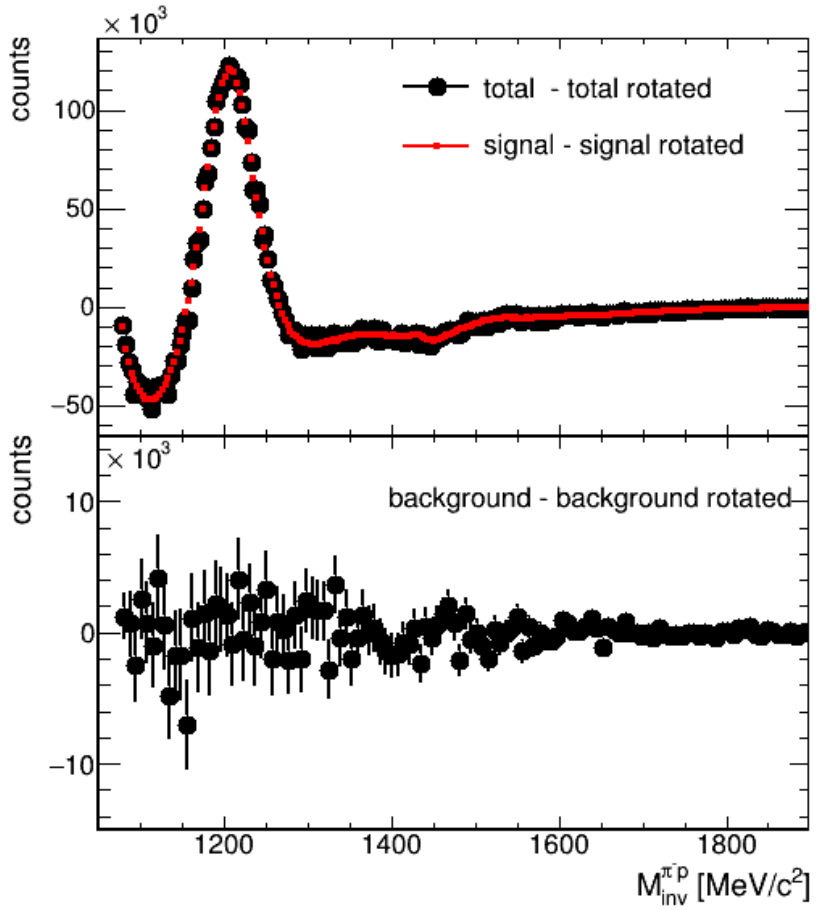

$$\mathcal{B} = \hat{\mathcal{U}}(\mathcal{B})$$

Test on simulation

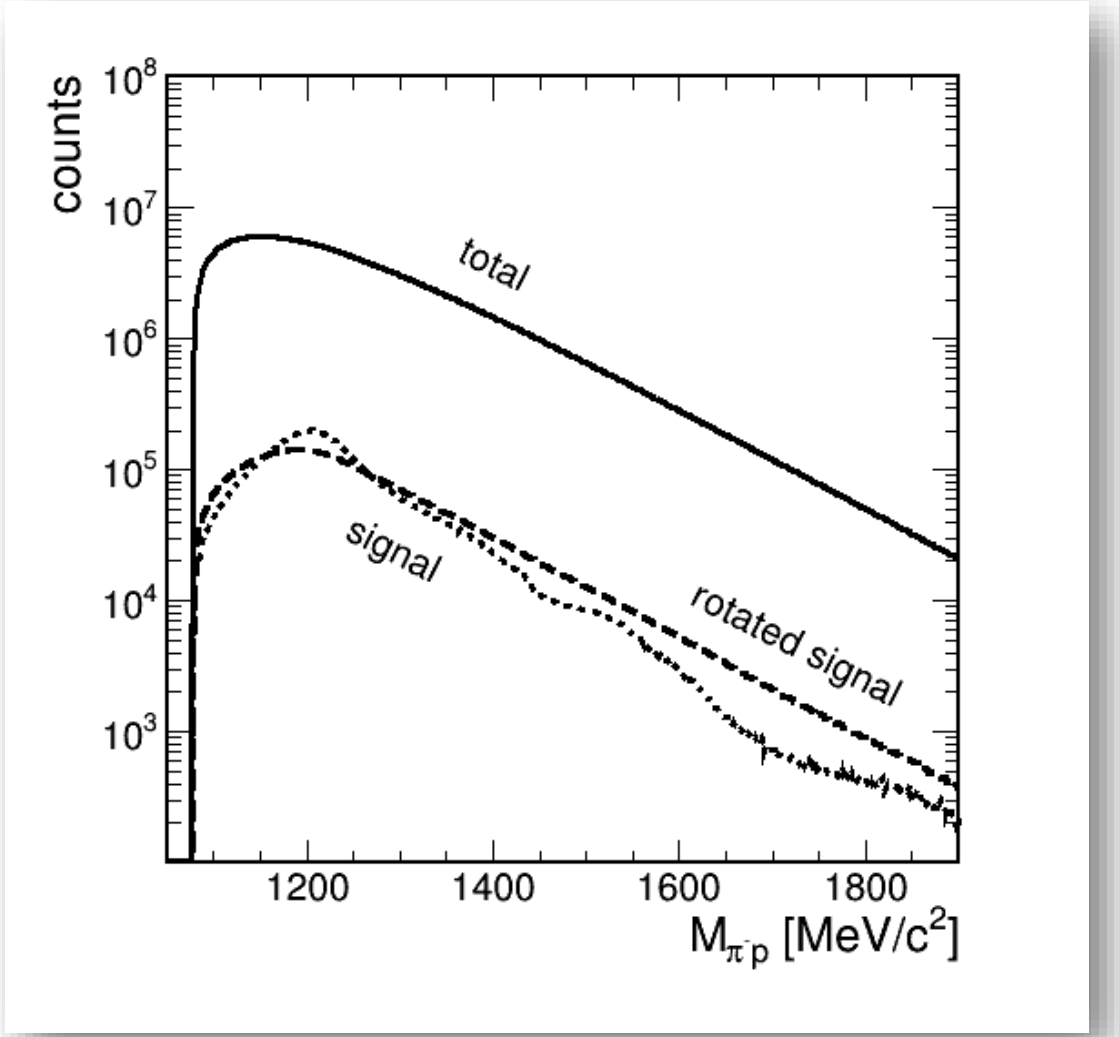

Not only the difference rises in the invariant mass!
The **transverse momentum** and the **angular** distributions behave in the same fashion

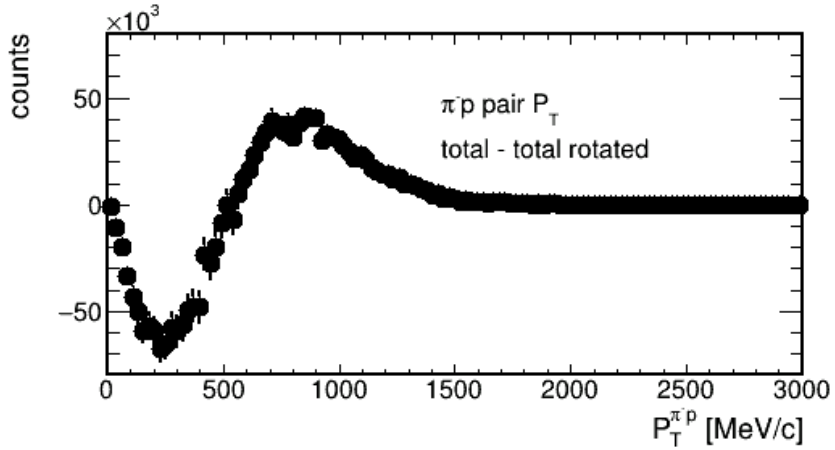

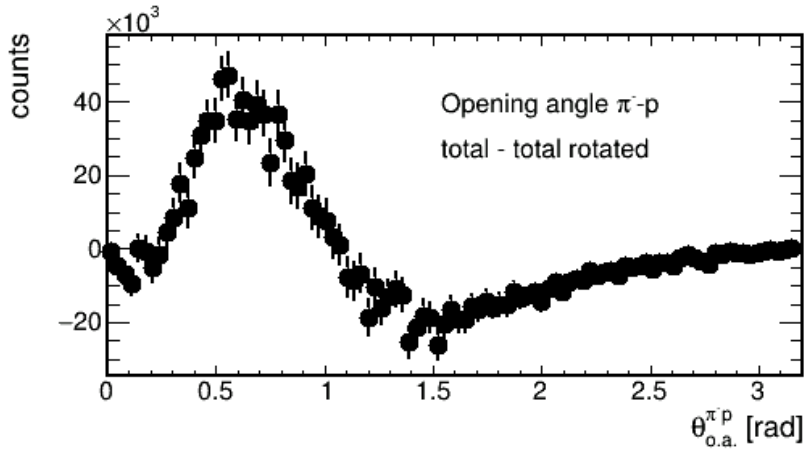

$$\mathcal{S}^{k+1} = \max\{\mathcal{T} - (\hat{\mathcal{U}}(\mathcal{T}) - \hat{\mathcal{U}}(\mathcal{S}^k)), 0\}$$

Test on simulation

P_T < 365 MeV/c

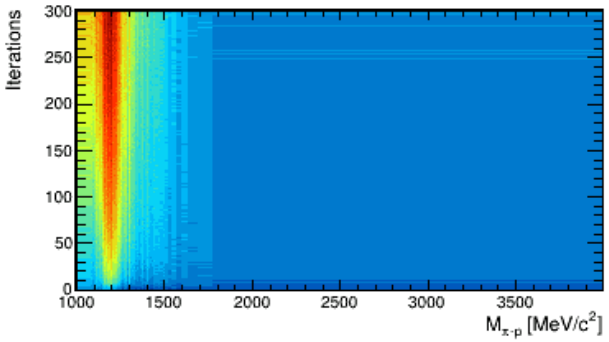

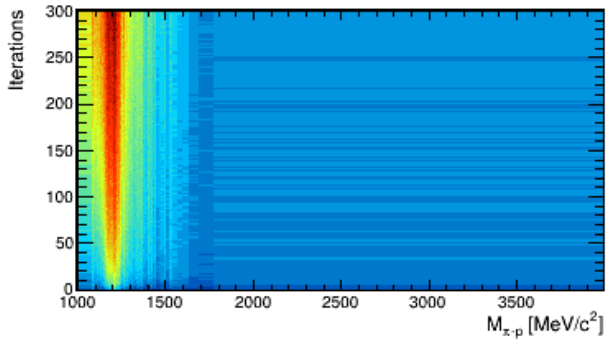

365 - 545 MeV/c

545-720 MeV/c

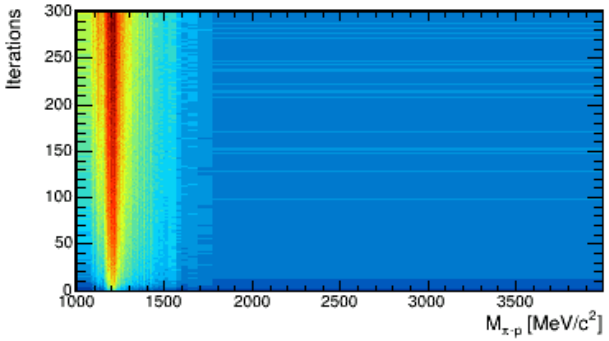

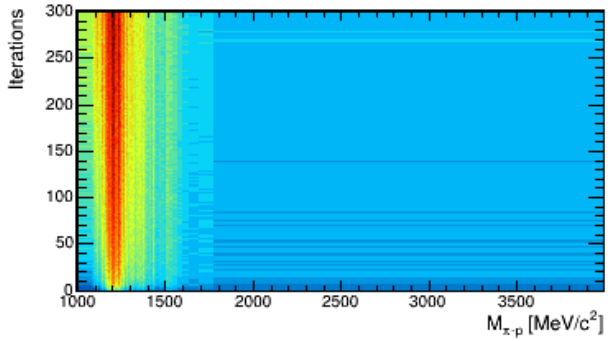

720-940 MeV/c

P_T > 940 MeV/c

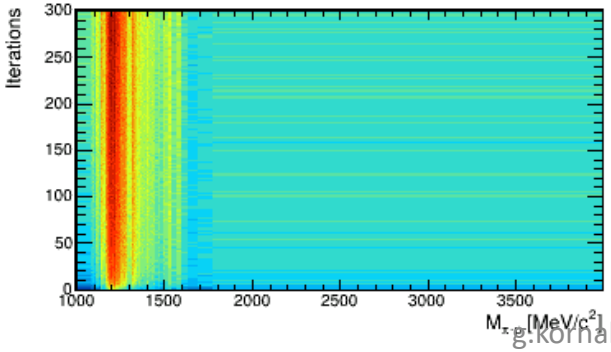

After 300 iteration signal continues to grow. Max{ }, ignores existence of bin-to-bin statistical fluctuations, and this creates an artificial signal rise: “statistical rise”

$$\mathcal{S}^{k+1} = \max\{\mathcal{T} - (\hat{\mathcal{U}}(\mathcal{T}) - \hat{\mathcal{U}}(\mathcal{S}^k)), 0\}$$

Test on simulation

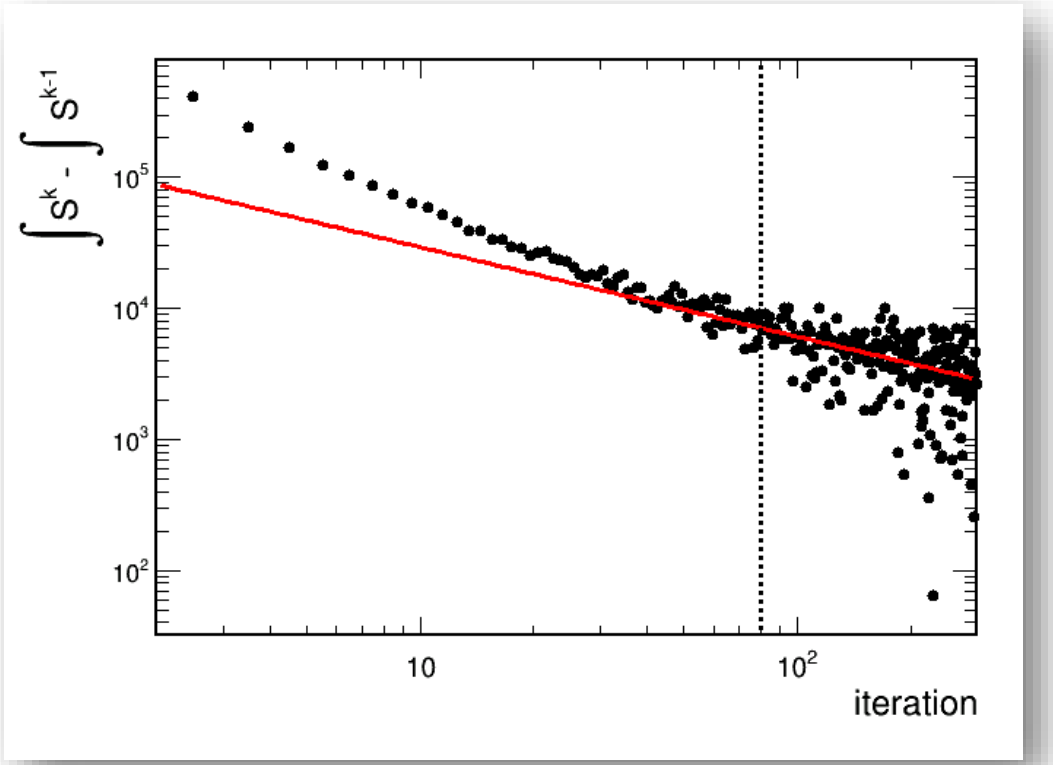

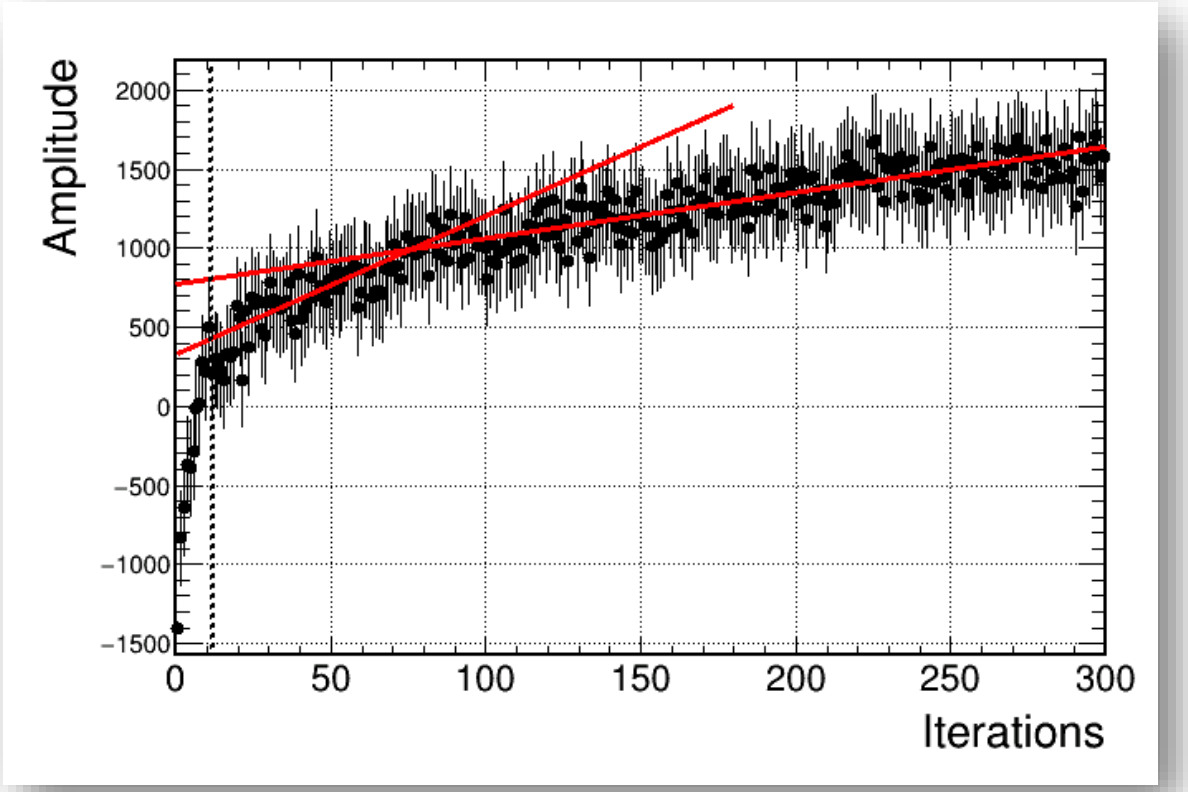

$$\mathcal{S}^{k+1} = \max\{\mathcal{T} - (\hat{\mathcal{U}}(\mathcal{T}) - \hat{\mathcal{U}}(\mathcal{S}^k)), 0\}$$

Test on simulation

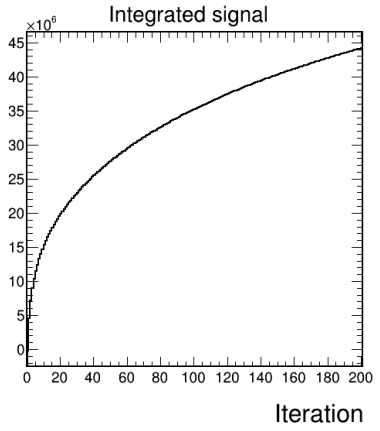

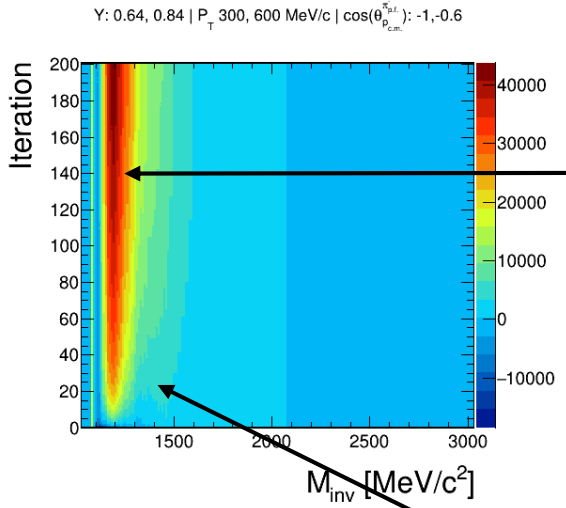

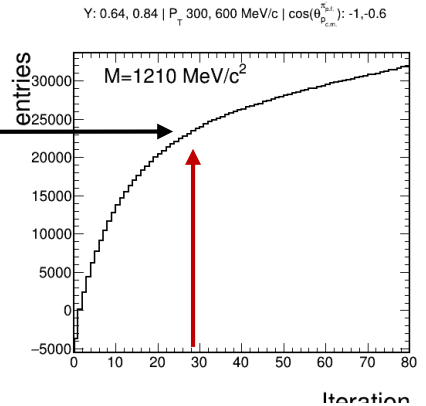

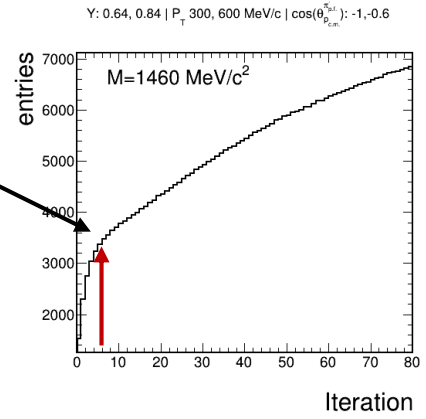

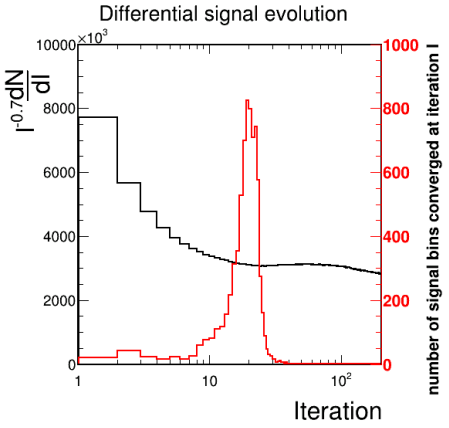

The algorithm is continuously incrementing the signal

The evolution of each bin in the 4-D matrix is evaluated: transition from fast growth into slow statistical rise

The differential total signal rise and the iteration at which the optimum value is reached are consistent

Test on simulation

Mult-differential result

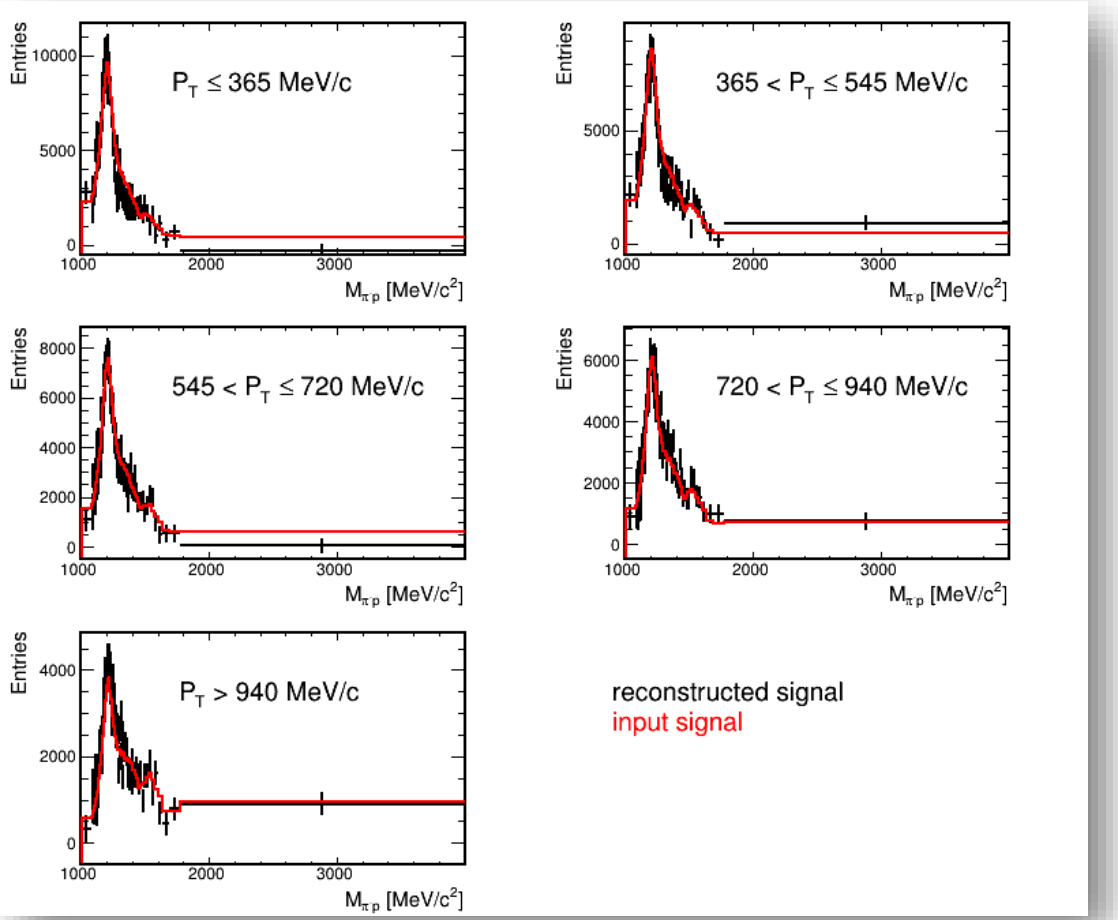

Test on simulation

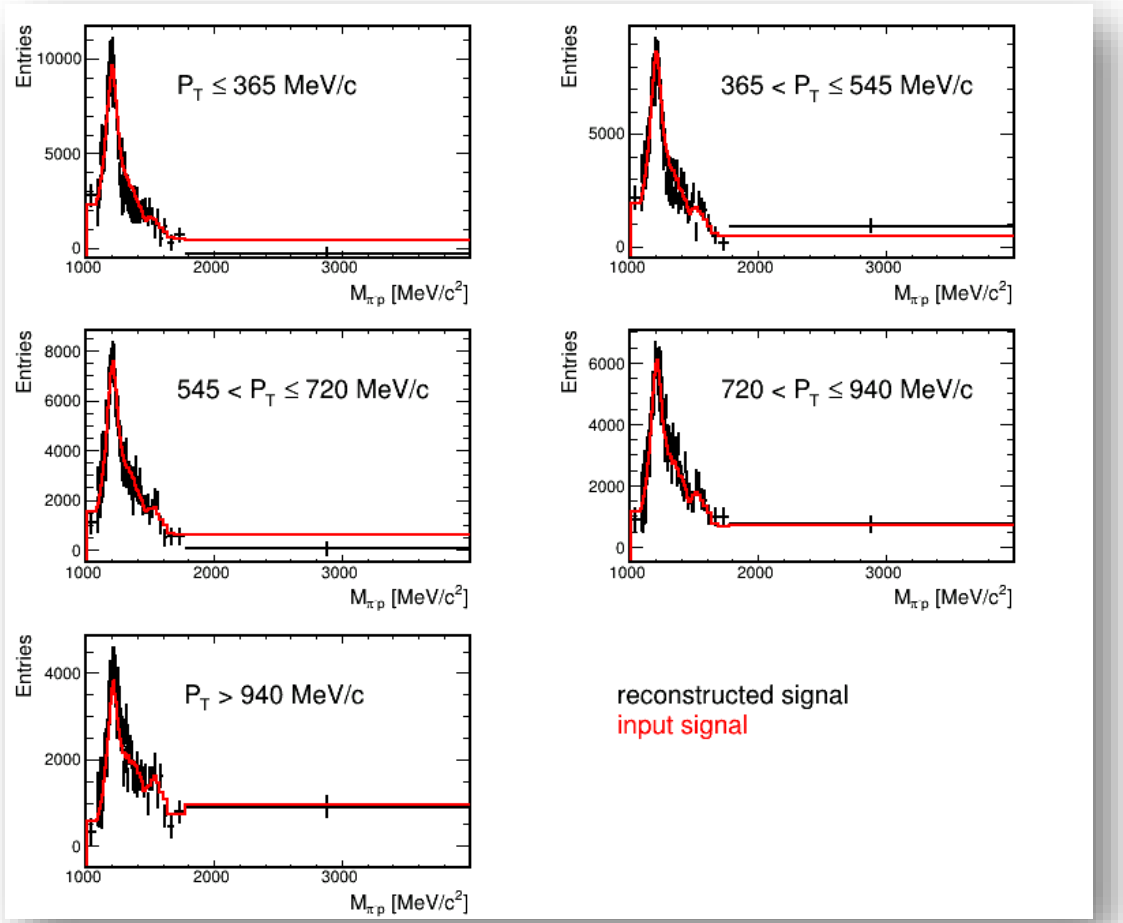

Mult-differential result

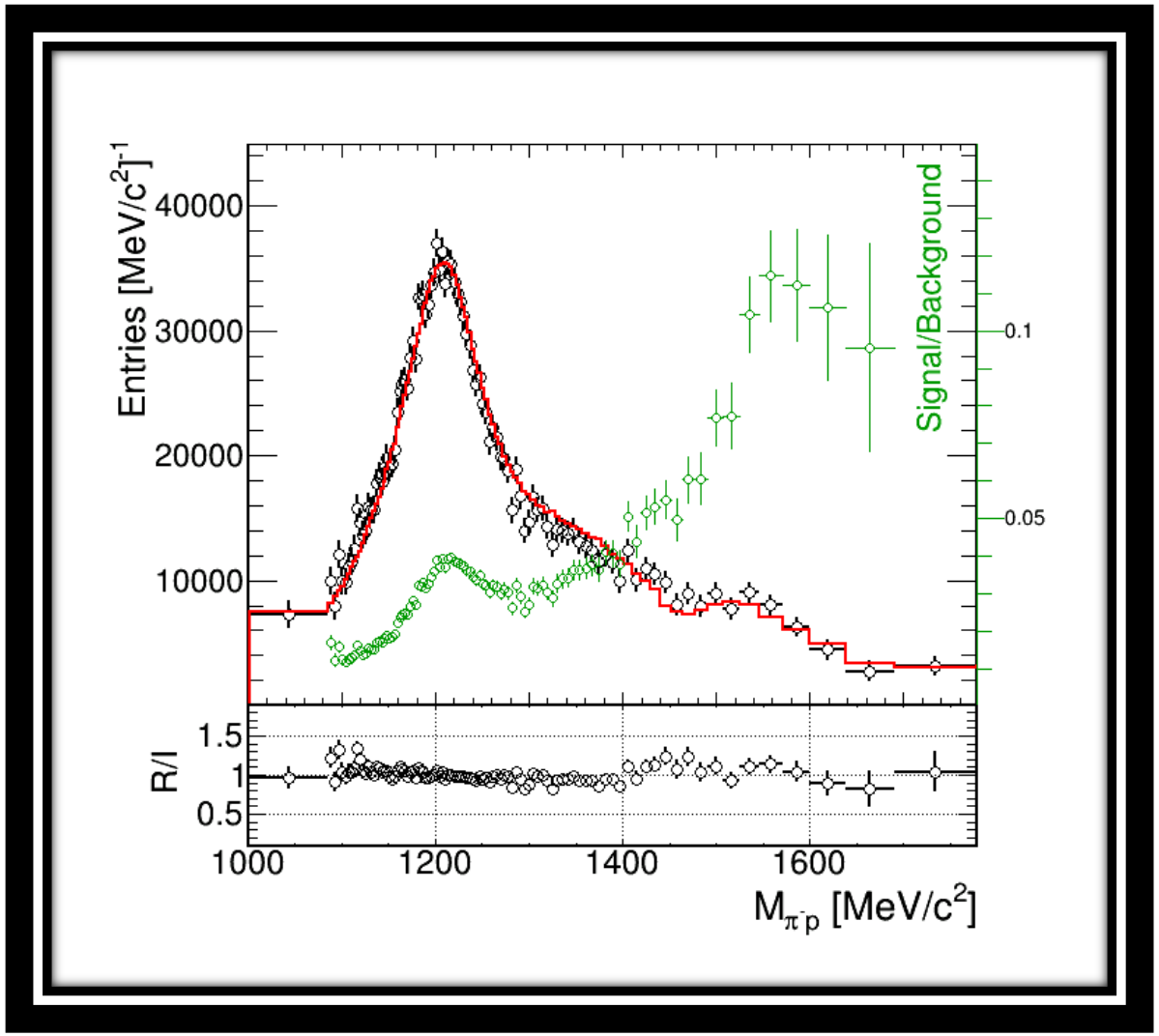

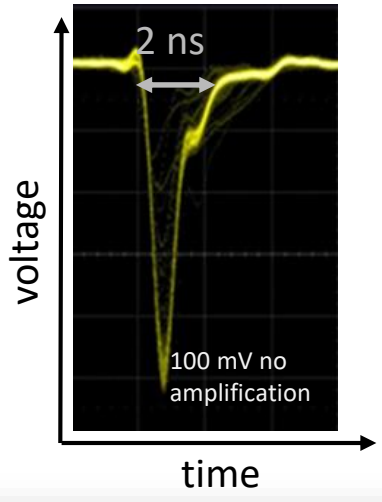

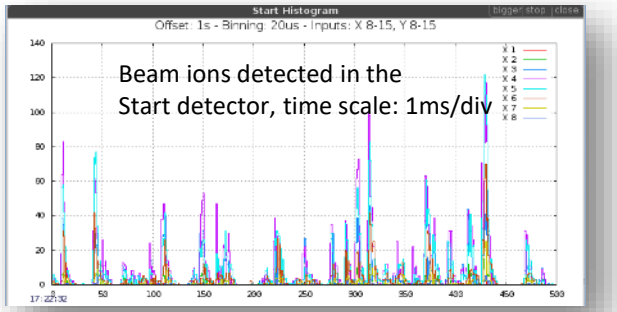

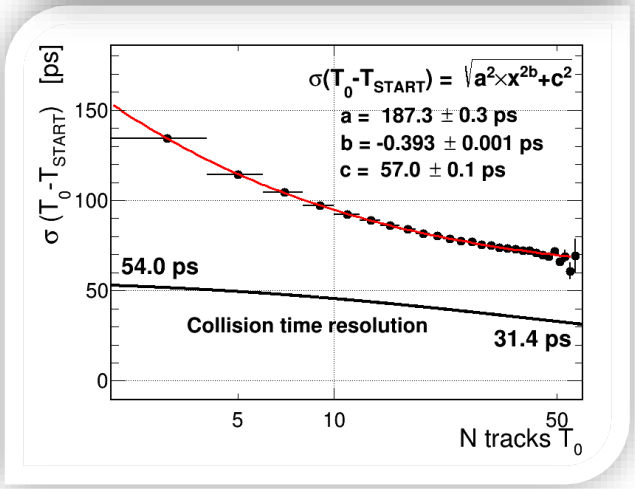

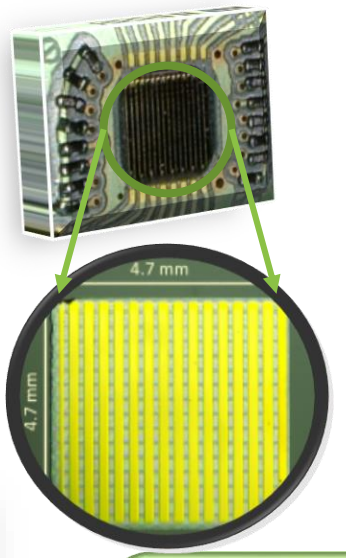

Beam size (3σ)
1.3 x 0.8 mm²

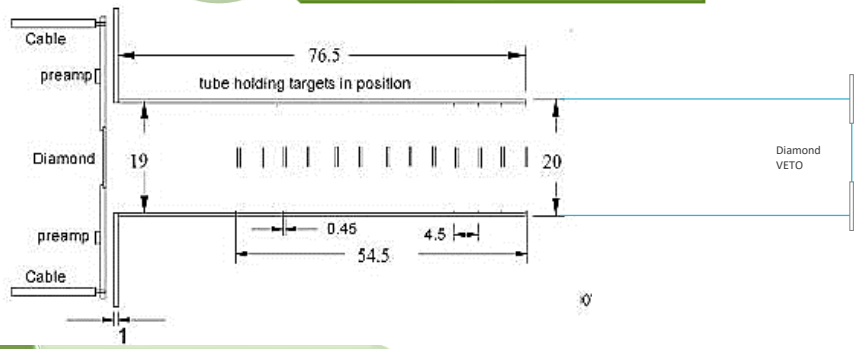

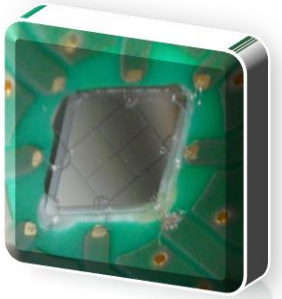

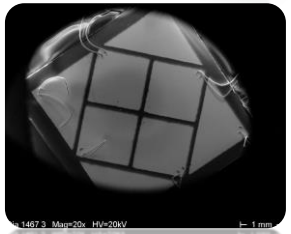

Detector specs:

- scCVD diamond
- thickness 67µm
- Strip width 200 µm
- Gap width 90 µm

- size: 4.5 mm x 4.5 mm
- detector thickness: 70 µm
- detector time precision: ~50 ps

8 -segment detector

Dedicated electronics:

- Multi-hit TDC, 17 ps res.
- Detector resolution 42 ps

Mean 4-weeks Time resolution 54 ps
From analysis with high quality tracks

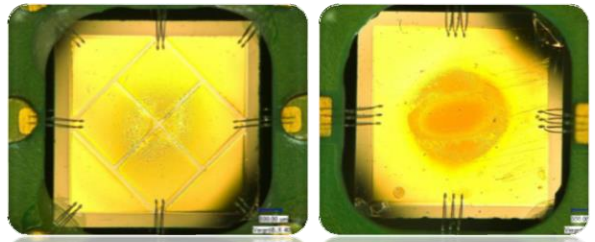

Irradiated by 3 x 10^{11} Au (1.23 AGeV) ions during 5 days

g.kornakov@gsi.de

Virtual photons from Au+Au at $\sqrt{s} = 2.42$ GeV

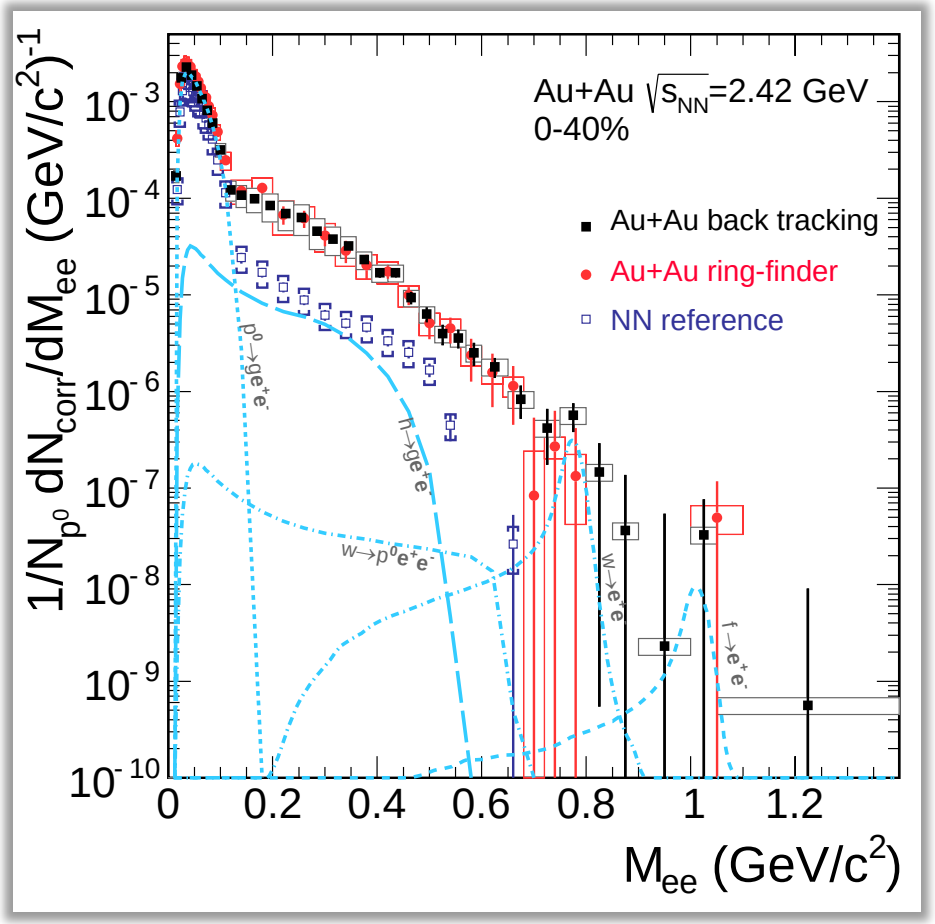

[HADES] Submitted

- Dilepton mass spectra
- Cocktail includes: π^0, η, ω, ϕ measured in the same experiment.
- Reference NN spectra

$$\frac{dN_{ref}^{NN}}{dM_{ee}} = \left(0.54\frac{dN^{pp}}{dM_{ee}} + 0.46\frac{dN^{np}}{dM_{ee}}\right)\langle A_{part}\rangle$$

Excess yield → true in-medium radiation

g.kornakov@gsi.de

Virtual photons from Au+Au at $\sqrt{s} = 2.42$ GeV

Acceptance corrected excess yield

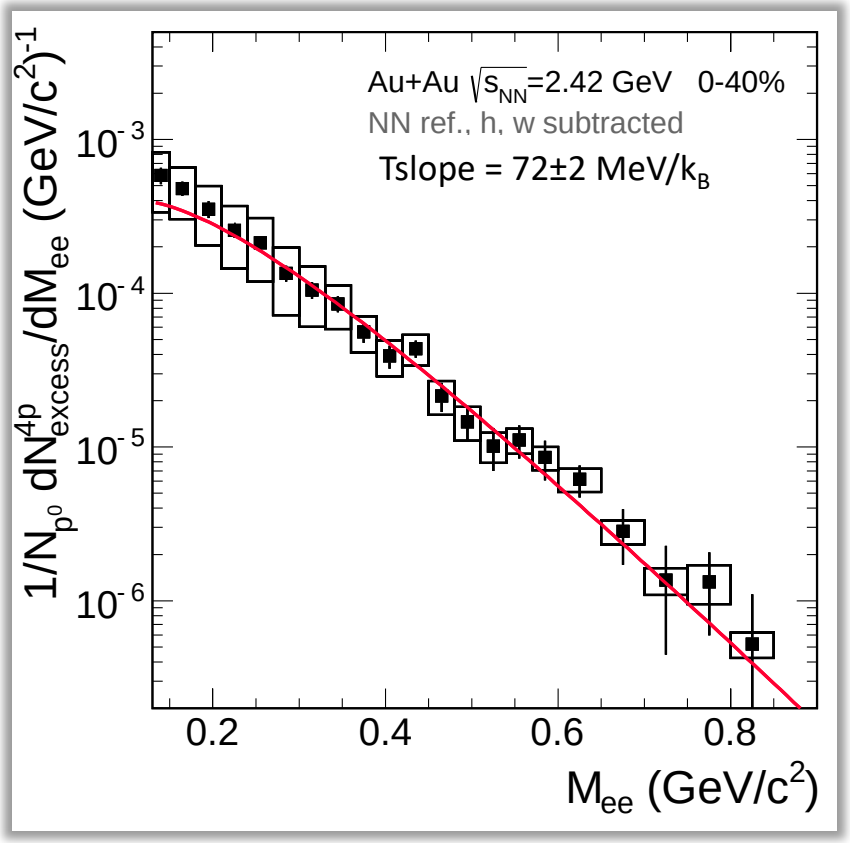

[HADES] Submitted

Excess yield obtained after subtracting:

- π^0, η, ω, ϕ (freeze-out)
- Reference NN spectra

Thermometer of the emitting source

Exponential fall of the spectrum

$T = 72 \pm 2$ MeV/k_B

g.kornakov@gsi.de

Excess yield of virtual photons from Au+Au at $\sqrt{s} = 2.42$ GeV

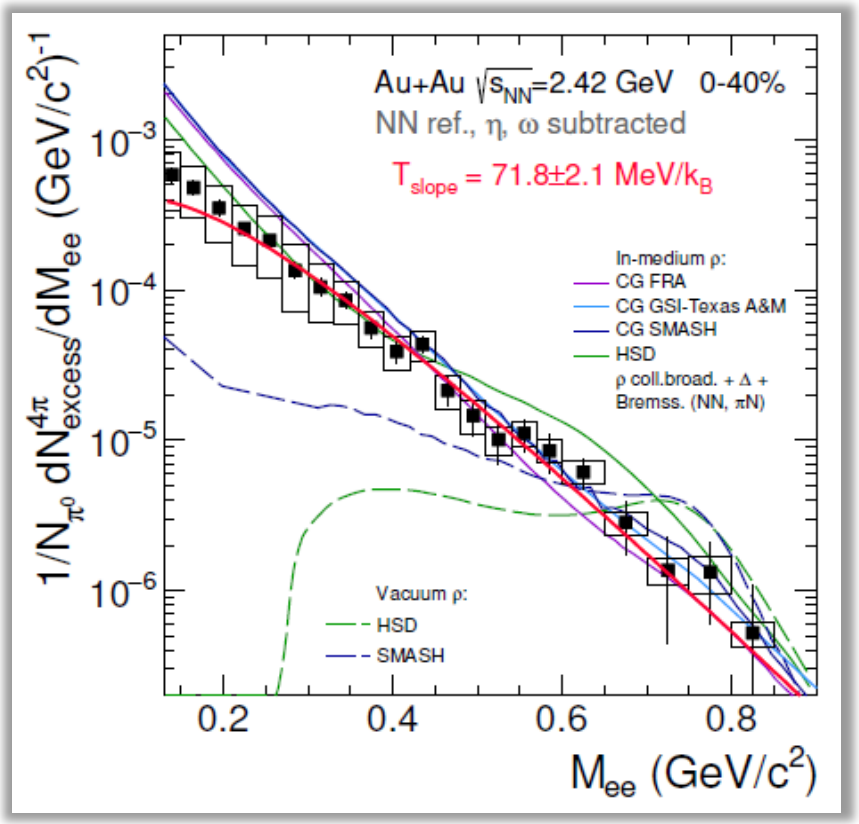

- Strong broadening of the in-medium ρ due to direct ρ-hadron scattering

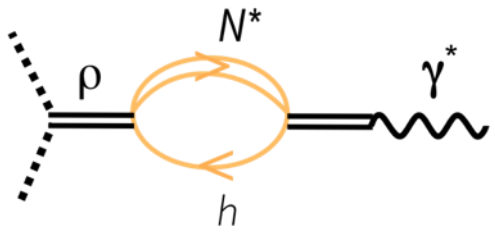

- Thermal rates folded over coarse-grained UrQMD medium evolution works at low energies
- Supports baryon-driven medium effects at SPS, RHIC, LHC

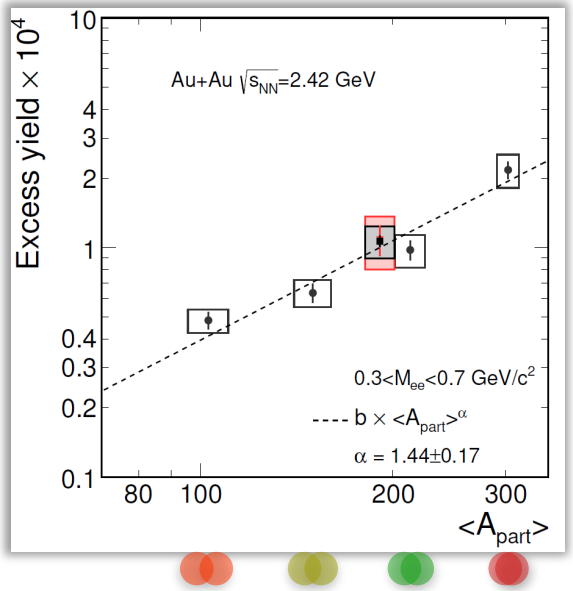

Coarse Graining (CG): ρ in-medium spectral function with thermodynamic parameters from transport

CG FRA: Phys. Rev. C 92, 014911 (2015)
CG GSI-Texas A&M: Eur. Phys. J. A, 52 5 (2016) 131
CG SMASH: arXiv:1711.10297 [nucl-th]
HSD: Phys. Rev. C 87, 064907 (2013)

Medium radiation goes beyond incoherent superposition of NN collisions (like $A_{\mathrm{part}}^{4/3}$)

→**Dilepton chronometer** of the collision time:

$$N_{\mathrm{ee}} \sim A_{\mathrm{part}} \cdot A_{\mathrm{part}}^{1/3} \sim V \cdot \boldsymbol{\tau_{\mathrm{fireball}}}$$

g.kornakov@gsi.de

Excess yield of virtual photons from Au+Au at $\sqrt{s} = 2.42$ GeV

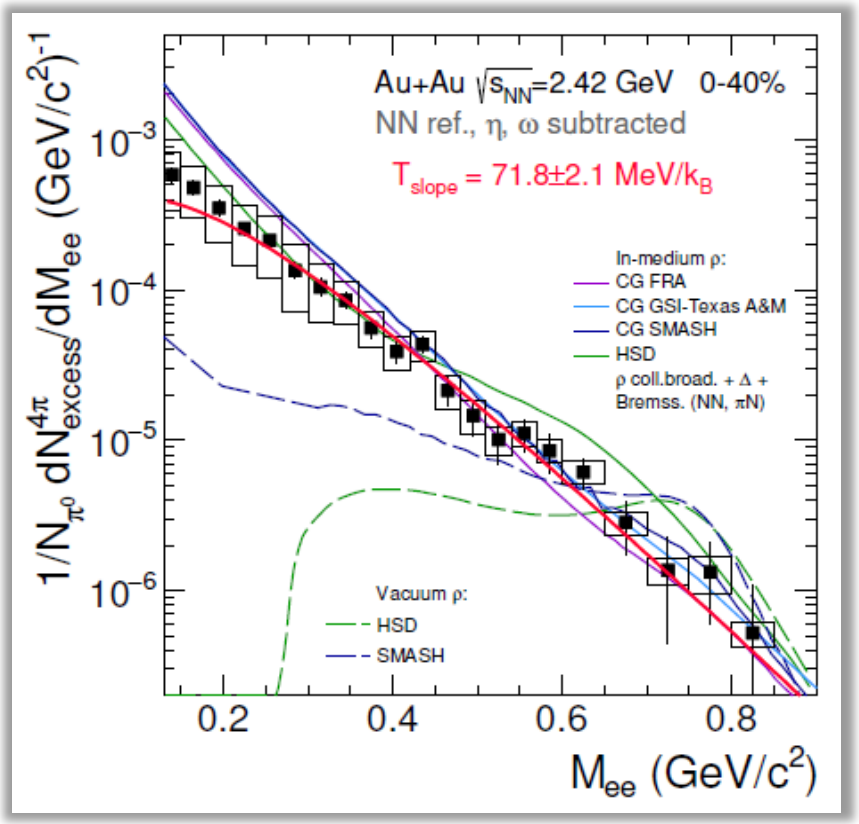

Coarse Graining (CG): ρ in-medium spectral function with thermodynamic parameters from transport

- Strong broadening of the in-medium ρ due to direct ρ-hadron scattering

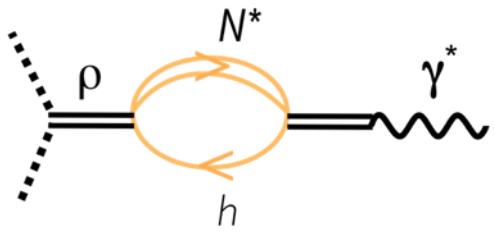

- Thermal rates folded over coarse-grained UrQMD medium evolution works at low energies
- Supports baryon-driven medium effects at SPS, RHIC, LHC

Robust understanding across QCD phase diagram

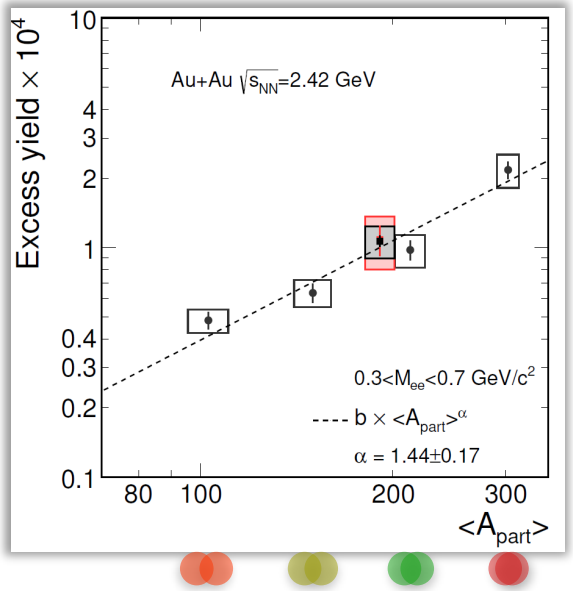

Medium radiation goes beyond incoherent superposition of NN collisions (like $A_{\mathrm{part}}^{4/3}$)

→**Dilepton chronometer** of the collision time:

$$N_{\mathrm{ee}} \sim A_{\mathrm{part}} \cdot A_{\mathrm{part}}^{1/3} \sim V \cdot \boldsymbol{\tau_{\mathrm{fireball}}}$$

CG FRA: Phys. Rev. C 92, 014911 (2015)
CG GSI-Texas A&M: Eur. Phys. J. A, 52 5 (2016) 131
CG SMASH: arXiv:1711.10297 [nucl-th]
HSD: Phys. Rev. C 87, 064907 (2013)

g.kornakov@gsi.de

Coupling mechanism of the ρ to baryons: π induced reactions

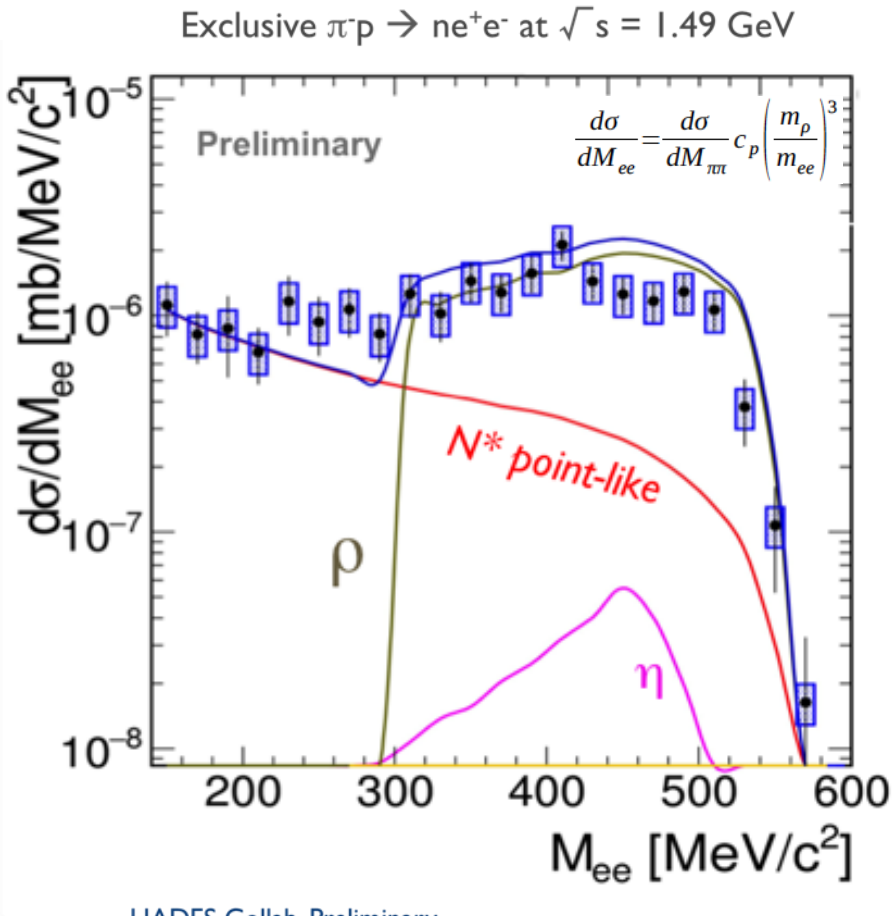

HADES Collab. Preliminary
E. Speranza, B. Friman et al., Phys. Lett. B764 (2017) 282
Ramalho, Peña, Phys.Rev. D95 (2017) 014003

- GSI: worldwide unique combination of π beams (at low energies) with dilepton spectrometer
- Access to time-like *em* transition FF of baryons

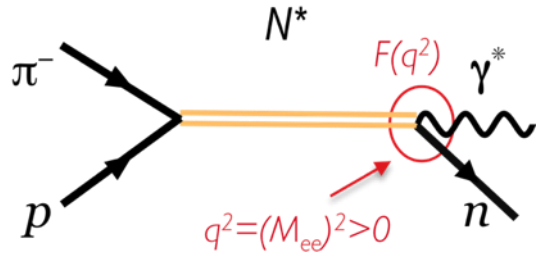

- First measurement demonstrates the dominant role of intermediate ρ propagation in $N^* \rightarrow Ne^+e^-$ transition
- In accordance with strict VMD (the basis of emissivity calculations for QCD matter)

g.kornakov@gsi.de